The modulatory effect of dominance rank on social perception in the mouse hypothalamus

Neven Borak

A dissertation submitted in partial fulfilment

of the requirements for the degree of

Doctor of Philosophy

of

University College London.

The Francis Crick Institute

University College London

June 24, 2024

I, Neven Borak, confirm that the work presented in this thesis is my own. Where information has been derived from other sources, I confirm that this has been indicated in the work.

Abstract

Studies of the neural basis of social dominance hierarchies have focused on how status is learned and represented in a thalamocortical circuit involving mainly the mediodorsal thalamus, the anterior cingulate cortex and the medial prefrontal cortex (mPFC). However, it is unclear how this circuit integrates sensory information about others and leads to distinct behavioural phenotypes for dominant and subordinate individuals in a wide repertoire of social behaviours. This thesis proposes that this is achieved through top-down modulation of the sensory representations of social cues in two hypothalamic areas involved in behavioural decision-making: the medial preoptic area (MPOA) and the ventromedial hypothalamus (VMH). In vivo miniscope recordings in these areas in male mice reveal rank-dependent modulation of neuronal excitability and tuning properties in response to female conspecifics. These functional features in turn predict the propensity for social interaction with females as well as sexual mounting. The position of these nodes in the social cognition pathway with known connectivity to olfactory sensory inputs combined with rank-dependent modulation led to the hypothesis that they serve as integration nodes for information about an animal's own social rank and that of opponents. It was confirmed that mice detect the rank of unfamiliar opponents through olfactory signals and the encoding of both own and opponent rank variables was individually investigated, however, neither was represented in these areas. Instead, a novel function for the hypothalamus was described in encoding two semi-stable variables with slow dynamics: competitive context and winning state. Finally, a circuit model is proposed where monosynaptic mPFC projections to the hypothalamus achieve sensory modulation and influence winning performance against conspecifics. Optogenetic

manipulation of mPFC projections to the MPOA and VMH during competitive behaviour was performed, however, no effect on winning performance was found, instead suggesting a multisynaptic modulatory mechanism or diffuse release of a neuromodulator.

Impact Statement

Low social status has well-documented damaging effects on both physical and psychological health in both humans and animals. At least some of these effects, especially on mental well-being, are attributed to the tendency towards social avoidance in subordinate individuals, which itself has a strong relationship with poor health outcomes. Additionally, by generalising one's low social status in one community to interactions with new groups of people, subordinates impair their ability to assume a higher rank in novel social contexts. Despite the associations between low social rank, low social engagement, and poor physical health, it is not well understood how social status affects social competence.

This thesis investigates how sensory representations of conspecifics are modulated by self-perceived dominance rank in male mice. It addresses the absence of sensory integration in the current understanding of the dominance circuit, even though hierarchical behaviour is highly adaptive and relies not only on own rank but also that of conspecific opponents. It characterises rank-dependent modulatory effects on social perception at the level of specific brain areas at single-cell resolution. Specifically, neuronal tuning and response amplitude properties in response to female conspecifics differed across males of different ranks. Furthermore, these metrics correlated with the level of chemoinvestigatory and sexual engagement with the female. Modulation of sensory responses to social cues could therefore be one mechanism by which low rank renders others less salient or rewarding, with social isolation as a consequence. Furthermore, these changes were found in two hypothalamic areas, whose involvement in hierarchical behaviour had not been investigated before. These findings therefore expand the theoretical understanding of the domi-

nance circuit, propose a conceptually novel mechanism for rank to affect behaviour, and have important translational implications for the mechanism behind lower social engagement among subordinate individuals.

The thesis also investigates how the rank of conspecifics is detected and proposes a model of own and opponent rank integration. The sensory modality used to detect conspecific rank is determined using sensory deprivation experiments. The sufficiency of both the main and accessory olfactory systems to detect the rank of even unfamiliar mice demonstrates that mice can generalise their rank to interactions with strangers and provides the basis for understanding why moving to a new social environment is insufficient to improve self-perceived social status. It also offers two potential pathways through which opponent rank information could reach the dominance circuit that encodes own rank. The thesis investigates the non-volatile pathway in more detail and proposes the two hypothalamic areas that are modulated by own rank as integration nodes, which combine the two streams of information containing own and opponent rank representations. This concept has implications not just for the encoding of hierarchical relationships, but the encoding of self and other as a wider problem in the neuroscience and psychology fields. While the integration node hypothesis was rejected, the work offers valuable technical insights for assay design, as well as robust decoder model evaluation standards due to the unique generalizability constraints in this type of analysis.

Acknowledgements

This work would not have been possible without the supervision of Jonny Kohl, I thank him for his guidance and support over the past 3 and a half years. Members of my thesis committee, Andrew Mackaskill, Elena Dreosti, and Petr Znamenskiy, have also provided invaluable input on the direction of the project throughout my PhD. Andrew and Elena were also my supervisors during my rotation year and equipped me with the skills and knowledge to tackle the PhD head on. I also wish to thank the Wellcome Trust and the UCL neuroscience PhD programme committee for giving me the opportunity and funding to pursue this project for the past 4 and a half years.

Everyone in the Kohl lab, which has grown significantly since I first joined, has been an invaluable source of support, motivation, scientific advice, and friendship through these years. I particularly want to mention Mingran and Francesco, with whom I formed the first cohort of PhD students in the lab and who became good friends, flatmates, confidantes, and fellow coffee addicts. Many of you from the lab and those just passing through helped me with things I knew little about. Thank you to Sophie Wood for helping me with surgeries when I was still training to do them myself, to Paula Rodriguez for showing me how to do histology on tissues that are not as soft as a brain, Irene for troubleshooting our olfactory bulb ablation protocols together, to Mingran for long discussions about computational techniques and big picture thinking about my project when the going got tough, and Janice Kim, the first person I ever mentored, for her enthusiasm in joining the project, learning, and contributing to every experiment she could.

Equally, I want to say thank you for the support of my family, who always stood behind me and made it possible for me to study abroad, even if I chose a subject that does not even exist back at home. My partner Jack, whom I met during the first few months in London and who stuck around through a global pandemic is a survivor of my PhD as much as I am. I don't know what I would have done without Gustavo, who taught me to explore other parts of myself when I became too entangled in the roller coaster of the PhD. Thanks to you I discovered dance at The Place and (re)discovered acting at Guildhall, the teachers and fellow students of which have helped me find a community in a city where they can be difficult to find. There are many others that I have met during my time at UCL and who have made my PhD experience better and for that, I thank you.

Contents

List of Figures

List of Tables

Acronyms

AAV Adeno-associated virus.

ACC Anterior cingulate cortex.

AE Autoencoder.

AOB Accessory olfactory bulb.

AUC Area under the curve.

AVT Arginine vasotocin.

c- Caudal.

CCA Canonical correlation analysis.

ChR2 Channelrhodopsin 2.

CI Confidence interval.

CV Cross-validation.

d- Dorsal.

DA Dopamine.

DR Dimensionality reduction.

eEPSC evoked excitatory post-synaptic current.

Esr1 Estrogen receptor 1.

FOV Field of view.

GLM General Linear Model.

GRIN Gradient refractive index.

Hb Habenula.

ILA Infralimbic cortex.

IPN Interpeduncular nucleus.

l- Lateral.

LH Lateral hypothalamus.

LOOO Leave-one-opponent-out.

m- Medial.

MDT Mediodorsal thalamus.

MeA Medial amygdala.

MOB Main olfactory bulb.

MPOA Medial preoptic area.

NAc Nucleus accumbens.

OE Olfactory epithelium.

OFC Orbitofrontal cortex.

PAG Periaqueductal gray.

PBS Phosphate buffered saline.

PCA Principal component analysis.

PFA Paraformaldehyde.

PFC Prefrontal cortex.

PIR Piriform cortex.

PL Prelimbic cortex.

PLS Partial least squares.

POA Preoptic area.

PR Progesterone receptor.

PSTH Peristimulus histogram.

PV Parvalbumin.

RSA Representation similarity analysis.

SKF Stratified K-fold.

SVM Support vector machine.

v- Ventral.

VIP Vasoactive intestinal peptide.

VMH Ventromedial hypothalamus.

VNO Vomeronasal organ.

VTA ventral tegmental area.

Chapter 1

Introduction

1.1 Hierarchies solve a resource allocation problem

Social animals face a resource allocation problem: resources that the community needs to survive are often scarce and available supplies are exceeded by the collective needs of the group. A hierarchical organisation is the evolutionarily preferred strategy for resolving this problem, where a single animal or a group of individuals retain preferential access to group resources (Tibbetts et al., 2022). Human societies are highly hierarchical as well although with substantial complexities, such as participation in multiple simultaneous hierarchies (e.g., domestic, workplace, friendships), formalised hierarchies that do not necessarily align with implicit hierarchies, and social ranking based on constructed concepts (Hawley, 1999). While many of these features of hierarchies cannot be replicated in animal models, their ubiquity across social species as well as research on the neural basis of dominance point to an evolutionarily ancient mechanism that enables this type of social structure.

Theories of why hierarchical organisation seems favoured over egalitarian community structures suggest that it avoids constant within-species physical conflict for resources since the access hierarchy is implicitly understood by all participants and injury is avoided (Drews, 1993). Indeed, stable hierarchies with little or no rank switching appear to result in lower testosterone, stress hormone, and ag-

gression levels across all group members compared to unstable hierarchies (Knight and Mehta, 2017). Hierarchies are also proposed to enhance the reproductive success of dominant group members, thus applying an additional evolutionary selective pressure. Indeed, subordinates do have lower reproductive success (D'Amato, 1988; Thor and Carr, 1979) and dominants are more likely to also sire dominant offspring (Kleshchev and Osadchuk, 2014), suggesting there is some propagation of advantageous traits via this mechanism.

1.2 Dominance-dependent modulation of innate social behaviour

Social behaviours such as mating, aggression, parenting, and grooming are innate, meaning that they do not require training. The association of these behaviours with evolutionarily ancient subcortical brain areas has led to the outdated perspective that these behaviours are "hard-wired" and offer very little flexibility, compared to the learned behaviours facilitated by the cortical areas and the hippocampus. However, the expression of innate social behaviours is highly flexible and depends on the presence of the correct motivational state (Wei et al., 2021). For example, the propensity for sexual behaviour is regulated by past sexual experience in male mice (Yang et al., 2022; Remedios et al., 2017), while repeated experience of winning aggressive fights in males leads to a more aggressive phenotype in the future (Stagkourakis et al., 2020). Past experiences can therefore lead to stable plasticity changes that promote specific behavioural responses in the future. Similarly, hormonal states associated with the oestrus cycle modulate sexual receptivity in female mice (Inoue et al., 2019), lactation results in a switch from female sexual receptivity to aggression when interacting with males (Liu et al., 2022), while hormonal changes associated with pregnancy prime female mice for parental behaviour (Ammari et al., 2023). Finally, innate social behaviour is highly sexually dimorphic, meaning that the same social cues elicit distinct behavioural responses depending on sex (Stowers and Liberles, 2016). These internal states therefore flexibly modulate the expression of otherwise stereotyped social behaviours on multiple timescales.

Some states, such as those associated with the circadian and oestrus cycles can be highly transient, while others are semi-stable (e.g., pregnancy), and even permanent (e.g., sex). This variability in timescales is reflected in multiple mechanisms of internal state encoding, namely, neuromodulatory and endocrine signalling, maintenance of an internal state via recurrent self-sustaining activity, and stable plasticity changes (Flavell et al., 2022).

Dominance status is yet another internal state acquired through social experience (Zhou et al., 2017) and maintained over relatively long timescales as long as the group hierarchy remains stable. Variability in social status results in distinct behavioural phenotypes for dominant and subordinate individuals. The nature of these differences is highly variable across species due to a multitude of hierarchical structures that social animals employ (Tibbetts et al., 2022). Nonetheless, rank-dependent differences in behavioural phenotype, especially with respect to sociability, sexual behaviour, and resource control (Tibbetts et al., 2022), highlight the role of social status as a modulator of innate behaviour. However, the neural mechanism through which rank affects behavioural decision-making is not well understood.

Social behaviour can be conceptualised as a sensorimotor transformation, where the brain represents the relevant sensory features of a social cue and transforms them into a behavioural decision and subsequently motor instruction that ultimately leads to an observable behavioural response (Wei et al., 2021). Areas involved in this transformation frequently exhibit neuronal tuning to both the sensory features of the social cue as well as specific behaviours with varying levels of selectivity (Karigo et al., 2021; Stagkourakis et al., 2023). In this model, internal states can achieve distinct behavioural outcomes by either manipulating the sensory representation of the social cue (Ammari et al., 2023; Remedios et al., 2017; Yang et al., 2022; Stowers and Liberles, 2016), or by triggering switching in the activation of mutually exclusive neural populations which promote opposing behavioural responses, e.g., aggression versus mating (Karigo et al., 2021) and exploration versus defensive avoidance (Gründemann et al., 2019).

In the case of dominance, the modulatory mechanism has not been systematically explored at a similar level of mechanistic detail, however, evidence from human studies suggests that social status may be affecting the perceptual end of the sensorimotor transformation. For example, observing an individual perceived to be low-status is associated with diminished sensorimotor mirroring activity compared to observing high-status individuals (Gutsell and Inzlicht, 2010; Avenanti et al., 2010), while faces of high-status individuals are easier to recognise (Ratcliff et al., 2011). Studies in humans and primates have also identified an attentional bias, where lower-ranked individuals spend more time visually attending to their dominant counterparts, perhaps with the aim of either vicariously learning more about the shifting hierarchical relationships in the group, or to detect signs of aggression from the dominant and territorial claims over resources that the subordinate should avoid (Jones et al., 2010; Chance, 1967; Deaner et al., 2005; Shepherd et al., 2006). Similarly, in the mouse model, research has identified cells tuned to own behaviour as well as cells tuned to the behaviours of others in the prefrontal cortex, an area strongly involved in status encoding (Kingsbury et al., 2019). However, the subordinate mice had a larger proportion of cells selectively tuned to conspecifics compared to dominant counterparts, supporting the attentional bias hypothesis and higher sensory salience of dominant individuals at the neuronal level. Together these findings suggest that dominance status may be modulating the sensory representations of social cues to precipitate rank-dependent behavioural phenotypes.

1.3 Adverse effects of low social status

While hierarchical social organisation may have evolutionary benefits, it also entails substantial disadvantages for subordinate individuals. Low socioeconomic status in humans is a strong predictor of disease, poor immune function, short life expectancy, and psychiatric morbidity (Sapolsky, 2004; Johnson et al., 2012). While wealth-associated differences in lifestyle, healthcare, and food quality may explain some of these health outcome disparities, there is evidence that they do not depend on absolute income levels and living standards, but rather on the relative income

within a society (Wilkinson, 1997), demonstrating a contribution of social status in its own right. Likewise, these harmful effects of low status are also present in social animals, where the confounds of healthcare access and lifestyle differences are absent (Cavigelli and Chaudhry, 2012).

Of particular concern is the link between low social status, psychiatric conditions, and social avoidance. Chronic social defeat drives isolation (Challis et al., 2013; Franklin et al., 2017) and defensive behaviours such as fleeing (Nelson et al., 2019) in rodent models, while work in humans shows that low socioeconomic individuals have poorer quality social relationships. For example, low socioeconomic status men in Sweden reported lower perceived levels of social integration, social activity and emotional support compared to high-status counterparts (Rosengren et al., 1998). These coping mechanisms sacrifice an individual's innate need for social interaction and community belonging in exchange for the reduced probability of further social defeat in the future. In mice, this isolation drive is generalised and not limited to individuals whom the defeated animal has already had a negative experience with (Challis et al., 2013). Defeated individuals are therefore hypervigilant and tend to err on the side of caution by evaluating unfamiliar or neutral social cues as potentially threatening, thus passing over opportunities for positive social interaction in the interest of avoiding the risk of negative interaction (Sloman, 1984). This hypervigilance may be contributing to the attentional bias towards dominants described earlier, which could preempt physical conflict by detecting signs of aggression from the dominant early. While social vigilance does attenuate the risk of conflict, it is also destructive to the subordinate's community belonging and support network, which are fundamental needs in many social species and certainly humans (Rosengren et al., 1998).

Generalised social avoidance and failure to meet social needs are a known risk factor for poor mental health outcomes (Chen et al., 2022a; Wei et al., 2023; Jenkins et al., 2023), while psychiatric symptoms such as anxiety, depression, and psychosis frequently drive further isolation precisely when community support is the most crucial (Linz and Sturm, 2013). Isolation also inhibits the individual's

ability to increase their status. In contrast with the common perception of dominants as tyrants, a much more successful strategy to attain high status in humans is prosocial behaviour, gregariousness, and adopting the function of a leader and role model that provides value to the group (Hawley, 1999; Chance, 1967). Similarly, the attentional bias towards focusing on the highest-ranking individuals entails that dominants spend their time in the group spotlight, meaning that withdrawn and fearful individuals struggle to gain the esteem of others.

In humans, large parts of the population are pushed into low socio-economic status by factors beyond their control with severe implications for physical as well as mental health. I argue that the associations between low social status, poor health, and diminished social engagement further reinforce low rank and reduce hierarchical mobility. These health effects also occur in animals, meaning that they are at least partially independent from wealth disparities and access to quality healthcare that confound their relationships with social status in humans. Understanding the representation of social rank on the individual level is therefore crucial to understanding an incredibly strong predictor of quality of life.

1.4 Neural circuits of social dominance

Social hierarchy research is conducted in a very wide variety of model systems as well as humans with considerable interspecies variability in group organisation, however, a few conserved brain circuits reappear in the literature. The current state of the field will be summarised particularly with reference to work in male mice, which is the model system used in this thesis. Studies focusing on the learning of hierarchical relationships have elucidated the importance of plasticity in two thalamic projections to the cortex. Specifically, glutamatergic projections from the mediodorsal thalamus (MDT) to the medial prefrontal cortex (mPFC) are potentiated in dominant individuals (Zhou et al., 2017; Wang et al., 2011), resulting in a more excitable mPFC in dominants. Activity from the mPFC was used to decode competitive performance in dyadic interactions in the tube test, a behavioural dominance assay, while optogenetic excitation of this area could be used to reversibly

manipulate the rank of an animal (Zhou et al., 2017). Strikingly, repeated excitation of the mPFC over 3 days resulted in a stable rank improvement. Subsequent work has revealed that early life stress during a critical developmental period biases the ratio of excitatory and inhibitory input to the mPFC in favour of inhibition, thus resulting in low social status in adulthood (Chen et al., 2022b; Ohta et al., 2020). Work on social defeat in mice also found that functional connectivity between the mPFC and the dorsal periaqueductal gray (PAG) is weakened in defeated individuals who were repeatedly exposed to an aggressive intruder (Franklin et al., 2017). The optogenetic inhibition of the projection from the mPFC to the dPAG was also found to induce social avoidance behaviour mimicking social defeat. While the defeat paradigm using an aggressive intruder is different from dominance paradigms where hierarchies are mostly stable and peaceful, these findings suggest a mechanism through which status representations in the mPFC can affect social approach and avoidance.

Involvement of the PFC was also demonstrated in human fMRI studies. Participants usually play competitive games against opponents whose rank is explicitly communicated (e.g. by showing different numbers of starts next to the opponent avatar (Zink et al., 2008)), or the game is not played against a human opponent and instead rigged to obtain the desired rate of winning determining the self-perceived rank against the opponents (Ligneul et al., 2016). Activations in both the mPFC (Ligneul et al., 2016; Zink et al., 2008) and the dorsolateral PFC subdivision (Zink et al., 2008; Ligneul et al., 2017) correlate with the dominance of the opponent as well as winning and losing. The mPFC is also involved in the encoding of expertise and intelligence of others in humans (Boorman et al., 2013; Bault et al., 2011), both of which are strongly related to the subjective perception of someone's social position. Furthermore, variation in dlPFC sensitivity to social rank correlated with participants' social dominance orientation (SDO) score (Ligneul et al., 2017). SDO is a psychological trait axis that describes the individual's belief in the legitimacy of social hierarchy over egalitarianism, their willingness to enforce hierarchies and the perception of existing social inequalities as inherently just (Pratto et al., 1994).

In addition to the mPFC, MDT neurons also project to the caudal anterior cingulate cortex (cACC), where they synapse onto local parvalbumin (PV) positive inhibitory interneurons (Nelson et al., 2019). The potentiation of MDT-ACC projections in dominants therefore leads to the inhibition of the ACC glutamatergic (VGLUT2 positive) pyramidal neurons (Nelson et al., 2019). The ACC has been associated with physical as well as social pain in human studies, which have highly overlapping neural substrates (Qu et al., 2011). Stroke-associated lesions of the ACC do not impair the detection of pain, however, it ceases to be perceived as unpleasant (Qu et al., 2011). The role of the ACC in encoding negative social valence was also demonstrated by lesions in mouse mothers, which resulted in diminished distress in response to pup calls, indicating a lower sensitivity to social pain (Stamm, 1955; Murphy et al., 1981). This suggests that the highly activated caudal ACC in subordinates is correlated with a perception of social pain or exclusion associated with low social status. Similarly to the mPFC, optogenetic manipulation of the ACC was successfully used to manipulate social rank in mice, albeit with the reverse trend to the mPFC, establishing an opposing influence of the two areas on rank (Nelson et al., 2019).

In simpler vertebrates such as Zebrafish which lack a clear homologue of the mamallian neocortex, the roles of the mPFC and cACC in regulating dominance-dependent winning are instead attributed to the two subdivisions of the dorsal habenula (dHb) and their projections to the interpeduncular pathway (IPN) (Chou et al., 2016). The lateral subdivision (dHbL) and its projections to the dorsal and intermediate IPN is associated with winning fights, whereas the medial habenular subdivision (dHbM) and its projections to the ventral IPN are associated with losing. Involvement of the habenula in dominance has not been studied in rodents so it is unclear whether the role in encoding own dominance status has been completely delegated to the prefrontal cortices in mammals or whether the habenula still serves a unique or perhaps redundant dominance function in higher vertebrates.

Returning to the rodent model, the dopaminergic system is also of interest due to the involvement of the nucleus accumbens (NAc), the ventral tegmental area (VTA), as well as prefrontal projections to these areas in dominance. The NAc has an interesting relationship between mitochondrial function and dominance. Namely, subordinates exhibit diminished mitochondrial function in the accumbens along with decreased neuronal excitability (Ghosal et al., 2023), while local mitochondrial inhibition using electron transport chain inhibitors reduces social rank (Hollis et al., 2015). Furthermore, projections from the infralimbic area (ILA), a subdivision of the mPFC, to the NAc enhance social approach behaviour (Fetcho et al., 2023). Similarly, in a social defeat paradigm higher NAc activity during social approach correlates with resilience to defeat (Willmore et al., 2022). Other work has shown that diazepam action in the VTA increases dopaminergic input to the NAc, which improves accumbal mitochondrial function through the D1 dopamine receptor and promotes dominant behaviour (van der Kooij et al., 2018). The VTA is reciprocally connected to the mPFC (Huang et al., 2020), which also expresses dopaminergic receptors and a functional segregation of dominance and subordinacy promoting neurons in the mPFC was identified based on the expression of either the D1 or D2 receptor respectively (Xing et al., 2022). These findings imply a feedback loop between the prefrontal cortices encoding rank and the dopaminergic circuitry encoding the salience and reward value of social stimuli. Figure 1.1 summarises these findings into a working circuit model.

1.5 Absence of sensory integration in the current circuit model

While efforts have been made to map some of the upstream inputs into the core thalamocortical mechanism (e.g., orbitofrontal cortex inputs to the MDT (Nelson et al., 2019)), the current circuit model offers no clear way for representations of own social status to interact with sensory information about the conspecifics. Hierarchical behaviour is highly contextual, meaning that the behavioural decision can vary drastically depending on whom an individual is competing against. The mouse

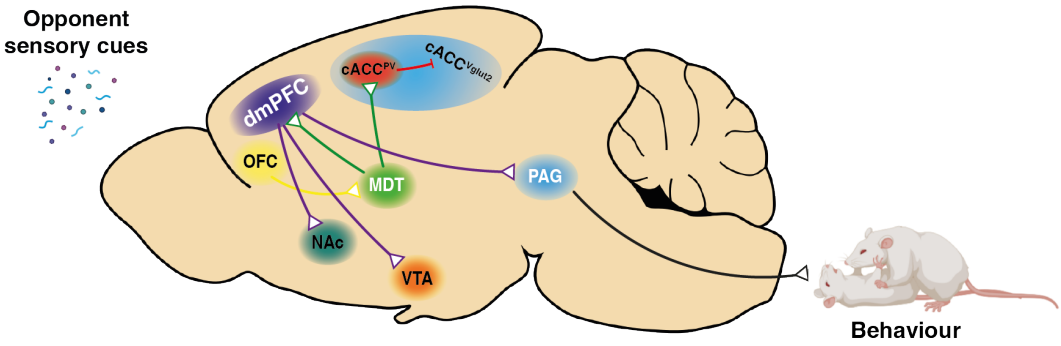

Figure 1.1: Current circuit model for encoding of own dominance rank in mice. MDT: mediodorsal thalamus. **dmPFC**: dorsomedial prefrontal cortex. **cACC^{PV}**: parvalbumin-expressing interneurons of the caudal anterior cingulate cortex. **cACC^{vglut2}**: vesicular glutamate transporter-expressing neurons of the caudal anterior cingulate cortex. **OFC**: orbitofrontal cortex. **NAc**: nucleus accumbens. **VTA**: ventral tegmental area. **PAG**: periaqueductal gray. Illustration created using BioRender.com.

with the same rank will withdraw from a scarce resource or assert its claim over it depending on the social status of any surrounding conspecifics. It is currently unclear what signals are used by rodents to detect the rank of conspecifics, where this variable is represented in the brain, and where it is integrated with representations of own rank. Furthermore, behavioural responses also depend on environmental context: In a scarce resource environment a mouse may yield preferential access to resources to a higher ranked conspecific, but there may be no need for that in a less constrained environment with plentiful resources. Rank therefore does not simply promote specific dominant or subordinate behaviours indiscriminately, at all times, and irrespective of social context. Understanding the way sensory inputs about social cues integrate with the existing dominance circuit is therefore crucial for understanding the situational flexibility of hierarchical behaviour. The following section describes the social perception circuitry in mice with a focus on candidate areas which might facilitate the encoding of conspecific social status.

1.6 Social perception in mice

Mice primarily use olfaction for social perception (Stowers et al., 2002; Dulac and Torello, 2003). For example, the ablation of vomeronasal sensory input through TRP2 (transient receptor potential channel 2) knockout results in the abolition of

conspecific sex discrimination (Stowers et al., 2002). This results in male sexual behaviour towards both male and female conspecifics and the absence of male-to-male aggression. Olfaction is therefore indispensable for adaptive social behaviour in mice. The murine olfactory sensory system is split into the main and accessory olfactory pathways as summarised in Figure 1.2 (Dulac and Wagner, 2006). The former begins in the olfactory epithelium where olfactory sensory neurons detect volatile odorants and project to the main olfactory bulb (MOB). MOB mitral cells in turn project to several areas, including the piriform cortex, the olfactory tubercle, the anterior cortical nucleus (ACN) and the entorhinal cortex. The ACN is a subdivision of the cortical amygdala that conveys olfactory information to the MPOA (Dulac and Wagner, 2006) and the medial amygdala (MeA) (Keshavarzi et al., 2015), which is activated in response to volatile cues in conspecific urine (Kang et al., 2009).

In contrast, non-volatile odorants which require direct contact of the animal with the odorant are detected in the vomeronasal organ (VNO). The VNO projects to the accessory olfactory bulb (AOB), which in turn projects to the bed nucleus of the accessory olfactory tract, bed nucleus of the stria terminalis (BNST), the MeA, and the posteromedial cortical amygdala (Dulac and Wagner, 2006; Imamura et al., 2020). The MeA therefore receives and integrates both volatile and non-volatile olfactory input (Kang et al., 2009; Keshavarzi et al., 2015). This amygdalar subdivision then projects to several hypothalamic targets, among them the MPOA and the VMH (Keshavarzi et al., 2014). The BNST, MeA, MPOA and VMH all have significant roles in regulating social behaviour (Chen and Hong, 2018). Furthermore, the MPOA (Kohl et al., 2018) and VMH (Lo et al., 2019) have onward connectivity to the brain stem, specifically the PAG at the behavioural execution end of the pathway, thus forming a social behaviour circuit from sensory input to behavioural outputs.

While the two olfactory pathways are initially segregated, there are a handful of subcortical areas, namely, the MeA, MPOA, and VMH, which receive input from both modalities. Since olfactory information passes through several nodes before reaching these three areas, they receive highly processed sensory input. This

is demonstrated in their tuning to abstracted variables relevant to social behaviour, for example, selective tuning for either male or female conspecifics (Li et al., 2017; Yang et al., 2022; Remedios et al., 2017). Additionally, these sensory representations are flexible depending on the animal's internal state. For example, sexual experience drives increased discriminability of female and male conspecific representations in the MeA and VMH (Yang et al., 2022; Remedios et al., 2017), while the hormonal changes associated with pregnancy in mothers increase the discriminability of pups from other social cues (Ammari et al., 2023). This also demonstrates that sensory representations in these areas are relatively low-dimensional since distinct social cues can be representationally highly similar in the absence of the appropriate motivational state (e.g., parental or sexual receptivity). This is in contrast with more high-dimensional representations of the sensory environment in upstream nodes of the pathway such as the main olfactory bulb, which are sensitive to small changes in the sensory stimulus (Cleland, 2014).

1.7 Evidence for rank-dependent modulation in the hypothalamus

Interestingly, the MPOA and VMH, which are two prominent downstream targets of both olfactory pathways, also exhibit evidence of modulation by own dominance status. A c-Fos study by Nelson et al. (2019) (Figure 1.3) found increased c-Fos expression in the VMH and decreased expression in the MPOA of high-ranking mice after a tube test, a dominance assay which forces non-aggressive competition between pairs of mice (Wang et al., 2011; Fan et al., 2019). This activation pattern was reversed in low-ranking animals. Additionally, dominant female mice have higher levels of estrogen alpha and beta receptors as well as oxytocin receptor mRNA in the VMH compared to subordinate females (Williamson et al., 2019), while subordinate male mice who newly assume a dominant role show elevated gonadotropin-releasing hormone levels in the MPOA (Williamson et al., 2017). Dominance research in Zebrafish also identified differences in the numbers of arginine vasotocin expressing (AVT^{+}) cells in the preoptic area (POA). There are more

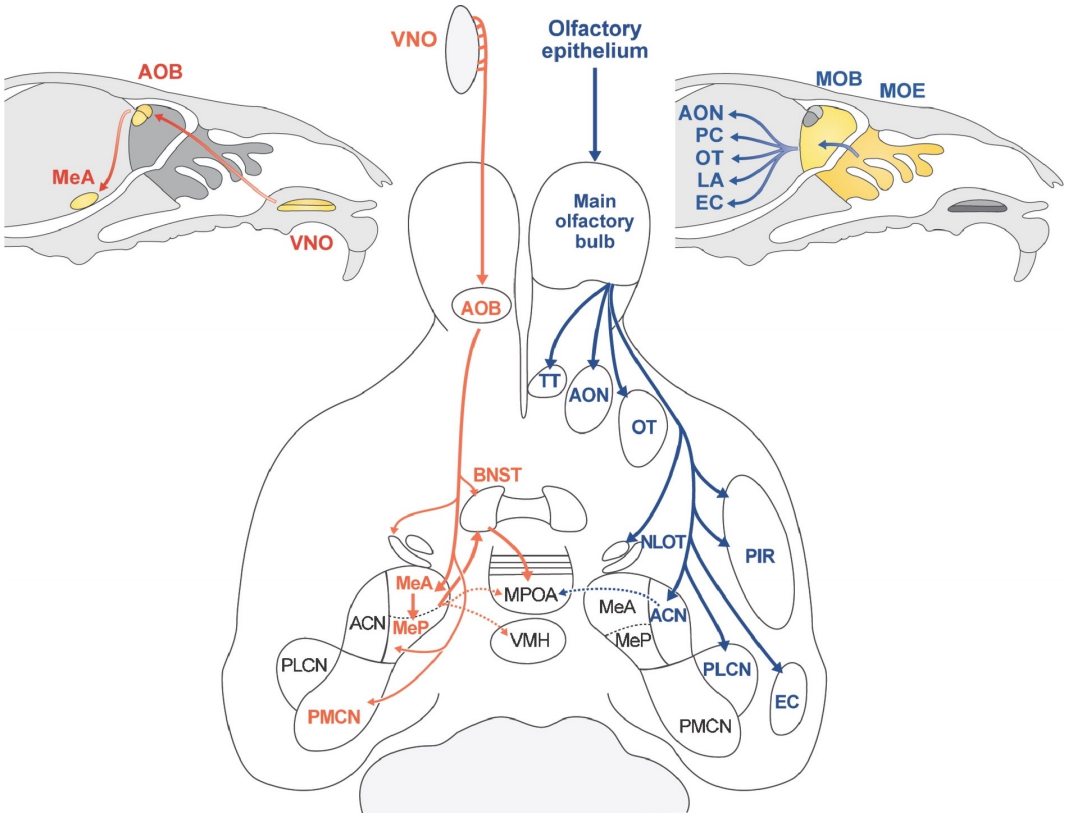

Figure 1.2: The projection patterns of the volatile and non-volatile olfactory systems in mice. Red arrows show the non-volatile (accessory) olfactory pathway, while blue arrows show the volatile (main) olfactory pathway. **VNO**: vomeronasal organ. **AOB**: anterior olfactory bulb. **BNST**: bed nucleus of the stria terminalis. **MeA**: medial amygdala. **MeP**: posterior division of the medial amygdala. **PMCN**: posteromedial cortical amygdaloid nucleus. **MOB**: main olfactory bulb. **MOE**: main olfactory epithelium. **TT**: tenia tecta. **AON**: anterior olfactory nucleus. **OT**: olfactory tubercle. **PC/PIR**: piriform cortex. **LA**: lateral amygdala. **NLOT**: nucleus of the lateral olfactory tract. **ACN**: anterior cortical nucleus. **PLCN**: posterolateral cortical amygdaloid nucleus. **EC**: entorhinal cortex. Adapted from Dulac & Wagner (2006).

AVT^+ cells in the magnocellular POA of dominant fish and more AVT^+ cells in the parvocellular POA of subordinate fish (Larson et al., 2006). This indicates a vasotocinergic mechanism to activate distinct subpopulations within the POA that could result in distinctly dominant and subordinate behavioural phenotypes. Another study in mice examined c-Fos expression in response to presented urine from dominant and subordinate male donors (Lee et al., 2021). Here the VMH showed differential expression depending on the rank of the urine donor, suggesting a sensory representation of the social status of conspecifics combined with modulatory influence from own rank in the same area. The following section therefore reviews the role of these two areas in social cognition in more detail, before discussing the implications of rank-dependent modulatory input for this function.

1.8 Functional features of the MPOA and VMH

The VMH is primarily a glutamatergic area (Lo et al., 2019), while the MPOA is approximately 80% GABAergic (Moffitt et al., 2018). The two nodes are reciprocally connected and drive social behaviours in a subpopulation-specific manner as demonstrated by manipulation experiments, while simultaneously exhibiting robust responses to social olfactory cues locked to chemoinvestigation episodes (Ammari et al., 2023; Remedios et al., 2017; Wu et al., 2014; Kohl et al., 2018; Karigo et al., 2021; Lin et al., 2011). Neuronal subpopulations with distinct functional features

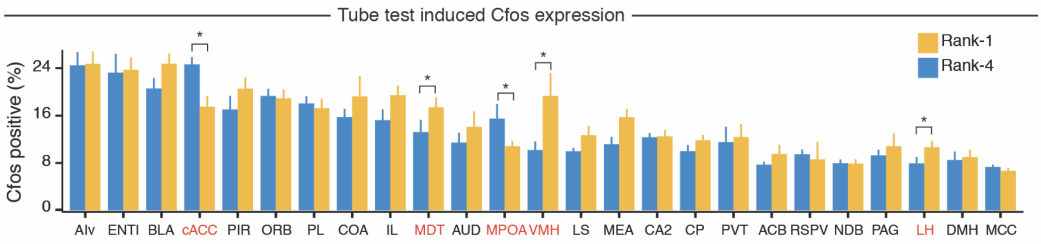

Figure 1.3: Differences in c-Fos expression between dominant (rank-1) and subordinate (rank-4) mice following the tube test. cACC: caudal anterior cingulate cortex. **MDT**: mediodorsal thalamus. **MPOA**: medial preoptic area. **VMH**: ventromedial hypothalamus. **LH**: lateral hypothalamus. Brain areas in red indicate statistically significant differences in c-Fos expression between dominant and subordinate mice. Linear mixed effects model with Tukey post hoc test, * $p < 0.05$. Adapted from Nelson et al. (2019).

in terms of sensory sensitivity and driving behaviour also have distinct projection patterns (Kohl et al., 2018; Wang et al., 2019), thus a single area can yield a wide repertoire of social behavioural responses.

Many examples of the state-dependence of innate social behaviours involve these two areas. In males, the VMH has been shown to encode a semi-stable defensive state (Kennedy et al., 2020) in its dorsomedial subdivision and an aggressive state (Lin et al., 2011; Nair et al., 2023) in its ventrolateral subdivision. It also encodes a sexually motivated state in both sexes (Ishii et al., 2017; Nomoto and Lima, 2015; Yang et al., 2013). Conversely, the MPOA encodes a hormone-dependent parental motivational state in females (Kohl et al., 2018; Ammari et al., 2023), while in males it is involved in sexual motivation through a dopaminergic signalling mechanism (Dominguez and Hull, 2005). Additionally, hormonal modulation of neurotensin-expressing MPOA cells was shown to regulate social approach (McHenry et al., 2017). These areas therefore contain both sensory and behaviour-tuned subpopulations susceptible to modulation by internal states. The prevailing model of their function in social cognition is therefore one of behavioural decision-making, where relevant sensory features about the conspecific are extracted (e.g., sex, age, familiarity) and integrated with the motivational state (e.g., sexual receptivity or aggressive state), in order to choose the best behavioural response.

1.9 Hypotheses

Evidence of rank-dependent modulatory input to the MPOA and VMH led to four main hypotheses. Firstly, the confluence of dominance-related modulatory input and olfactory sensory input in the hypothalamus suggests that the MPOA and VMH could serve as integration nodes for information about own and conspecific rank. Secondly, own dominance rank may be modulating the sensory representations in these areas, thus affecting the way conspecifics are perceived. Indeed, the poor social network and isolation reported by low-status individuals suggest that their inability or unwillingness to socially engage with others may be derived from a skewed perception of others as inherently threatening instead of rewarding. Thirdly,

due to the combined involvement of the MPOA and VMH in a wide repertoire of social behaviours and their causal role in the execution of these behaviours through projections to the PAG, their modulation by dominance status could be one mechanism for achieving a uniquely dominant or subordinate behavioural phenotype. While the direct mPFC-PAG projection proposed by Franklin (2017) provides a mechanism for the mPFC to affect behaviour more directly, it is specific to escaping an aggressive conspecific that has chronically attacked the defeated mouse. This is an unlikely scenario in most hierarchies since their purpose is to dispense with constant in-group conflict. In contrast, the hypothalamic modulation mechanism is more general in the number of behaviour types that can be affected. Additionally, the numerous subcortical projections of the mPFC could allow rank to modulate behaviour at multiple stages of social cognition in parallel. Finally, I propose that rank-dependent modulatory input in the hypothalamus is achieved through direct synaptic input from the mPFC.

1.10 Thesis overview

To test these hypotheses I first establish the validity of the behavioural dominance assay and document the rank-dependent behavioural differences in Chapter 3. I also investigate the sensory modality used to detect the rank of conspecifics through a series of sensory deprivation experiments. In Chapter 4, I proceed with cellular resolution miniscope recordings from the MPOA and VMH during free social behaviour in dominant and subordinate mice and demonstrate the rank-dependent modulation of social perception in these areas. I also correlate functional differences in neuronal excitability and tuning to behavioural differences between ranks. Chapter 5 investigates the information encoding properties of both hypothalamic areas. Specifically, I focus on decoding of own and opponent rank variables from neural activity, as well as the prediction of competitive performance from neural activity. Finally, I perform anatomical and manipulation studies to investigate the circuit basis of the proposed model (Chapter 6).

Chapter 2

Methods

2.1 Animals

All animals used in this project were from a C57BL/6J background obtained from The Francis Crick Institute Biological Research Facility. Male pups with the same date of birth were weaned directly into cages of four without subsequent addition or removal of animals to prevent disruption of the hierarchy. Mice remained group-housed for all experiments on a 12h:12h day/light cycle. All experiments were performed in mice between 8 and 52 weeks of age during the dark phase. Mice were shaved either on the left or right flank, above the tail, or upper back to easily distinguish them in top-down recordings. Food and water were available ad libitum except during water restriction protocols.

2.2 Behavioural profiling

2.2.1 Tube test

As described by Fan et al. (2019) the tube test was performed in a 30 cm long transparent plastic tube with an inside diameter of 30 mm. For mice with implants, tubes with a 10 mm gap along the length of the tube were used to accommodate the implant tether. The tether gap was widened at both tube ends to prevent mice from getting stuck while exiting the tube. Used tubes were cleaned with bleach

and 70% ethanol to remove olfactory stimuli after every test. Before testing, each mouse was trained for 2 days to enter the tube and pass through it alone 10 times. In testing sessions, mice were tube tested in a round-robin design, namely, every mouse against all of its cagemates. The order of the pairs was randomised for each session, including the side of the tube on which each mouse was inserted. Hierarchies were considered stable when the dominant and subordinate mice exhibited consistent tube test outcomes for at least 3 consecutive days.

2.2.2 Elo rating

Given that all mouse pairs were tested in a round-robin design, it was not necessary to consider data sparsity or under sampling of a particular animal, hence the Elo rating was chosen as the scoring system that converts binary tube test outcomes to continuous scores and by extension hierarchical rankings (Elo, 2008). In the Elo rating system, all animals begin with the same number of points (here 1000), which they win or lose from each other through tube tests. The score of mouse A is updated after a tube test based on the following update rule:

$$R'_a = R_a + K(E_a - S_a)$$

Where R_a and R'_a are the existing and updated scores of mouse A respectively, K (set to 100) is the scaling factor determining the maximum number of points transferred from loser to winner in a single match, E_a is the expected match outcome and S_a is the actual outcome. S_a is either 0 or 1 indicating a loss or win for mouse A, while E_a is a real number between 0 and 1. The expected outcome of the match is a probability measure determined based on the existing score difference between the two mice:

$$E_a = \frac{1}{1 + 10^{((R_b - R_a)/400)}}$$

Where R_a and R_b are the current Elo scores of mice A and B respectively. This system results in more points being transferred when the match outcome is unlikely, namely, when the winner has a lower score than the loser. When the expected and actual outcomes are identical, no points are transferred.

2.2.3 Hierarchy stability metrics

While the Elo rating allows the mice to be ranked based on tube test outcomes, it does not indicate whether they are always winning and losing against the same opponents, which is crucial for evaluating the stability of the hierarchy. For this, the following measures were used: The consistency index measures the proportion of opponent pairs that had the same tube test outcome as in the previous testing session. It therefore ranges from 1 when all tests in the round robin had the same outcome as the previous session and 0 when all tests are inconsistent with the previous session. The stability index was adapted from work by Neuman et al. 2011 as a measure of rank changes per individual over a rolling 2-day window. Formally, it is the sum of absolute rank changes (C) between two consecutive testing days d and $d+1$ weighted by the standard Elo rating of the highest-ranking animal involved in a rank change (w) and divided by the total number of animals in the hierarchy (N):

$$S = \frac{(C_d + C_{d+1}) * w}{N}$$

The standard Elo score scales the score of an animal to the interval $[0,1]$ where 0 and 1 are the lowest and highest scores of any animal in the hierarchy respectively. This weighting captures the finding that rank changes at the top of the hierarchy are much more disruptive to the overall stability of the group compared to rank changes among lower-ranked members. Finally, transitivity is a binary metric with a value of 1 when the hierarchy is linear and does not have loops such as $A > B, B > C, C > A$, and 0 otherwise.

2.2.4 Water competition assay

Mice with stable tube test hierarchies and known Elo scores were habituated to drinking water delivery via bottle for 1 week. A custom bottle collar was designed, which only allowed one mouse at a time to drink from the bottle. After the habituation, the bottle was removed and the mice were water-deprived for 12 hours. Food remained available ad libitum. After 12 hours of water restriction, the water bottle was reintroduced and the behaviour was recorded for 10 minutes. For each mouse,

I quantified the total time spent drinking in seconds, and the latency until the first drinking episode from the introduction of the water bottle. Additionally, pushing success was defined as the proportion of successful attempts to push another mouse away from the drinking spout and occupy it, while resisting push success was defined as the proportion of pushing attempts by other mice that were successfully resisted so that the spout occupant did not change.

2.2.5 Winner effect modelling

A winner effect entails that winning a tube test increases the probability of winning the next test. This would increase the likelihood of consecutive wins (and consecutive losses) compared to outcome switches. The expected proportion of consecutive outcomes and outcome switches in a linear hierarchy without a winner effect was simulated empirically. Consecutive outcomes in a round-robin design with any number of players are twice as frequent as outcome switches, irrespective of the number of animals in a hierarchy. This was used as the null distribution indicating the absence of a winner effect, against which the actual frequency of consecutive outcomes was tested using a Chi-square goodness-of-fit test.

2.2.6 Resident-Intruder test

Mice found to be dominant or subordinate in the tube test were individually tested for aggressive behaviour in the home cage while the cagemates and enrichment objects were removed. The resident mouse was habituated in the recording chamber for 10 minutes, followed by an introduction of a middle-ranked unfamiliar intruder mouse from another cage. The mice were allowed to freely interact for 10 minutes before the removal of the intruder.

2.2.7 Sexual behaviour assay

Testing of sexual behaviour was performed as the resident-intruder test with a female intruder. However, due to difficulties in observing robust sexual behaviour - perhaps because the males were virgins - a few variations of sexual receptivity priming before the assay were trialled: Firstly, the swapping of soiled bedding between the male and female cages for one or more days before the test reportedly

increases sexual receptivity known as the Whitten effect (Whitten, 1956). Since that approach was unsuccessful in enhancing sexual behaviour, hormonal priming of ovariectomised females as reported by Inoue et al. (2019) was trialled next. This involves the subcutaneous injection of 10µg 17-ß estradiol benzoate (Sigma-Aldrich) in 100 µl sesame oil (Sigma-Aldrich) 2 days before the assay, 5µg 17-ß estradiol benzoate in 50µl sesame oil 1 day before the assay, and 50µg progesterone benzoate (Sigma-Aldrich) in 50µl sesame oil on the day of the assay.

2.2.8 Social preference test

Social preference testing was performed in a 3-chamber design, where the tested mouse occupies the middle chamber (l*w 40*23 cm) flanked by two smaller chambers (l*w 10*23 cm), one containing an inanimate object and the other containing a middle-ranked unfamiliar conspecific on the other (Figure 2.1). The walls were made of transparent plastic, however, a mesh gate (l*h 100*50 mm) between the main chamber and the two stimulus chambers allowed the passage of olfactory stimuli. The recorded mouse was placed in the middle chamber and allowed to explore without the stimuli present for 10 min. Afterwards, both the object and the conspecific were simultaneously placed in the smaller side chambers for 10 minutes. The chamber was cleaned with 70% ethanol between tests to remove olfactory stimuli while the locations of the object and conspecific were alternated to prevent the accumulation of social odorants on one side of the testing chamber. The floor of the chamber was white to allow automated location tracking of the black mouse using image thresholding in the Ethovision software (Noldus). 5cm zones around the gates with the object and the conspecific stimulus were defined in addition to a neutral zone in the middle of the chamber. The percentage of total assay time spent in these zones was calculated.

2.2.9 Behavioural Analysis

All behaviour was recorded using a top-down infrared high-speed camera (Basler Ace GigE, acA 1300-60gmNIR). Behavioural recordings were manually annotated using the BORIS software (Friard and Gamba, 2016), specifically the first contact

and episodes of chemoinvestigatory sniffing, anogenital sniffing, grooming, attack, and sexual mounting. The first two categories were merged into a single chemoinvestigation behaviour. In the case of tube tests, the entire test period was annotated along with the first contact and episodes of pushing, resisting and retreating. Behaviour duration was defined as the percentage of time spent performing a particular behaviour. Behaviour length was defined as the mean behavioural bout duration in seconds. Behavioural frequency was calculated as bouts per minute. Behavioural metrics for resident-intruder assays were quantified in a 90-second window after the introduction of the conspecific (i.e., excluding the 1-minute baseline period). This is because mice have the strongest motivation to interact with the intruder just after first contact, but they become habituated later in the assay and return to baseline behaviour of mostly exploring the cage. Figure 2.2 shows the duration of chemoinvestigation of female intruders evaluated over several time windows from intruder introduction. Engagement with the intruder drops towards the end of the assay in both dominants and subordinates, which diminishes rank-dependent behavioural in social engagement observed just after intruder introduction. 90 seconds is a time window where mice exhibit peak rank-dependent differences in behaviour. This habituation factor is not relevant in the tube test, hence tube test behaviours were evaluated over the entire test period.

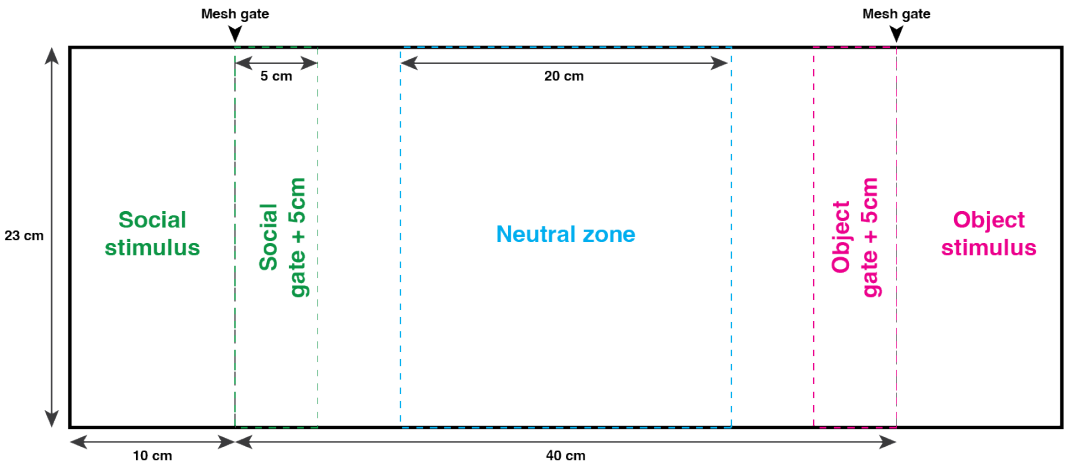

Figure 2.1: Diagram of the three-chamber social-preference assay.

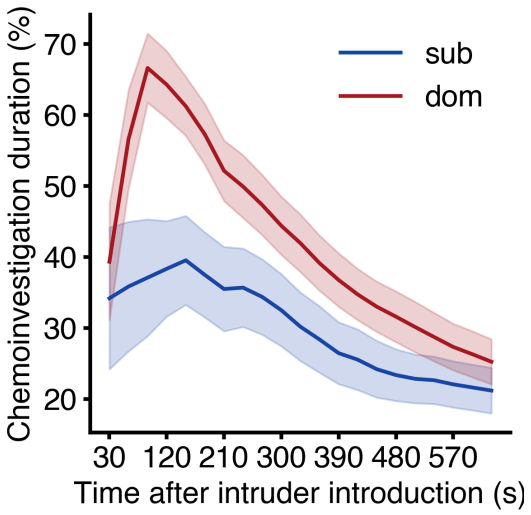

Figure 2.2: Rank-dependent differences in chemoinvestigatory behaviour over different time windows from intruder introduction. Error shading represents ± SEM.

2.3 General surgical procedures

Mice were administered preoperative analgesia (0.15 ml Carprofen in 200 ml drinking water) one day before surgery and for 2 days following the surgery. Anaesthesia was induced using 4% isoflurane and maintained at 1.5% isoflurane in oxygen-enriched air. The head was fixed using a stereotaxic frame (Model 940, Kopf Instruments). Meloxicam (10 mg/kg body weight) and Buprenorphine (0.1 mg/kg body weight) were administered by subcutaneous injection after induction and prior to the procedure. The relevant skin area was disinfected with chlorhexidine and surgery was performed aseptically. Body temperature was maintained at 37°C using a rectal temperature probe and heat pad (Harvard Apparatus). Eyes were protected using an ophthalmic ointment (Viscotears, Alcon). The skin was closed using Vicryl sutures (Ethicon). Mice were recovered in a heated recovery chamber until mobile.

2.4 Sensory deprivation

2.4.1 Castration

Both testes were aseptically removed via the scrotal approach in groups of males with determined hierarchies (Guilmette et al., 2015). All males in a cage were castrated on the same day and group-housed immediately after recovery. Castration surgeries were performed by Sophie Wood (The Francis Crick Institute Biological Research Facility).

2.4.2 Olfactory ablation

The olfactory epithelium was ablated using intraperitoneal injection of 100 mg methimazole (Cambridge Bioscience Ltd.) per kilogram of body weight (Håglin et al., 2021). Methimazole was prepared fresh on the day of injection as a 10 mg/ml solution in sterile water for injection. Hierarchy generalisation was tested 24 hours after injection. Methimazole injection at this dosage often causes some temporary weakness and lack of activity for the animal which could interfere with normal tube test behaviour. A subcutaneous injection of meloxicam (10 mg/kg body weight) and buprenorphine (0.1 mg/kg body weight) as analgesia an hour before behavioural testing successfully abolished any adverse effects of methimazole on behaviour.

Vomeronasal input was ablated through a bilateral stereotaxic injection of 130 nl of N-methyl-D-aspartate (Cambridge Bioscience Ltd.) into the accessory olfactory bulb (AOB) adapted from the procedure reported by Erskine et al. (2019) (Erskine et al., 2019) for total olfactory bulb ablation. AOB injection coordinates: AP 3.1, ML 1.00, DV 1.75. NMDA was prepared as a 10 mg/ml solution in 1% PBS. Mice were recovered for 3 days after surgery before behavioural testing. For combined vomeronasal and olfactory ablation the NMDA injection was performed first, followed by intraperitoneal methimazole injection after the 3-day surgery recovery period and subcutaneous analgesia an hour before testing.

2.4.3 Nose H&E staining

Mice were sacrificed by pentobarbital overdose (100 mg/kg body weight) and perfused with formalin. The heads were stored in formalin for 12h at room temperature. The heads were dissected keeping only the bony nasal cavity. The tissue was washed with PBS 3 times and kept in 10% EDTA (in PBS) at 4°C for decalcification, followed by 3 more PBS washes. Samples were dehydrated, embedded in paraffin wax and cut into 2–4 μm thick transverse sections using a Leica CM1950 cryostat and stained with Haematoxylin-Eosin following the standard protocol (Feldman and Wolfe, 2014). H&E histology was performed by Paula Rodriguez Villamayor.

2.4.4 Nissl staining

Mice were sacrificed by pentobarbital overdose (100 mg/kg body weight) followed by transcardiac perfusion with 4% paraformaldehyde (PFA) in PBS. Brains were dissected from the skull and kept in 4% PFA overnight. PFA was removed and the brains were washed with fresh PBS 3 times before slicing at 60μm thickness using a vibratome. Olfactory bulb vibratome slices were washed in 1% PBS with 0.1% Triton-X (Sigma-Aldrich) for 5 minutes, followed by two washes in 1% PBS for 5 minutes each. Slices were protected from light from this step onward. Neurotrace Nissl stain (Thermo Fisher N21482, 1:100 dilution in PBS) was applied for 10 minutes, followed by two more PBS washes for 5 minutes each. All steps were performed at room temperature. Slices were mounted on Superfrost slides (Thermo Fisher Scientific) using the Vectashield mounting medium with DAPI (Vector Laboratories Inc.). Slices were imaged using the Vectra Polaris (Akoya Biosciences) slide scanner and Zeiss LSM 710 confocal microscope.

2.5 Calcium imaging

2.5.1 Surgery

A stereotaxic craniotomy was performed. Mice were injected with 300 nl of AAV1-Syn-jGCaMP7s-WPRE (Addgene 104487) using a glass pipette. Injection coordinates: MPOA (AP 0, ML 0.5, DV 5.05), VMH (AP -1.5, ML 0.78, DV -5.8), MeA

(AP -1.6, ML 2.25, DV 4.95). The gradient index (GRIN) lens (600μm diameter, 7.3mm length) with attached baseplate (Inscopix Inc.) was implanted 0.2mm ventrally from the injection site. The implant was cemented in place using UV dental cement (RelyX Unicem, 3M) followed by Superbond dental cement (Prestige Dental). The skin was sutured tightly around the implant.

2.5.2 Assays

The recorded mouse was habituated in its home cage with the cagemates and enrichment removed for 20 minutes after mounting of the miniscope. A 1-minute baseline recording was acquired before the introduction of any stimuli, for the subsequent calculation of the change in fluorescence relative to baseline. Home cage interaction with an unfamiliar male and female intruder was recorded for 10 minutes. The male intruder was a confirmed rank 2 mouse (just below the dominant). The female intruders were freely cycling and were therefore in a random estrus state on the day of the recording. Following the male and female intruder assays, at least three tube tests against the same unfamiliar intruder were recorded using an adapted tube that accommodates miniscope tethering. The baseline for tube tests was also recorded in the home cage. The recorded mouse was returned to the home cage between every tube test. The entry side of the tube was alternated for each test.

For the opponent rank decoding dataset, an adaptation of the above assays was used. In the resident-intruder paradigm, 3 cages of 4 mice with known hierarchies were introduced sequentially into the recorded resident's home cage. This resulted in four rank labels for the opponent rank decoder. The order of intruder presentation was randomised to avoid decoding based on signal decay over time. Intruders were in the resident's cage for 90 seconds, followed by a 60-second rest period between intruders. After the first round of presentations (12 intruders) was completed, there was a 20-minute break, followed by the second round of presentations. In the tube test version of this paradigm, the two mice determined the duration of interaction and were separated after every test - the recorded mouse was returned to the home cage. The same 20-minute rest period between presentation rounds was used.

For the anaesthetised presentation paradigm, urine was collected from the intruders by scruffing them over a grate with a petri dish positioned below. This prevents the urine from being immediately absorbed into the animal's fur. The urine was stored at -20°C if not used immediately. The recorded mouse was injected intraperitoneally with 100 mg/kg body weight ketamine and 10 mg/kg body weight xylazine. The righting and pedal reflexes were used to confirm unconsciousness and recording began 15 minutes after injection. A urine sample for each intruder was presented sequentially by dipping a disposable applicator brush into the urine and presenting it to the recorded mouse's nose without touching the nose for 3 seconds. A fresh brush was used for each urine sample. Following completion of the assay, mice were monitored until full recovery from anaesthesia.

2.5.3 Imaging

Implanted mice were imaged 8 weeks after surgery at the earliest to allow satisfactory calcium indicator expression as well as clearance of any inflammatory response around the lens, which reduces image quality. Calcium recordings were acquired using the nVista system (Inscopix Inc.) and the associated acquisition software at 20 Hz using 475nm LED light. The power was individually adjusted between 0.1 and 0.3 mW / mm^2 based on the calcium indicator expression in each animal to obtain a good dynamic range without saturation. Miniscope acquisition was synchronised with behavioural video recording using a custom workflow in the Bonsai Software (Neurogears).

2.5.4 Histology

Mice were sacrificed by pentobarbital overdose (100 mg/kg body weight) followed by transcardiac perfusion with 4% PFA in PBS. Brains were dissected from the skull and kept in 4% PFA overnight. PFA was removed and the brains were washed with fresh PBS 3 times before slicing at 60μm thickness using a vibratome. Slices were air-dried onto SuperFrost Plus adhesion slides (Thermo Fisher Scientific) and mounted using the Vectashield mounting medium with DAPI (Vector Laboratories Inc.). Slides were imaged using the Vectra Polaris (Akoya Biosciences) slide scan-

ner. Histological imaging was used to determine whether the lens was implanted in the desired area, as well as to confirm there were no obvious signs of cell death in the imaged area based on cell morphology and the presence of cellular debris.

2.5.5 Calcium recording preprocessing

The signal from calcium recordings was preprocessed using the Inscopix Data Processing Software (Inscopix Inc.). Recordings were spatially and temporally downsampled to half the original resolution and to 10 Hz. Rapid noise signal and slow drift in signal (e.g. due to bleaching) were removed using a spatial bandpass filter with a lower threshold of 0.005 oscillations per pixel and an upper threshold of 0.5 oscillations per pixel. Motion correction was performed followed by signal normalisation to mean fluorescence during the baseline period (F_0): $\frac{\Delta F}{F_0} = \frac{F - F_0}{F_0}$. PCA-ICA based automated cell detection was performed, followed by manual curation of the resulting cell-set.

2.5.6 Evoked activity analysis

Manual behavioural annotations were used to extract PSTHs (peristimulus time histograms) surrounding a behavioural event. Each PSTH was comprised of a 2-second baseline period before the start of the behavioural event and a 2-second response period following behaviour initiation. Magnitude differences between neural responses in dominants and subordinates were tested using the z-scored response section of the PSTH. Z-scoring of the PSTH activity samples (x) was performed by using only the baseline phase to compute the mean (μ) and standard deviation (σ) of the fluorescence signal and then scaling the entire PSTH: $z = \frac{x - \mu}{\sigma}$. To obtain a single-value estimate of the response amplitude for each cell, the absolute area under the curve (AUC) of the response phase of the PSTH was calculated. Amplitude AUCs were Poisson distributed, so a log transform was applied to normalise the distribution. Tuning to a behavioural event was determined for each cell through an independent t-test between the baseline and response sections of the PSTH surrounding that behavioural event (without prior z-scoring). Statistical significance at the 5% level indicated a tuned cell, whereas the sign of the t statistic indicated

whether it was positively or negatively tuned. The t statistic was also used as a continuous tuning index. The first contact with a social stimulus resulted in the most robust and highest amplitude neural responses, followed by rapid desensitisation during subsequent chemoinvestigations. The first contact responses were therefore used for tuning and response amplitude analyses, as well as the decoding of intruder rank.

2.6 Modelling

Logistic regression classifiers, support vector machine classifiers, principal component analysis, partial least squares, as well as all cross-validation and scoring procedures were implemented using the Scikit-learn Python package. The implementation details for representational similarity analysis, canonical correlation analysis and autoencoders are detailed below. Activity recordings were standardised before any machine learning model training. Standarisation removes signal magnitude differences between features (cells), by subtracting the mean feature signal and scaling to unit variance: $z = (x - \mu)/\sigma$, where μ is the mean signal and σ is the standard deviation.

2.6.1 Representational similarity analysis

RSA was implemented using the RSAtoolbox Python package reported by Nili et al. (2014). For each recorded mouse, PSTHs evoked by chemoinvestigation of male and female intruders were extracted. The baseline phase of the PSTH was discarded, while the response phases were stacked into a single M x N x O matrix, where M were conditions (i.e. male intruder, female intruder), N were cells and O were timepoints. This matrix was used to initialise the RSAtoolbox *Temporal-Dataset* class. The time dimension was converted into additional samples of the existing conditions (e.g. female intruder representation at time t, t+1, ... t+n) using the *convert_to_dataset* method. The dissimilarity matrices between conditions were then calculated using the Euclidean distance metric. The average Euclidean distance across time points was reported as the representational dissimilarity between male and female encodings for each mouse.

2.6.2 Logistic classifier

A logistic classifier is a generalized linear model with a logistic (sigmoidal) linker function, which is used to predict a binary dependent variable, such as discreet classes. The linear part of the model is equivalent to multiple linear regression:

$$Y = \beta_0 + \beta_1 X_1 + \beta_2 X_2 + ... + \beta_n X_n$$

Where Y is the dependent variable, X are observations for n regressors and β are the estimated parameters which linearly scale the contribution of each regressor. This gives continuous values for $Y \in \mathbb{R}$, which is transformed using the sigmoidal function to obtain an estimate of the probability of a class between 0 and 1:

$$S(Y) = \frac{1}{1+e^{-Y}}$$

The Scikit-learn implementation of the logistic classifier fits a separate logistic model for each of the data classes and uses the class with the highest probability as the model prediction for a given observation. A predictive weight β is fit for each neuron in the behavioural decoders reported in Chapter 5. The weights of the tube test outcome decoder in particular were used as an estimate of whether (and how strongly) a neuron is associated with winning compared to losing in the tube test. These estimates were correlated with each neuron's tuning preference to social stimuli.

2.6.3 Ordinal logistic classifier

Given ordinal labels $j = 1, 2, 3, ...J$, the ordinal adaptation of the logistic classifier estimates the cumulative probability that the prediction Y is j or lower:

$$P(Y \leq j|X) = \frac{1}{1+e^{-(\theta_j - (\beta_1 X_1 + \beta_2 X_2 + \ldots + \beta_k X_k))}}$$

In addition to feature loadings β, the set of thresholds θ_j for each label j is also estimated. The probability of a specific label j is estimated as the difference in cumulative probabilities for label j and the ordinal category below it, $j-1$:

$$P(Y = j|X) = P(Y \leq j|X) - P(Y \leq j-1|X)$$

The label with the highest estimated probability is selected as the model prediction.

2.6.4 Competitive behaviour prediction

Logistic classifiers were used for predicting the tube test context, winning/losing and push/retreat/resist behaviours. For tube test context prediction, activity data from the entire recording was used, whereas for prediction of tube test winning and push/retreat/resist behaviours the recordings were first segmented to discard the intervening home cage sections, followed by concatenation of these segments into a single continuous activity recording. Activity data was standardised before entry into the model. The model was implemented using $l2$ regularisation with regularisation parameter $C = 1.0$. The mean performance was evaluated using 5-fold cross-validation using a stratified K-fold data splitting procedure. Since activity samples close in time are similar and therefore cannot be considered completely independent, sample shuffling before splitting was not performed to avoid data leakage between the training and testing datasets.

2.6.5 Canonical correlation analysis

For two datasets X, Y with unequal dimensionalities, CCA linearly projects both datasets into a common coordinate space (Hotelling, 1936). For each dimension j of this common space, there is a pair of canonical weight vectors a_j, b_j, which linearly project the original datasets into the latent space. The projections of the two datasets are known as canonical components $u_j = \langle a_j, X \rangle$ and $v_j = \langle b_j, Y \rangle$ for canonical dimension j. CCA optimises the common space so that the canonical components are maximally correlated:

$$\rho_j = max \frac{\langle u_j, v_j \rangle}{\| u_j \| \| v_j \|}$$

The concept can be extended to an arbitrary number of datasets. The CCA model was implemented using the Python package PyRCCA reported by Bilenko & Gallant (2016) (Bilenko and Gallant, 2016). Fitting was performed on activity evoked by the chemoinvestigation of a female intruder. A PSTH with a 2-second window before and after the first episode of chemoinvestigation was extracted for each recorded mouse. CCA can simultaneously function as a dimensionality reduction method, since the common latent space of two datasets is limited by the dataset with the lowest number of features, in this case, cells. The smallest recording contained 7 cells, which was therefore set as the desired number of CCA components. PyRCCA implements a regularised form of CCA, where an $l2$ penalty is applied to the canonical weights. The optimal regularisation parameter was cross-validated such that the cross-animal Pearson correlations were maximised in the testing fold. The optimal regularisation parameter was $C = 5$, which was used for all reported CCA models.

2.6.6 Intruder rank classifier

Calcium recordings were first segmented to extract the 2-second PSTH from the first contact with each intruder. These first contact episodes were concatenated into a single dataset and standardised. The dimensionality reduction method was applied to the dataset with the best 3 latent components retained. For the supervised dimensionality reduction method (i.e., partial least squares), the intruder ranks were used as the supervising sample labels. The reduced dataset was used to evaluate the opponent rank classification performance of a logistic regression model using 12-fold cross-validation and either a stratified K-fold or leave-one-group-out data splitting procedure. $l2$ regularisation with the regularisation parameter set to $C = 1.0$ was applied to the fitting of the logistic model.

The autoencoder was a custom implementation using the Keras Python package. It was comprised of symmetrical encoder and decoder blocks, separated by a 3-neuron bottleneck layer. Both blocks had input and output layers with dimensionality equivalent to the number of cells in the dataset and 4 hidden layers. The dimensionality of the hidden layers was linearly interpolated between the sizes of

the input and bottleneck layers. All layers except the input and output layers had ReLU activations. The loss was the mean squared error between the input and output layer activations. Autoencoders were trained over 20 epochs of training using a batch size of 32 samples. Following training, the activations of the bottleneck layer were extracted for each of the dataset samples to obtain an activity signal reduced to 3 dimensions.

2.6.7 Model evaluation

2.6.7.1 Weighted F1 score

Since the number of samples from different classes was uneven for most datasets (e.g. a mouse does not spend the exact same amount of time winning and losing tube tests), the weighted F1 score was used to avoid overestimating the performance of a model which always simply predicts the most frequent class. The F1 score ranges ($F1 = \frac{2*P*R}{P+R}$) between 0 and 1 and includes the precision of the model ($P = \frac{True\ positives}{True\ positives+False\ positives}$) as well as recall ($R = \frac{True\ positives}{True\ positives+False\ negatives}$). Precision measures the accuracy of the positive predictions, whereas recall measures the ability of the model to predict all positive instances of a class. The weighted F1 calculates the F1 score for each of the classes i and weights it by the frequency of each class (w) before obtaining the mean F1 score across all classes: $F1_{weighted} = \frac{\sum_i w_i * F1_i}{\sum w_i}$. The weighted F1 performance of the models was statistically compared to the performance of the same model trained on shuffled class labels. The mean shuffled performance was estimated by performing 100 permutations of the target labels.

2.6.7.2 Ordinal mean absolute error

The ordinal mean absolute error evaluates the mean absolute difference between the true and predicted values of a target ordinal variable Y for samples i:

$$\sum_{i=1}^{N} \frac{||(Y_{true_i} - Y_{pred_i})||}{N}$$

2.7 Viral tracing

Mice underwent stereotaxic craniotomy and were injected with 100 nl of AAV2-CB7-CI-eGFP-WPRE-rBG (AddGene 105542) unilaterally in either the dorsomedial prefrontal cortex (AP 2.43, ML 0.52, DV 1.27) or caudal anterior cingulate cortex (AP 0.65, ML 0.17, DV 0.95). 2 weeks after surgery was allowed for satisfactory viral expression. Mice were subsequently sacrificed by pentobarbital overdose (100 mg/kg body weight) followed by transcardiac perfusion with 4% PFA in PBS. Brains were dissected from the skull and kept in 4% PFA overnight. PFA was removed and the brains were washed with fresh PBS 3 times before slicing at 60μm thickness using a vibratome. Slices were air-dried onto SuperFrost Plus adhesion slides (Thermo Fisher Scientific) and mounted using the Vectashield mounting medium with DAPI (Vector Laboratories Inc.). Slides were imaged using the Zeiss Axioscan slide scanner (PL and cACC injections) or the Vectra Polaris (Akoya Biosciences) slide scanner (ILA injections).

2.8 Optogenetics

All mice from cages with known hierarchies underwent craniotomy with bilateral stereotaxic injection of 125 nl of AAV5-hSyn-hChR2(H134R)-EYFP (Addgene 26973) into the infralimbic area (AP 1.7, ML 0.4, DV 2) and implantation of a dual fibre-optic cannula (Doric) into the MPOA (AP 1.7, ML 0.4, DV -4.9) or VMH (AP -1.5, ML 0.5, DV -5.6). Mice were habituated in the home cage for 10 minutes after tethering of the implant to the patchcord with all cagemates and enrichment objects removed. Each mouse individually underwent tube tests against all of its cagemates with and without optostimulation. The patchcord was tethered to the mouse in both conditions. The stimulated mouse was returned to its home cage after every tube test. The stimulation protocol was based on work by (Padilla-Coreano et al., 2021), namely, patterned stimulation at 100 Hz with a duty cycle of 0.9 at 10 mW (5 mW per fibre). The actual light power coming through the implant was measured before the experiment. The order of the light on and off conditions was alternated for each mouse.

2.9 Statistics

Statistical analysis and plotting were performed using GraphPad Prism (GraphPad Software) and custom Python scripts. Wherever multiple data were derived from the same animal, for example, multiple cells from the same recording, a mixed effect GLM was used to control for the correlations between data derived from the same source. In all instances of mixed effects GLMs in the thesis, the animal ID was used as the random effects variable. References to a controlled variable mean that a variable was included in a linear model (including special cases such as ANOVAs) as a regressor in addition to the variable of interest. Thus any effect found for the variable interest cannot be attributed to the controlled variable. This was used to control for any differences between the MPOA and VMH when evaluating the behavioural decoders in Chapter 5 and optogenetic effects in Chapter 6. Significance labels indicate $p > 0.05 : n.s., p < 0.05 : *, p < 0.01 : **, p < 0.001 : ***, p < 0.0001 : ****$.

Chapter 3

Behavioural characterisation of mouse social hierarchies

3.1 Introduction

This chapter validates that stable and linear hierarchies can be determined as described in the literature and that the behavioural differences between ranks reported elsewhere can be replicated using our animals and experimental setups. I also extend previous work by investigating the ability of mice to generalise their rank from their usual social group to interactions with completely unfamiliar mice and investigate the sensory modality used to detect the rank of unfamiliar opponents.

Several behavioural tests to determine rodent social hierarchies have been developed. Early tests relied on the examination of dyadic interactions in the home cage or open field setting, with a particular focus on aggressive and defensive behaviours to determine the winner and loser in each pair (Machida et al., 1981). These approaches implicitly assume that aggressiveness reliably correlates with hierarchical status in rodents, however, recent studies have found no such relationship (Zhou et al., 2017; Nelson et al., 2019). Presumably, the purpose of the hierarchy is to dispense with the need for constant in-group conflict.

More recent approaches have therefore focused on competition for scarce resources, such as the hot spot test. In these assays a reward such as a warm spot on the floor of a cold enclosure can only be accessed by one mouse at a time, thus exposing the hierarchy by measuring which animals have preferential access to that resource. The entire group can be tested at once with these assays and recreates a naturalistic problem which has evolutionarily been solved through hierarchies. Nevertheless, these assays require significant behavioural annotation which is inconvenient in research settings and can result in ambiguous hierarchy inference depending on the behavioural metric that is chosen. For example, one mouse may be the dominant based on the latency until warm spot occupancy, but another may be the dominant based on the duration of the warm spot occupancy.

The tube test provides an alternative to these naturalistic assays by providing a binary win-lose outcome through dyadic interactions. As described by Fan et al. (2019) two mice are inserted into the opposite ends of a tube that is too narrow for an adult mouse to turn around. They are therefore forced to walk forward into the tube where they meet the other mouse. In turn, the more dominant mouse pushes its opponent out of the tube. By testing every pair of mice in a group using a round-robin design, a binary winner outcome is obtained for each pair. These outcomes can then be converted into continuous dominance scores for each mouse using scoring systems such as the Elo rating (Elo, 2008) used for ranking chess players. While this test might be less naturalistic, it dispenses with behavioural annotation, can be performed quickly with simple materials, and provides an unambiguous hierarchy as long as the test outcomes for the same mouse pairing are consistent. Furthermore, hierarchies inferred using the tube test correlate well with those inferred from naturalistic reward competition assays (Wang et al., 2011). The usefulness of the tube test as a dominance readout is validated in this chapter for use in subsequent experiments.

While the tube test is a paradigm which forces a competitive confrontation between two animals in an effort to expose a binary hierarchical relationship, social status also affects behaviour in more benign social interactions. There has been a particular focus in the literature on aggression, sexual behaviour, and anxiety. Many have found significant effects, however, there are studies claiming contradictory findings in all of these categories (Varholick et al., 2021). This may be because dominance-related behavioural differences have been shown to vary based on group dynamics, especially hierarchical stability as well as the size of the group (Williamson et al., 2017). These factors can lead to a reversal of the behavioural correlates of dominance, for example, in stable hierarchies subordinates show higher anxiety than dominants, but the reverse is true in unstable hierarchies (Williamson et al., 2017). Some of these crucial factors may not be immediately obvious, hence it was suitable to document the concrete behavioural differences that appear in our mice and experimental environment, before proceeding with the investigation of the neural basis of any such differences in the coming chapters. I focus in particular on aggression towards unfamiliar males, chemoinvestigatory interest in females, and affinity for social interaction.

3.2 Validation of the tube test assay

Three metrics were used to evaluate the quality of the hierarchies obtained using the tube test: Stability entails that the ranking of the animals does not change over time. Consistency ensures that mice are consistently winning and losing against the same opponents, rather than behaving probabilistically, for example, winning a third of the tests irrespective of the opponent's identity. Finally, the transitivity requirement is satisfied when the hierarchy is linear and there are no loops (e.g., $A > B$, $B > C$, hence $A > C$). The tube test paradigm successfully produced hierarchies with stable dominant and subordinate mice, although frequent rank changes between middle-ranked mice were common. Hierarchies were considered stable when the dominant and subordinate mice performed consistently in all tube tests for at least 3 consecutive days. In addition, consistency, stability and transitivity

metrics were computed for each testing day to aid the evaluation of the hierarchy's stability. The example Elo rating plot over several testing days and the average stability metrics across all cages (Figure 3.1) show the typical behavioural dynamics in this test. Stability is initially low but increases and plateaus by testing day 5 on average. Pushing, retreating, and resisting the opponent's push are three commonly annotated tube test behaviours (Figure 3.2). Pushing behaviours were significantly different between mice from opposite ends of the hierarchy, with dominants pushing more frequently ($t(21) = 2.50, p = 0.0125$) and spending more time doing so ($t(21) = 2.58, p = 0.00979$).

3.2.1 Tube test hierarchies are not based on fixed differences in behavioural phenotype

One concern is that consistent and transitive tube test outcomes could be achieved based on trait behavioural differences between mice instead of differences in rank. For example, "dominant" mice might simply have a stronger behavioural tendency to push and will therefore consistently "win" against opponents who happen to be

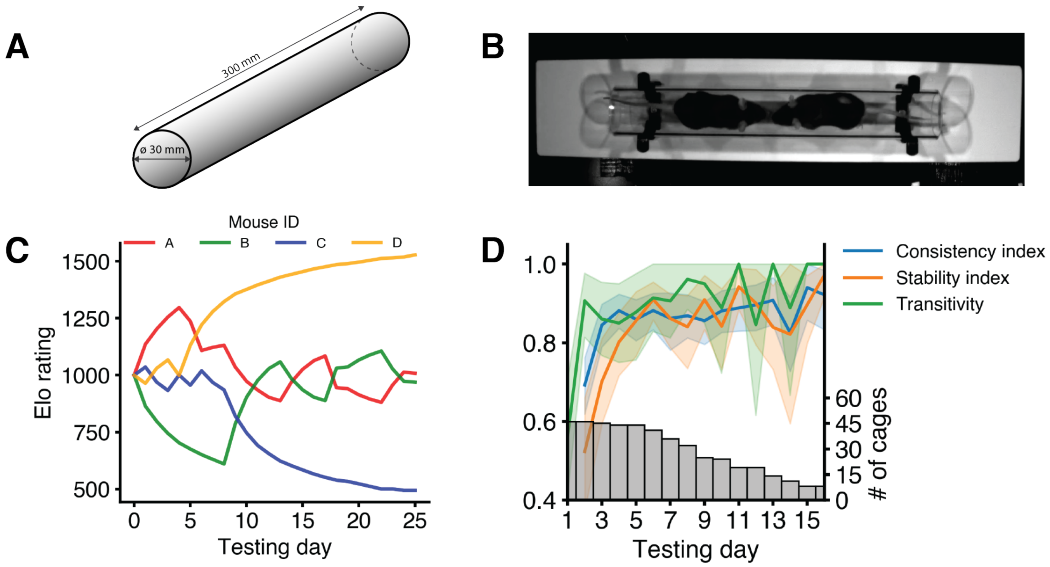

Figure 3.1: The tube test reveals stable social hierarchies in group-housed mice. (A) Diagram of tube dimensions. **(B)** Example image from a recording of a tube test. **(C)** Elo ratings for a representative example hierarchy over several testing days. **(D)** Average hierarchy stability metrics across all cages over time. $N = 46$ cages. Error shading represents 95% CI.

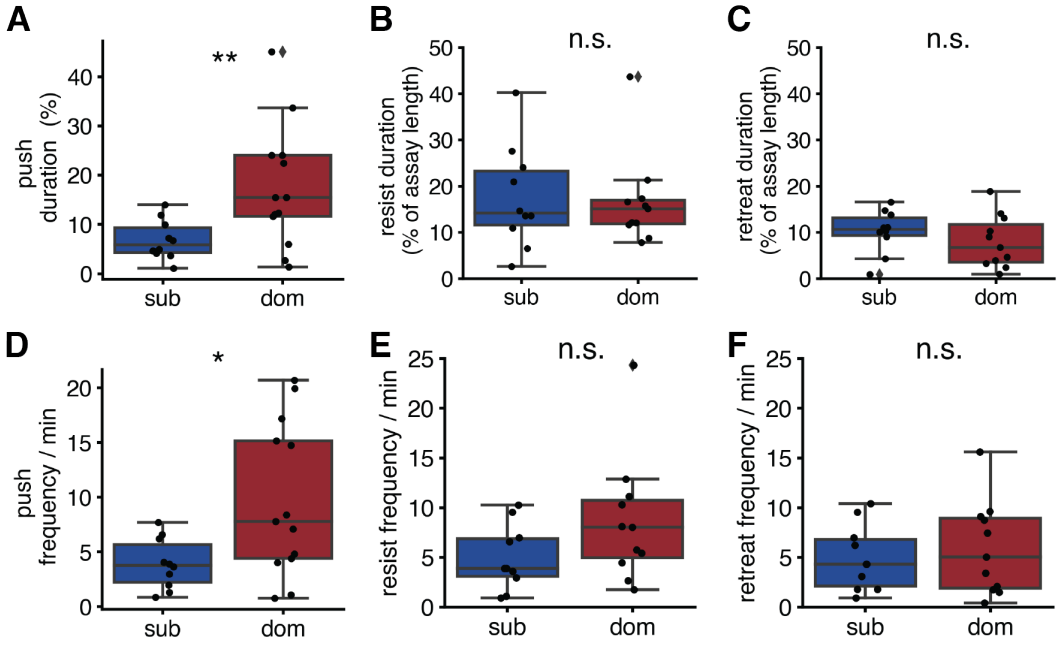

Figure 3.2: Rank-dependent differences in pushing, retreating and resisting behaviours in the tube test. **(A-C)** Assay time spent pushing, resisting opponent's push, and retreating across ranks. **(D-F)** Frequency of pushing, resisting and retreating across ranks. Independent t-tests, $N = 11$ dominant mice, $N = 10$ subordinate mice. Error bars represent 95% CI.

less inclined to push and more inclined to retreat. This hypothesis rests on the assumption that mice have a fixed propensity for pushing and retreating in the tube test, rather than dynamically adapting their behaviour depending on the rank of their opponent. To address this concern, the behavioural phenotype of the same animal across winning and losing trials was quantified in Figure 3.3. This data shows that mice push more in tube test trials that they win compared to losing trials (Repeated measures ANOVA testing the effect of winning on behaviour duration while controlling for within-animal effects: $F(1,13) = 20.7, p = 0.000551$), and vice versa, retreat more in trials that they lose ($F(1,13) = 54.3, p < 0.0001$). No difference was found for resisting ($F(1,13) = 1.9, p = 0.190$). This demonstrates that the same mouse has a variable behavioural strategy in the tube test depending on its opponent, rather than a fixed tendency to push as opposed to retreat.

The initial period of instability is interesting because it suggests that some learning process is occurring during that time. Since mice were weaned together and were in most cases cohoused as littermates since birth, there had been plenty of time for hierarchies to form before the first tube test at week 8 of age at the earli-

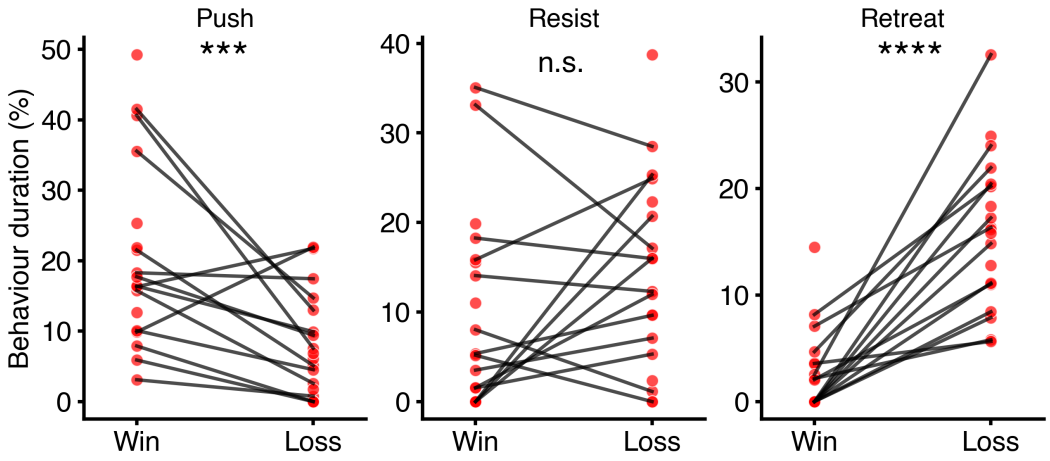

Figure 3.3: Mice have different behavioural strategies in winning and losing tube test trials. The duration of behaviour as a percentage of the total tube test trial duration is shown for pushing (**left**), resisting (**middle**) and retreating (**right**). Data pairing indicates the same animal in winning and losing trials. Unpaired data points indicate animals who won or lost all trials. Repeated measures ANOVA, N=23 mice.

est. Indeed, others have reported the existence of stable hierarchies in mice before weaning (Bicks et al., 2021). The expectation is therefore that by week 8 an established hierarchy could be simply read out without a learning period. There are two potential explanations for this behaviour: firstly, if hierarchies are formed through a series of antagonistic encounters over resources, the laboratory environment with ad libitum food and water may not provide ample enough opportunities for such conflict. In contrast, the tube test forces them into an encounter with a binary outcome and could therefore trigger a hierarchy learning process in adulthood. Anecdotally, spontaneous aggression in the home cage was frequently observed following a tube testing session, which could mean that testing elicits new rounds of competition either to establish a new hierarchy for which there was previously no purpose or to renegotiate a previously settled social order. The second possibility relates to the animals adapting to the experimental apparatus and the requirements of the test. For example, there can be a reluctance of either mouse to push in early tests, hence the outcome is achieved by one of the mice retreating without the winner ever doing anything. Such a winner may not last in subsequent sessions when their opponents become more accustomed to pushing.

3.2.2 The winner effect

Despite these explanations of the learning period, the possibility that the mice are learning something unrelated to the hierarchy had to be addressed. In particular, some studies have reported the existence of winner effects, where a mouse that has just won a conflict will be emboldened and continue to win the following encounter (Fuxjager and Marler, 2010; Fuxjager et al., 2011). The order of the tube tests in a round-robin was randomised to mitigate this possibility. Additionally, a winner effect entails that winning is not dependent on the identity of the opponent, but rather on the sequence in which they are presented, which is incompatible with the high consistency index seen in my data. it would also mean a higher likelihood of consecutive winning and losing. The expected frequency of outcomes as well as outcome switches that theoretically result from a transitive hierarchy was modelled and compared to the empirically observed distribution in Figure 3.4. While the latter was sign10ificantly different from the theoretical prediction (Chi-squared $\chi^2 = 10.2, df = 3, p = 0.004$), the frequency of consecutive wins or losses was in fact modestly lower than the expected distribution, hence no evidence of a winner effect was found.

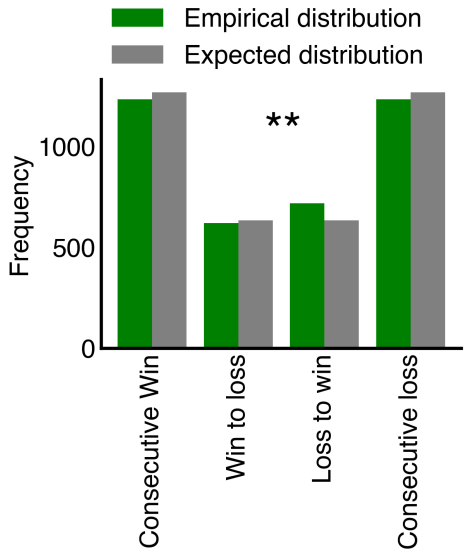

Figure 3.4: The frequency of consecutive wins and losses is lower than expected and therefore winner effects are not observed in the data. Chi-squared test, $N =$ 3812 tube tests.

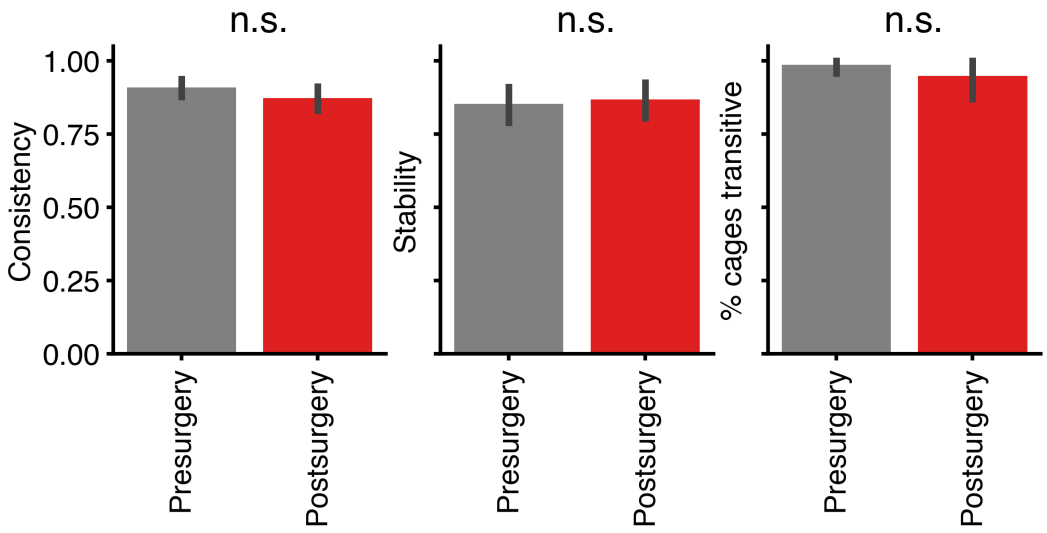

Figure 3.5: Hierarchical stability metrics are not disturbed following surgery. Consistency (**left**), stability (**middle**), and transitivity metrics (**right**) before and after surgery was performed on at least one of the mice in the hierarchy. Paired t-tests, $N = 13$ cages. Error bars represent 95% CI.

3.2.3 Resilience to surgical intervention

Since the dominant and subordinate mice underwent surgeries in most of the experiments in the following chapters, it was necessary to verify that surgery did not disrupt the established hierarchy. To that end, hierarchy stability metrics were quantified for the five testing sessions before and after surgery for each cage undergoing surgery in Figure 3.5. None of the three stability metrics were significantly altered following surgery (consistency index: $t(12) = 1.21, p = 0.248$, stability index: $t(12) = 0.31, p = 0.766$, transitivity: $t(12) = 1.08, p = 0.301$, paired t-tests), hence experimental intervention could occur without perturbation of the hierarchy.

3.2.4 Reward competition

Previous work has shown that hierarchies obtained by tube test correlate with other more naturalistic assays of hierarchy, for example, the hot spot assay where mice compete to occupy a warm spot in a cold assay chamber (Wang et al., 2011). Competing for a resource is perhaps one of the most naturalistic social dominance paradigms. In work by Padilla-Coreano et al. (2021) mice were trained to expect reward in the form of sucrose water upon presentation of an auditory cue. How-

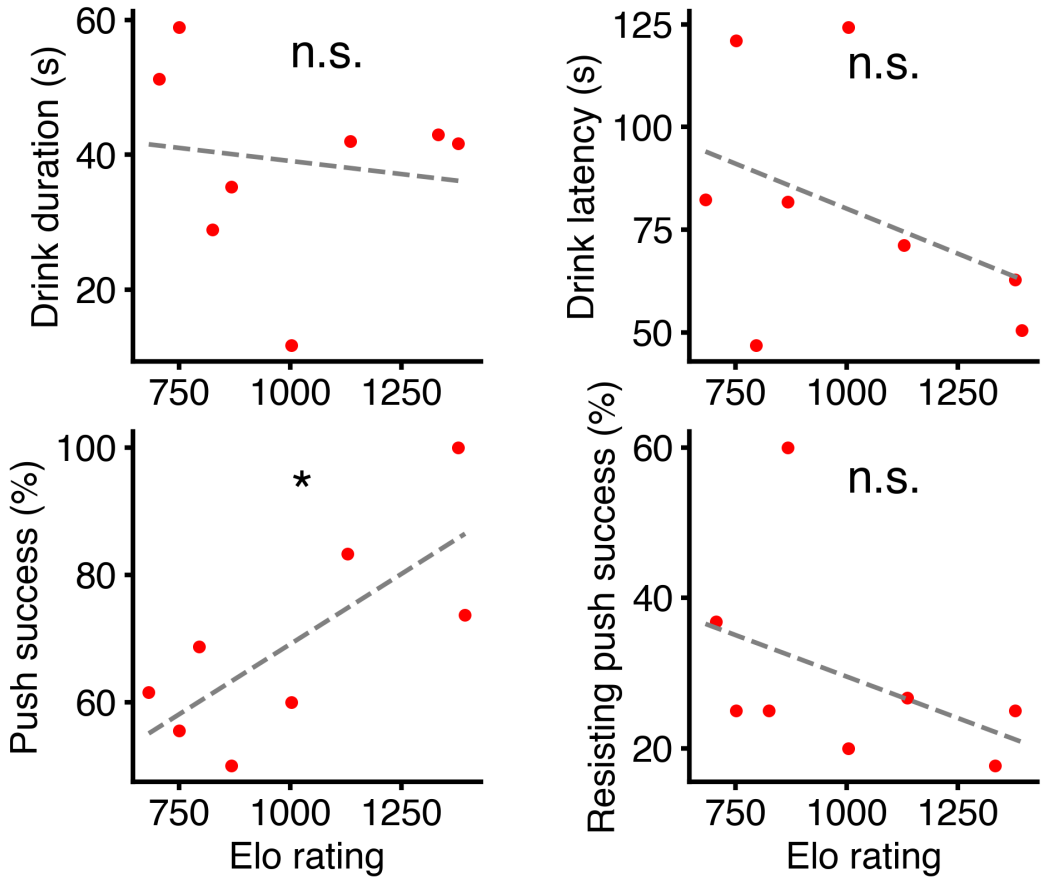

Figure 3.6: Successfully pushing an opponent away from a resource is associated with high tube test Elo score. Associations between tube test elo scores of each mouse and its performance in the water competition assay in terms of drinking duration, drink latency, success in pushing competitors away from the water spout and success in resisting pushing attempts from others. Statistics indicate results of linear regressions predicting Elo score from behavioural metrics of reward competition success. $N = 8$ mice.

ever, the spout from which the reward could be obtained could only accommodate one mouse at a time, thus incentivising competition. Mice were assayed in pairs and the winner was determined based on reward spout occupancy, latency to spout occupancy and how successful mice were in pushing their opponent away from the spout. Cued reward presentation represents significant assay and training optimisation and since this was not the main focus of the project, I used a simplified adaptation of this paradigm, where mice with a known tube test hierarchy were water-deprived for 12 hours and subsequently presented with water through a spatially constrained spout. The entire cage was assayed at the same time rather than

pairs of animals and the same metric of reward competition as in the original study were quantified. Figure 3.6 shows the results of linear regressions predicting behavioural measures of competitive success in this paradigm from the animal's tube test Elo rating. An animal's pushing success showed a significant association with its Elo score ($p = 0.033$), but the spout occupancy duration, latency and resisting pushes from the opponent did not. These discrepancies may have resulted from design alterations from the reported assay. The drive to quench thirst is perhaps less persistent than obtaining a reward that is not tied to physiological needs. The mice that access the water first may stop being thirsty and then allow lower-ranked mice to drink as well. Over the course of the assay, this could attenuate differences in spout occupancy. Additionally, since the presentation of the water is not cued, latency is a less reliable metric, since mice further away from the spout may notice that it is present later than the closer ones. The poor associations of the reward competition metrics measured here with the tube test Elo rating therefore likely reflect the design differences compared to the original experiment by Padilla-Coreano et al. (2021).

3.3 Generalisation of in-group hierarchies to interactions with strangers

One of the characteristics of human hierarchies is that past experience can be used to rapidly infer the social status of strangers and one's own status relative to a stranger. The existence of robust hierarchies between familiar mice has been well documented, however, it was unclear whether mice are capable of similar inference about stranger conspecifics. Indeed, one study notes that the emergence of stable hierarchies in the tube test relies on at least some degree of group-housing - tube testing single-housed males fails to produce stable hierarchies on its own, but allowing the same mice to also interact freely in a resident-intruder paradigm stabilises the hierarchy in the tube test (Nelson et al., 2019). This suggests that familiarity is crucial and that dominance is therefore tied to a specific social identity and past interaction history with that individual. To test this idea more explicitly, in-group

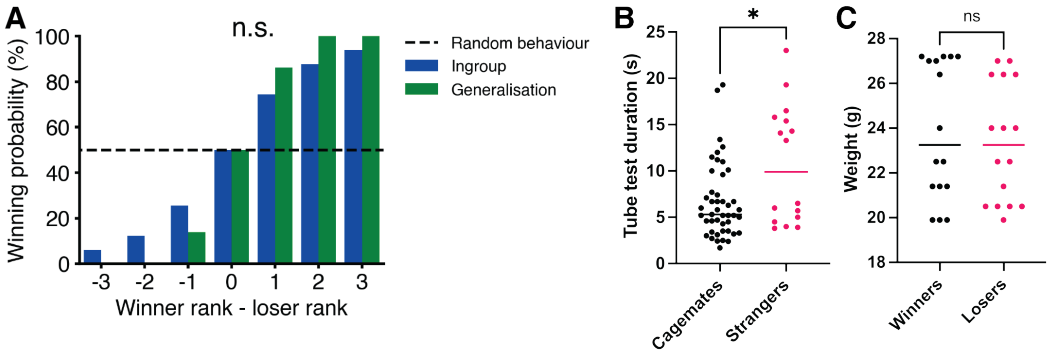

Figure 3.7: In-group dominance rank is robustly generalised to unfamiliar mice. (A) The frequency of rank differences between winners and losers when tube testing cohoused mice (in-group, $N = 2589$ tube tests) or unfamiliar mice from separate cages ($N = 30$ tube tests). Mann-Whitney U-test. **(B)** Tube tests between unfamiliar mice ($N = 16$ tube tests) are longer in duration compared to tests among cagemates ($N = 45$ tube tests). Mann-Whitney U-test. **(C)** Body weight is unrelated to winning potential against unfamiliar opponents. Mann-Whitney U-test, $N = 16$ tube tests.

hierarchies were determined as described using the tube test in two separate cages. Mice of known in-group rank were then paired with an unfamiliar mouse from the other cage. Figure 3.7 shows the winning probability in this experiment depending on the rank difference between the winner and the loser mouse. Negative rank difference indicates that the lower-ranked animal had won and vice versa. In the case of perfect generalisation, the winning probability where the rank difference is negative to any degree should be 0%, and 100% if it is positive. However, some errors are present even in the in-group tube test paradigm and hence this error rate was used as the control. The winning probabilities from the in-group tube test in Figure 3.7 show that errors are more common if the difference in ranks is smaller, i.e. a dominant loss against a subordinate is extremely uncommon, but inconsistent test outcomes between animals close in rank are more frequent. The distribution from the generalisation experiment closely follows this pattern and a one-sided Mann-Whitney U-test did not find the distribution of winner-loser rank differences in the generalisation paradigm ($N = 30$ tests) to be significantly lower compared to the in-group paradigm ($N = 2589$ tests) ($U = 44225, p = 0.915$). This means that mice behave consistently with their in-group rank, even when the opponent is unfamil-

iar and not a member of their usual hierarchy. Nonetheless, the average tube test duration was somewhat longer in the generalisation paradigm compared to the in-group paradigm, suggesting that while rank can be inferred from unfamiliar opponents, social familiarity helps in resolving the conflict quicker, perhaps because the hierarchical relationship between the two mice is recognised more readily (Mann-Whitney U-test $U = 231, p = 0.0338$, cagemate control: $N = 45$ tests, stranger group: $N = 16$ tests). The olfactory signature of the unfamiliar opponent will be unique and therefore not especially informative, implying that a more general signal of rank is necessary for generalisation to be successful. One intuition is that mice can detect a physical attribute of the opponent that implies strength such as size or weight, however, an analysis of the body weights of the tube test winners and losers in the generalisation paradigm did not find an association between body weight and winning potential (Mann-Whitney U-test $U = 108, p = 0.499$, $N = 16$ tests). The following section therefore focuses on identifying the sensory modality that mice use to accurately detect the rank of even unfamiliar mice.

3.4 The sensory modality of murine social dominance perception

Determining the sensory modality used to detect the rank of unfamiliar opponents is crucial to forming circuit hypotheses about the encoding of opponent rank and where this information interacts with own rank representations. As discussed in the introduction, mice rely primarily on olfaction for social perception in general, while studies specific to dominance reported that there are differences in the production of some major urinary proteins (MUPs) such as darcin and MUP20 depending on rank (Roberts et al., 2010; Lee et al., 2017; Guo et al., 2015). Specific brain areas also show differential c-Fos responses to urine from mice of different ranks (Lee et al., 2021; Veyrac et al., 2011). In some cases, the rank of a mouse can even be increased through painting with dominant urine (Nelson et al., 2019). It is therefore likely that mice are detecting the olfactory pheromonal cues contained in urine to

infer the rank of an unfamiliar opponent. While this has been the general assumption in the literature, no studies so far have explicitly tested the necessity or sufficiency of specific sensory modalities for hierarchical behaviour.

To investigate this, a series of sensory deprivation experiments were conducted and the error rate in the generalisation paradigm was measured to determine whether specific modalities are necessary for opponent rank inference. The error rate from the regular tube tests among cagemates was retained as the control error rate. Figure 3.8 shows the winning probabilities depending on the rank difference between the winner and loser for these sensory interventions. I first excluded any role of the visual system, by performing a standard tube test among unfamiliar mice under infrared light, which is not visible to mice (Ma et al., 2019), in other words, in darkness. This did not affect the ability of mice to correctly infer the rank of unfamiliar opponents in the tube test (Mann-Whitney U-test $U = 20047.5, p = 0.253$, $N = 22$ darkness, $N = 2766$ control). Next, the initial strategy to disrupt pheromonal signalling was to castrate the mice, which is technically simpler than ablation of sensory modalities. Both the production of pheromones (Penn et al., 2022) as well as their perception (Schellino et al., 2016; Stowers and Liberles, 2016) is highly sex-dependent and thus regulated by gonadal sex hormones, which additionally function as pheromones themselves (Takács et al., 2017). Castration was expected to disrupt male-specific pheromonal dominance signalling, however, this intervention also did not affect generalisation performance ($U = 8259.0, p = 0.492$, $N = 9$ castration, $N = 2766$ control).

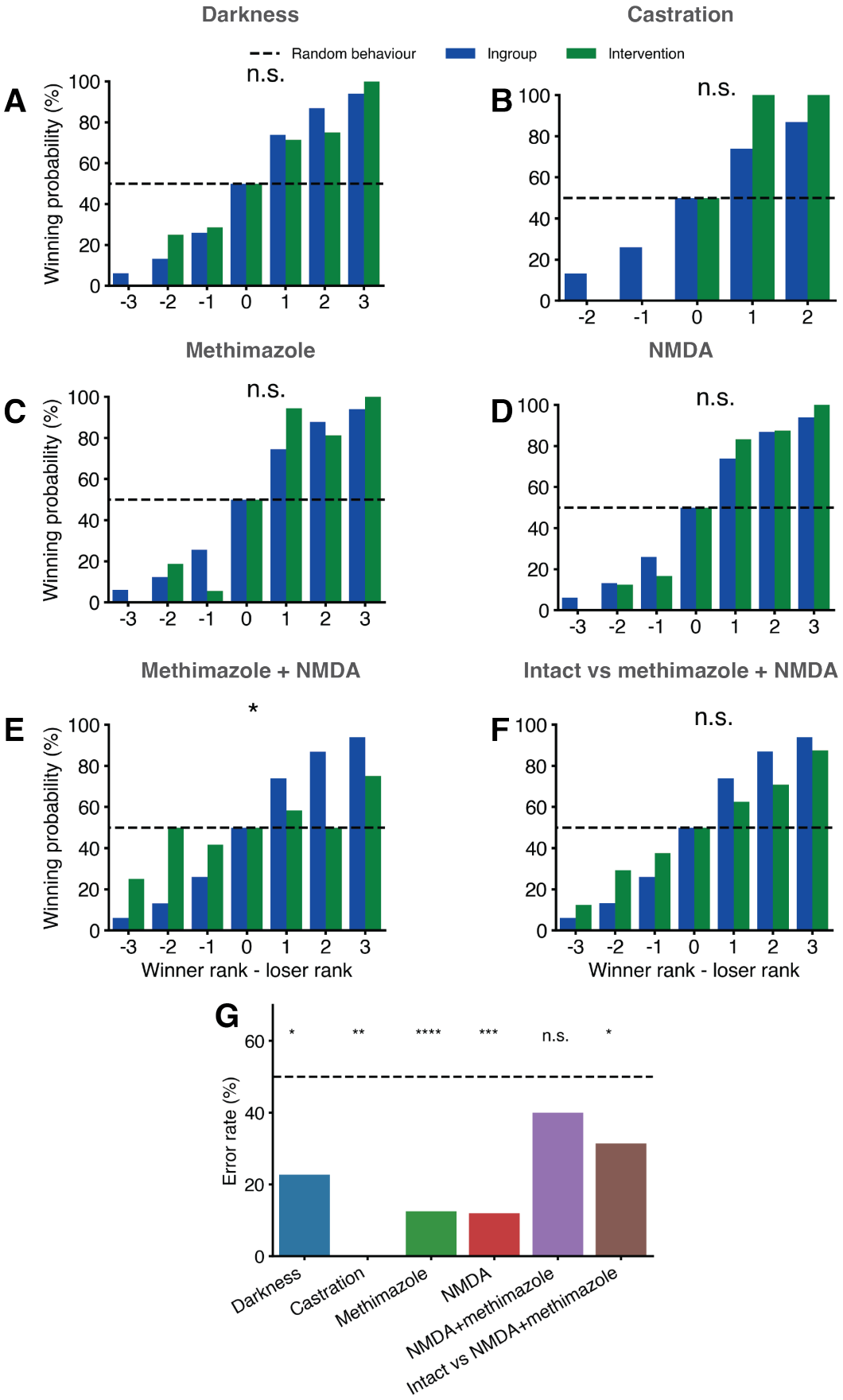
Darkness
Castration
Random behaviour
Ingroup
Intervention
A
B
n.s.
n.s.
Winning probability (%)
Methimazole
NMDA
C
D
n.s.
n.s.
Methimazole + NMDA
Intact vs methimazole + NMDA
E
F
*
n.s.
Winner rank - loser rank
Winner rank - loser rank
G
Error rate (%)
* ** **** *** n.s. *
Darkness
Castration
Methimazole
NMDA
NMDA+methimazole
Intact vs NMDA+methimazole

Figure 3.8: Simultaneous ablation of both volatile and nonvolatile olfaction impairs rank recognition. **(A-F)** The effect of sensory deprivation interventions on the distribution of winner-loser rank differences in the generalisation paradigm (tube tests between unfamiliar mice) compared to the in-group paradigm (tube tests between cohoused mice). The same intervention was applied to all mice in a condition, except in panel **F**, where mice with combined main and accessory olfactory ablation were tested against unfamiliar intact mice. The dotted line indicates a distribution where tube test winners are random without regard for the dominance rank of the two opponents. Statistics indicate the results of Mann-Whitney U-tests between the distributions of winner-loser rank differences in the in-group ($N = 2766$ tube tests) and the intervention conditions. $N = 22$ tube tests in darkness, $N = 9$ for castration, $N = 32$ for methimazole, $N = 25$ for NMDA, $N = 25$ for methimazole+NMDA, and $N = 35$ for methimazole+NMDA vs. intact mice. **(G)** The effect of sensory deprivation interventions on error rates (where the winner rank is lower ranked than the loser) in the generalisation paradigm. Binomial tests with Holm-Sidak correction.

Since there is no definitive evidence that the production of dominance signalling molecules is specifically affected by gonadal hormones, I moved on to complete lesioning of the volatile and non-volatile olfactory systems separately and in combination. Volatile olfaction was abolished using methimazole injections, which cause rapid and complete detachment of the olfactory epithelium (OE) and anosmia (Håglin et al., 2021). In contrast, vomeronasal sensation was abolished through stereotaxic injection of NMDA into the accessory olfactory bulb (AOB), which causes excitotoxic neuronal death (Erskine et al., 2019). Confirmatory histology for methimazole and NMDA injections is shown in Figure 3.10 and Figure 3.11 respectively. Interestingly, neither the OE ($U = 43776.5, p = 0.584$, $N = 32$ methimazole, $N = 2766$ control) nor AOB ablation ($U = 35679.0, p = 0.746$, $N = 25$ NMDA, $N = 2766$ control) resulted in impaired generalisation performance when used in isolation. However, the combined abolition of both volatile and nonvolatile olfaction did result in a significantly higher error rate ($U = 25162, p = 0.016$, $N = 25$ NMDA+methimazole, $N = 2766$ control). Additionally, a binomial test for this condition showed that the tube test error rate is not significantly lower than 50%, which indicates that outcomes are random and independent from the rank differences between opponents. Interestingly, when pairing a cage of mice that underwent the combined OE and AOB ablation with an intact cage, the generalisation still occurs ($U = 41140.0, p = 0.094$, $N = 35$ intact vs. NMDA+methimazole, $N = 2766$ con-

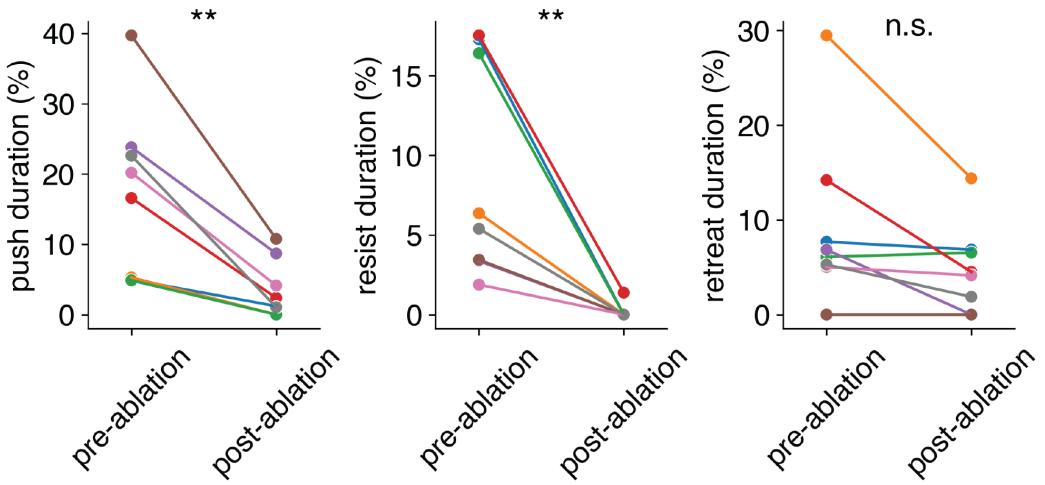

Figure 3.9: Combined main and accessory olfactory system ablation results in less active behaviour in the tube test. The mean behaviour duration (as a percentage of the total trial duration) for pushing, resisting, and retreating in the tube test before and after combined main and accessory olfactory system ablation. Repeated measures ANOVAs, $N = 8$ mice, pairing indicates the same animal.

trol). This suggests that the animal with intact sensation accurately detects the rank of the anosmic opponent and perhaps behaviourally leads the encounter towards the correct outcome. Additional behavioural analysis revealed mice that underwent combined main and accessory olfactory ablation continue to exhibit the usual tube test behaviours (Figure 3.9), however, they spend less time pushing and resisting (repeated measures ANOVAs testing the effect of olfactory ablation on pushing duration: $F(1,7) = 19.2, p = 0.0032$, resisting duration: $F(1,7) = 14.0, p = 0.0072$ and retreat duration: $F(1,7) = 5.3, p = 0.0547$).

3.5 Rank-dependent differences in social behaviour

There is substantial variability in the reported behavioural differences between mice of different ranks, often with contradictory findings (Varholick et al., 2021). While instinctive social behaviour is expected to be relatively stereotyped, it is highly sensitive to context, for example, group- or single-housing, whether the assay is performed in the home cage or dedicated apparatus, stress, mouse strain and other factors. It is important to establish which behaviours are different with our animals

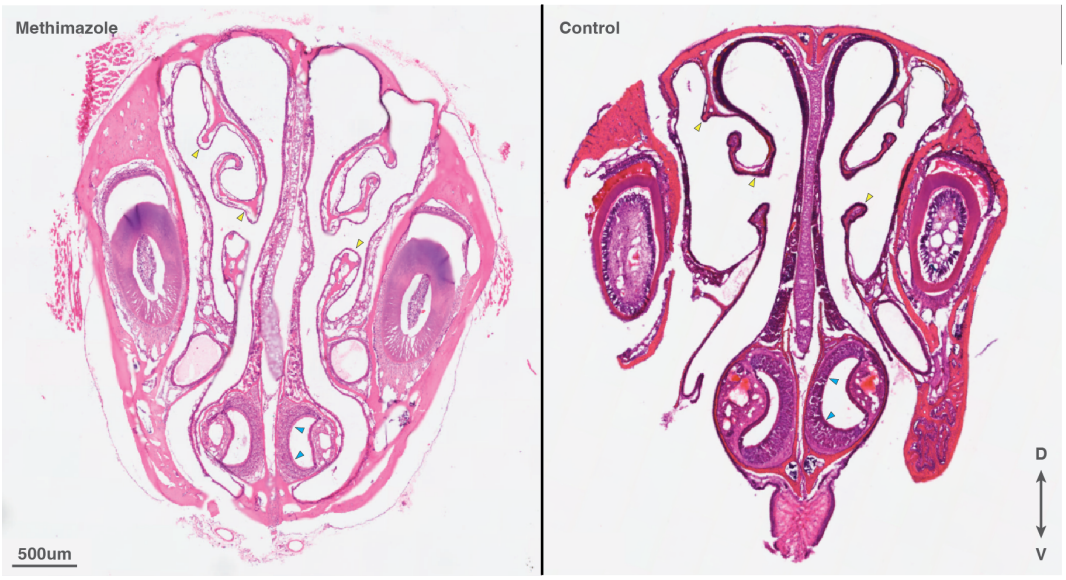

Figure 3.10: Confirmatory histology for olfactory epithelium ablation using methimazole. H&E stained nose sections from methimazole injected and control mice. Yellow arrows show detached olfactory epithelium and the corresponding attached areas in the control. Blue arrows show the vomeronasal organ which is unaffected in both conditions. Nose histology was performed by Paula Rodriguez-Villamayor.

and setups to guide the selection the selection of behaviours for functional recordings. Here I assayed some behaviours for which rank-dependent differences have previously been reported.

3.5.1 Aggression

Male-to-male aggression was tested using a resident-intruder paradigm, where an unfamiliar middle-ranked male (the intruder) is introduced into the home cage of another male (the resident). Figure 3.12 shows the percentage of time spent attacking the intruder ($t(5) = 0.32, p = 0.756$), the mean length of the attack bouts in seconds ($t(5) = 0.19, p = 0.858$), and the latency until the first attack bout ($t(5) = 0.43, p = 0.683$) none of which differed significantly between dominant and subordinate cagemates (paired t-tests). This is consistent with more recent studies in the field which also fail to find a hierarchical effect on aggression (Nelson et al., 2019), while more detailed investigations into factors such as hierarchy size and stability have shown that aggression differences are only present in unstable hierarchies (Williamson et al., 2017). Furthermore, optostimulation of the dmPFC,

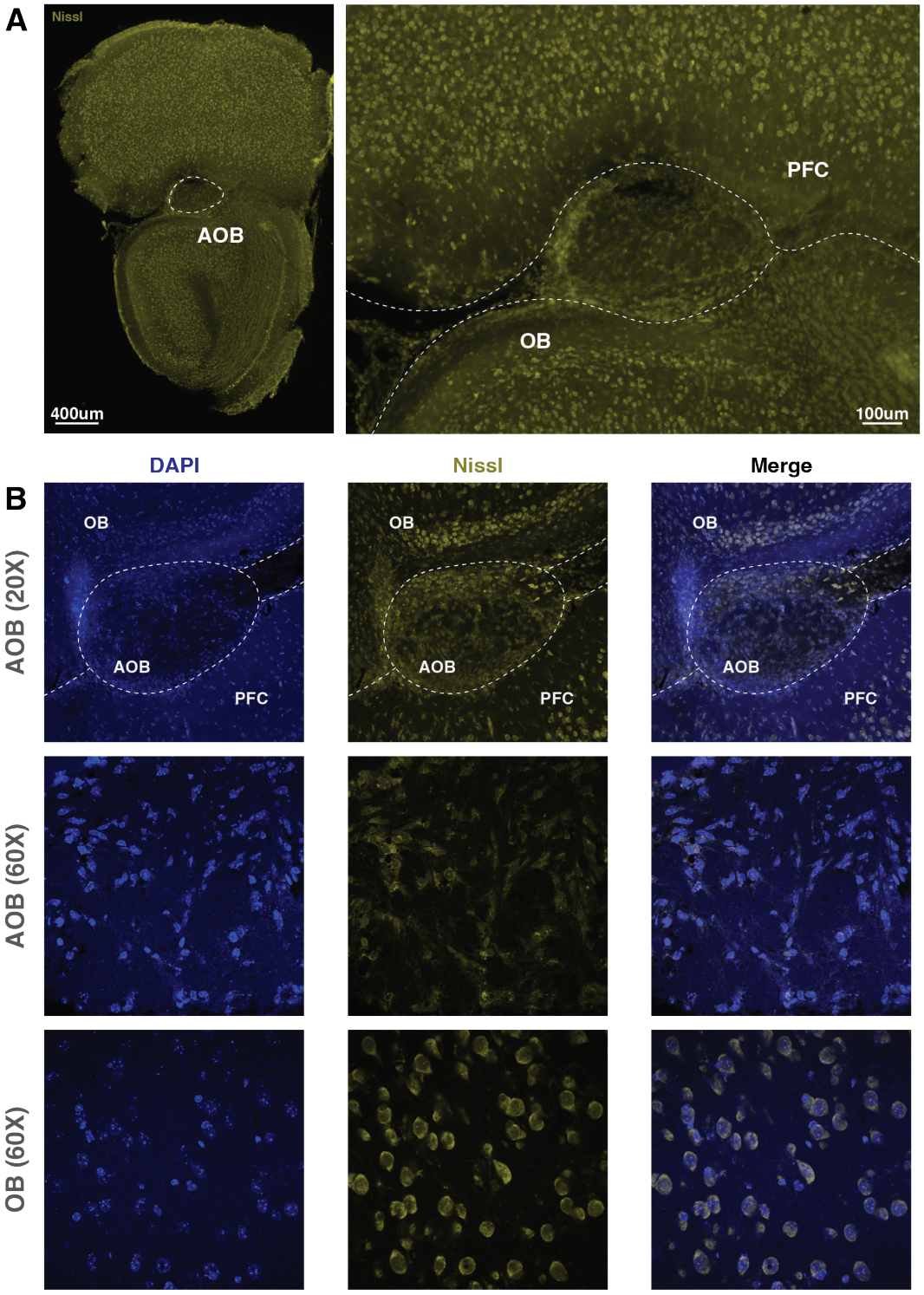

Figure 3.11: NMDA injection into the accessory olfactory bulb results in localised cells death. **(A)** 20x slide scanner images of the Nissl stained AOB sections. **(B)** 60x confocal images of the AOB with cellular morphology indicating cell death in contrast with MOB cells from the same slice.

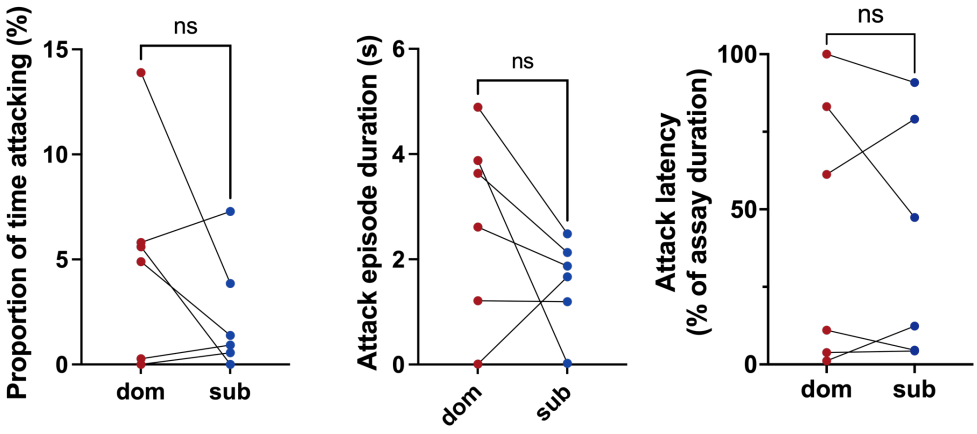

Figure 3.12: Differences in dominance rank do not affect aggression in mice. Left: Percentage of time spent attacking the male intruder among dominant and subordinate residents. **Middle:** Length of attack bouts in seconds. **Right:** Latency until first attack bout by the resident. Paired t-tests, $N = 6$ mice in each group. Pairing is between the dominant and subordinate from the same cage (cagemates).

which results in improved competitive success in the tube test did not simultaneously increase aggression (Zhou et al., 2017), demonstrating that the dominance and competition circuits are separate from the aggression circuit.

3.5.2 Sexual behaviour

Previous studies have found that subordinates are less likely to mate with females, even when they are isolated from their normal hierarchy (Kleshchev and Osadchuk, 2014) and that dominants sire more numerous offspring (D'Amato, 1988), presumably as a consequence of more frequent mating. Furthermore, females themselves prefer to mate with dominant males, due to attraction to MUPs such as darcin (Nelson et al., 2015; Carr et al., 1982). Sexual behaviour was initially tested using the same resident-intruder protocol but with a virgin female intruder for 10 minutes. Since no sexual behaviour was observed within that period, the recording was extended to 90 minutes, but only a single male engaged in sexual behaviour during that period. Sexually experienced females were used next, along with swapping of bedding material between the male and female cages for 3 days before the assay (the Whitten effect). The bedding carries urinary cues from the opposite sex and increases sexual receptivity in mice (Whitten, 1966). Since that did not improve

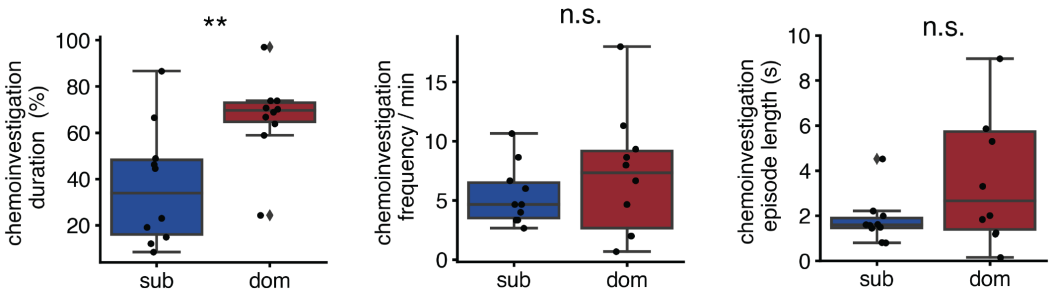

Figure 3.13: Dominants spend more time chemoinvestigating females. Left: Percentage of time spent chemoinvestigating the female intruder among dominant ($N = 12$ mice) and subordinate mice ($N = 10$). **Middle:** The frequency of chemoinvestigation bouts initiated by the resident. **Right:** The mean length of chemoinvestigation bouts. Independent t-tests. Error bars represent 95% CI.

the frequency of sexual behaviour, a more invasive approach with hormonal priming of the sexual receptivity in females was piloted. Subcutaneous injections of estradiol on days -2 and -1 before a sexual behaviour assay followed by a progesterone injection on the day of the assay have been shown to increase receptivity (Inoue et al., 2019). This procedure did not improve the frequency of sexual behaviour initiation by the males either. In place of reliable sexual behaviour, the behavioural metrics of chemoinvestigation as a proxy for sexual interest were quantified in Figure 3.13 instead. The dominants spent a significantly longer proportion of time chemoinvestigating the female intruder ($t(20) = 3.2, p = 0.00131$), although they did not do so more frequently ($t(20) = 0.66, p = 0.507$) or with a longer bout length ($t(20) = 1.5, p = 0.133$). That said, both of the latter two metrics have a non-significant trend towards higher frequency and bout length in dominants, which in combination likely lead to significantly more time spent interacting with the female.

3.5.3 Social preference

Previous work in humans (Rosengren et al., 1998) and animals (Challis et al., 2013) have suggested that low status and social defeat decrease sociability. This is likely to avoid future conflict with more dominant individuals and indeed the hierarchical organisation of some species compels lower-ranked individuals to live on the

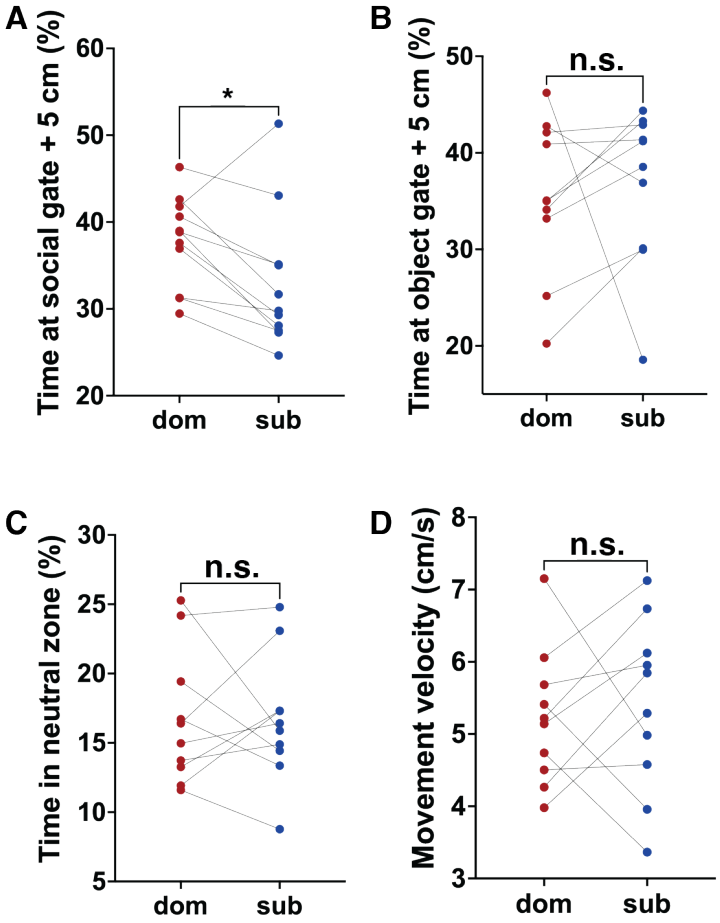

Figure 3.14: Dominants spend more time interacting with a social stimulus. Assay time spent in the 5 cm zone around the social **(A)** and object gates **(B)**. **(C)** Assay time spent in the neutral zone. **(D)** Average movement speed of the tested mouse. Statistics are paired between the dominant and subordinate cagemates. N=11 cages.

physical periphery of the community (Naud et al., 2016). Preference for social over inanimate stimuli was tested using a three-chamber social preference test (Figure 3.14). In this paradigm, the tested mouse is placed into a central chamber flanked by two smaller chambers separated by a mesh gate. One smaller chamber contains a social stimulus (an unfamiliar middle-ranked male) and the other an inanimate object (a roll of sellotape). The mesh gate ensures that the initiative to interact falls entirely on the tested mouse and the stimulus animal therefore cannot confound the measurements of sociability. The time spent in a 5 cm zone around each gate was quantified, along with time spent in a neutral zone in the

middle of the main chamber. In this paradigm, dominant mice spent more time in the close vicinity of the social stimulus compared to their subordinate cagemates (paired t-test, $t(10) = 2.76, p = 0.0203$). Importantly, the exploration of the object gate (Wilcoxon signed-rank test, $W(10) = 25, p = 0.232$), the neutral zone (paired t-test, $t(10) = 0.078, p = 0.940$), as well as the movement speed (paired t-test, $t(10) = 0.41, p = 0.689$) were the same between these groups. This indicates that these effects are not derived from differences in stress levels or overall exploratory drive. Interestingly, the mean level of sociability was strongly correlated between cagemates, suggesting that the group dynamics within each cage have a greater influence on individual motivation for social interaction than rank does.

3.6 Discussion

The aim of this chapter was to establish the characteristics of hierarchical behaviour in laboratory mice, especially replicating assay validity and determining what differences in social behaviour are observed with the specific mice and experimental environment used here. The results confirm the validity of the tube test for obtaining stable hierarchies that are resilient to experimental interventions, especially surgery. Importantly, these hierarchies rely on consistent tube test outcomes between the same pairs of mice, and not on a winner effect or a probabilistic winning rate irrespective of the opponent.

3.6.1 Aggression

The lack of differences in aggression has been confirmed by several recent studies (Zhou et al., 2017; Nelson et al., 2019). Unfortunately, there has been frequent conflation of dominance with aggression, high testosterone and low stress in older studies (Machida et al., 1981) to the extent where these measurements were used interchangeably. This is likely due to intuitions about animal behaviour that generalise very poorly across species and even across different group organisation within the same species. In mice alone, these variables appear in many combinations depending on the stability and size of the hierarchy. For example, aggression and stress differences are not observed in stable hierarchies, whereas aggres-

sion is high in subordinates and stress is high in dominants in unstable hierarchies (Williamson et al., 2017). Testosterone is reliably correlated with aggression (Nelson and Trainor, 2007), but not dominance. Indeed, several studies report a relationship between dominance and prosocial behaviour (Scheggia et al., 2022), which is certainly prominent in human high-rank individuals, where a dictatorial maintenance of one's status is generally a poor strategy outside specific environments like prisons or formal positions of authority (Hawley, 1999).

3.6.2 Sexual behaviour

In the sexual behaviour assays, it was unfortunately very rare to observe any mounting behaviour. Assay refinements involving the swapping of bedding between the male and female cages (i.e. the Whitten effect (Whitten, 1966)) several days before the assay, cohabitation of the male and female in separate home cages but in the same assay recording environment, as well as the use of sexually experienced females, did not noticeably improve the frequency of sexual behaviour during behavioural recordings. A level of reluctance is expected for sexually inexperienced males, especially ones that have not been single-housed. Single-housing for a week is a common method to increase territoriality in males and significantly increases the territoriality and frequency of sexual behaviour (deCatanzaro and Gorzalka, 1979). However, social isolation could have unpredictable effects on the social hierarchy within the former group, especially since males cannot be group-housed again after isolation to reestablish the hierarchy, due to high levels of inter-male aggression among formerly single-house males. Since the frequency of sexual behaviour was insufficient for statistically robust analysis, the general propensity for interaction with female intruders was analysed as a proxy measure of sexual motivation. This showed that dominants spend more time chemoinvestigating the females in line with higher reproductive success among dominants in other studies (Kleshchev and Osadchuk, 2014; Nelson et al., 2015). In summary, there are rank-dependent effects on competitive tube test behaviours, sexual motivation towards females, and social affinity towards males. The neural basis of these differences is explored in the coming chapters.

3.6.3 Rank inference

Finally, this chapter also investigated for the first time the ability of mice to generalise their rank to interactions with stranger mice. Their ability to do so was strikingly consistent and resilient to sensory deprivation, showcasing a substantial level of redundancy in detecting conspecific rank cues. Previous work on MUPs that are enriched in dominants such as darcin (Nelson et al., 2015; Guo et al., 2015; Luzynski et al., 2021) suggested that urinary signals could be used as universal dominance cues that allow rank inference without personal familiarity with a specific individual. However, the authors did not test this possibility, since they were focused on the ability of darcin to attract females. Another study reported c-Fos expression differences in several brain areas in response to urine obtained from dominant and subordinate donor males, including donors that were unfamiliar with the exposed mice (Lee et al., 2021). This again suggested that some dominance cue is present in the urine, however, no behavioural studies or manipulations were conducted by the authors to determine whether MUPs are indeed the primary cues for detecting rank and whether this information is sufficient to consistently recognise the rank of unfamiliar opponents.

This work is the first direct evidence that mice can in fact generalise dominance relationships using olfactory cues, while familiarity with the opponent still helps to resolve competitive encounters quicker. This seems to be the case in other species, for example, lizards who signal their dominance status through eyespots. Manipulating the eyespot signal does not perturb existing hierarchical relationships due to the redundancy afforded by identity recognition, but it does alter hierarchical relationships with unfamiliar opponents where that redundancy is absent (Korzan et al., 2007). The sensory deprivation experiments demonstrated that simultaneous ablation of both the main and accessory olfactory systems through combined methimazole and NMDA injection impairs the ability of mice to infer the dominance rank of an unfamiliar opponent and renders the tube test error rate indistinguishable from random behaviour. However, selective ablation of either olfactory pathway is insufficient to achieve this effect, meaning that the volatile and non-volatile modalities

provide redundant information about conspecific rank. By extension, this implies that there may be multiple olfactory dominance signals, some with volatile and others with non-volatile chemical properties. An important caveat of these experiments are the behavioural changes observed following the double olfactory ablation, namely diminished pushing and resisting. These changes are likely attributable to methimazole, which can cause signs of pain and reduced mobility for several days after injection. These symptoms were the reasons for painkiller (buprenorphine and meloxicam) injections hours before tube testing, which ensured that mice performed the tube test as usual, although behaviour was still diminished when quantified in detail. These behavioural effects could potentially confound the effects of sensory deprivation on rank generalisation.

The identification of the sensory circuit necessary for conspecific rank detection serves as the foundation for determining the anatomical location where this information interacts with thalamocortical representations of own rank. As discussed in the introduction, the MPOA and the VMH are two brain areas which receive both volatile and non-volatile olfactory input via the medial amygdala, while also showing evidence of modulation by own rank. They were therefore hypothesised as the integration nodes for the two streams of information. The next chapter therefore investigates the own rank-dependent modulation of the hypothalamus in much more detail compared to previous studies and identifies the exact functional features that are affected by this internal state, while Chapter 5 explores the information encoding properties of the MPOA and VMH to test the integration node hypothesis.

Chapter 4

Rank-dependent modulation of neural excitability and tuning properties

4.1 Introduction

The previous chapter found that rank-dependent behavioural differences are found in competitive behaviours in the tube test, social approach to unfamiliar male conspecifics and chemoinvestigatory interest in unfamiliar females. This thesis proposes that rank-dependent behavioural differences do not arise in a social vacuum, where, for example, dominant representations drive approach, sexual and competitive behaviours irrespective of the social environment, but rather that own rank representations interact and modulate the sensory perceptions of conspecifics. The MPOA and VMH have documented pheromonal sensitivity and therefore respond to conspecific cues (Dulac and Wagner, 2006; Stowers and Liberles, 2016) while also exhibiting differential c-Fos activation depending on own dominance status (Nelson et al., 2019). They were therefore selected as the candidate areas where rank-dependent modulation of social perception occurs. To investigate this hypothesis, mice with known dominant or subordinate status were implanted with endoscopic

lenses in either the MPOA or VMH for subsequent in vivo imaging of cellular-resolution neuronal activity during social interaction (Ghosh et al., 2011). This was followed by analysis of rank-dependent changes in evoked signal properties in response to male and female unfamiliar conspecifics as well as tube test behaviours.

4.2 Experimental pipeline

Figure 4.1 shows the experimental pipeline from implantation to imaging, histology, and signal analysis. Cage hierarchies were determined using the tube test. Once the hierarchy stability criteria described in Chapter 3 had been reached, the dominant and subordinate were stereotaxically injected with an AAV encoding the GCaMP7s fluorescent calcium indicator and implanted with a GRIN lens above the virus injection site in the MPOA or VMH in the same surgery session. Due to the substantial depth of the implantation, good signal quality was obtained around 6-8 weeks after surgery, with the typical field of view (FOV) yielding between 20 and 50 cells and up to 80 cells. The mouse was tethered to the miniscope in their home cage and recorded during free interaction with an unfamiliar middle-ranked male, an unfamiliar female, and several tube tests with an unfamiliar middle-ranked male. The free interaction recordings captured the sensory responses to both male and female stimuli during chemoinvestigation of the intruder, while the tube tests captured activity related to competitive behaviours, namely, pushing, resisting, and retreating. Following the recordings, the mice were perfused and the correct positioning of the GRIN lens in either the MPOA or VMH was verified histologically. Frequent reasons for the exclusion of an implanted animal were poor signal quality, mistargeted implantation, or change in social status. In total, recordings from 18 mice were accepted, 5 dominant and 5 subordinate animals implanted in the MPOA, as well as 5 dominant animals and 3 subordinate mice implanted in the VMH. The total cell yield across all accepted mice was 774 cells. Signal drift (e.g. from bleaching) and movement artefacts were removed from the recordings in the preprocessing steps and the cell regions of interest (ROIs) were detected automatically using the

PCA-ICA algorithm, followed by manual curation of the cell set. Behavioural annotations were used to extract the evoked calcium activity surrounding a stimulus or behavioural event (peristimulus time histograms or PSTHs).

4.3 Response amplitude

Previous work has shown that internal states can modulate the amplitude or gain of evoked responses in the hypothalamus to specific social cues (Nomoto and Lima, 2015). In this section, I investigated whether dominance rank as an internal state has a similar effect on evoked response amplitudes. As discussed in the introduction, the hypothalamus exhibits neuronal tuning to both sensory and behavioural triggers (Ammari et al., 2023; Karigo et al., 2021) and dominance rank could modulate responses to either category of triggers. The following analysis therefore extracted evoked responses to several cues, namely, chemoinvestigation of male and female unfamiliar intruders as well as pushing, resisting, and retreating behaviours in the tube test. The example recording in Figure 4.1 shows that the responses during the first contact with a new conspecific are the most robust, with significant attenuation of signal as the interaction continues. The following analyses therefore use PSTHs evoked by the the first instance of a social cue. Rank-dependent differences in the amplitude of first responses evoked by these cues are shown in Figure 4.2.

A summary response amplitude for each cell was defined as the absolute area under the curve (AUC) and a mixed effects linear model was used to test the effects of rank (indicated by significance labels) and brain area on the mean response amplitude, while controlling for correlations between cells from the same mouse (see Table 4.1 for detailed statistics). The amplitude of responses was generally higher during chemoinvestigation compared to tube test behaviours, while cell responses in dominants were generally higher amplitude than cells sourced from subordinates. Interestingly, the MPOA showed very weak population-wide responses to tube test behaviours with little difference in the response phase of the PSTH compared to the baseline phase, whereas VMH exhibited population-wide positive tuning to pushing and negative tuning to resisting. The modulatory effect of rank was significant

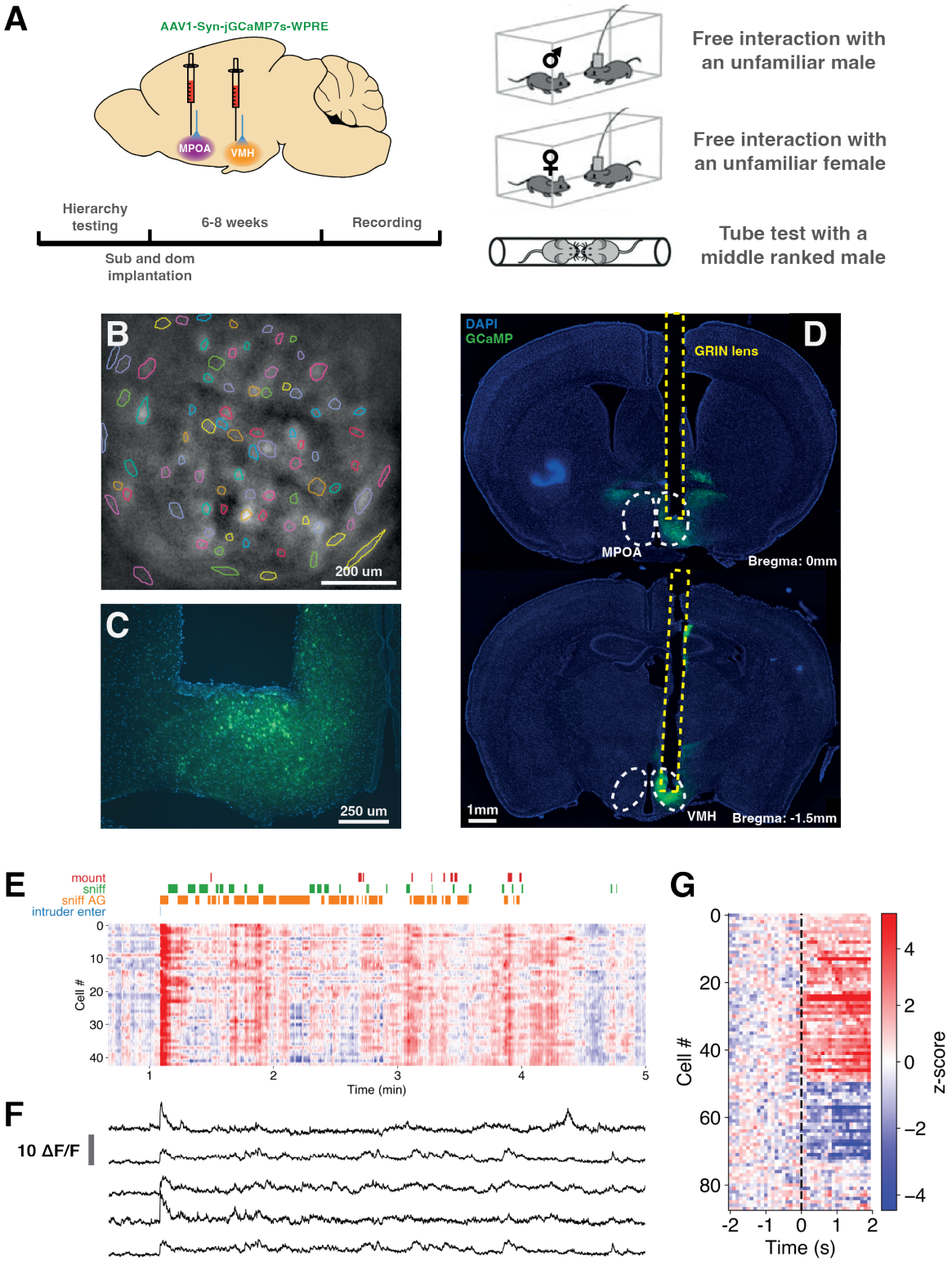

Figure 4.1: GRIN lens in vivo recording experimental pipeline. **(A)** Experimental design diagram. **(B)** Example FOV after preprocessing and cell detection. ROIs indicate the automatically detected and manually curated set of neurons **(C-D)** Example histology of the implantation sites. **(E)** Representative calcium recording during interaction with a female intruder with behavioural ethogram. The signal from each cell is interpolated to values between 0 and 1 for visualisation purposes. **(F)** Example raw activity traces from individual neurons from the recording in **E**. **(G)** Z-scored calcium activity surrounding a chemoinvestigation episode, with neurons sorted by tuning type (positive, negative and untuned).

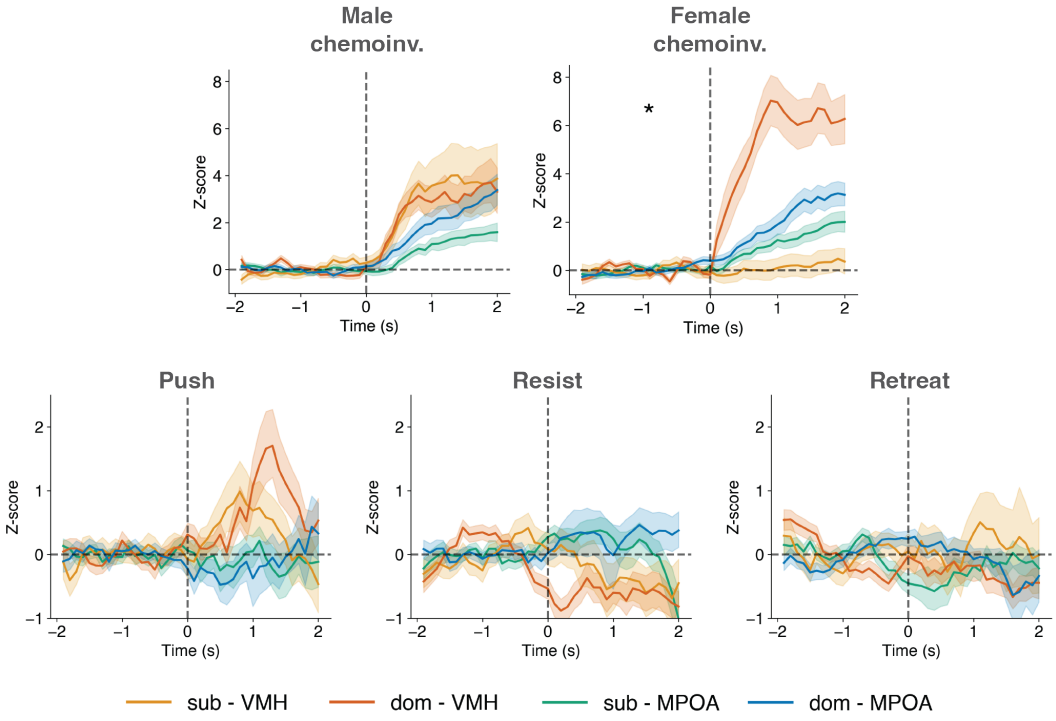

Figure 4.2: Dominance is associated with higher amplitude hypothalamic responses to female conspecifics. Z-scored PSTH diagrams during chemoinvestigation and tube test behaviours separated by social rank and brain area. The area under the curve of the response phase of the PSTH was used as a single-value estimate of the amplitude for each cell. Statistics indicate an effect of rank on response amplitude in a mixed-effects general linear model controlling for the effect of time and the source brain area of each cell ($N = 774$ cells, $N = 18$ mice, $N = 5$ mice for dom - MPOA, sub - MPOA, dom - VMH, and $N = 3$ mice for sub - VMH). Error shading represents 95% CI.

only during chemoinvestigation of females, but not during chemoinvestigation of male intruders or tube test behaviours. Brain area did not have a significant effect on response amplitude in any of the conditions. These data suggest that dominance increases evoked response gain when interacting with females in the same direction in both the VMH and MPOA.

4.4 Neuronal tuning

Previous work has shown that neural tuning properties in the hypothalamus can change due to internal states related to social experience (i.e., sexual experience) (Remedios et al., 2017). To investigate a similar mechanism of modulation by rank, the proportion of cells tuned to each of the social cues discussed so far was deter-

Table 4.1: Statistics for the mixed effects linear model predicting neural response amplitude from dominance rank and controlling for brain area.

	Rank				Brain area	
Behaviour	df - residuals	df - model	statistic	p	statistic	p
Male chemoinv.	767	3	0.74	0.462	1.19	0.235
Female chemoinv.	770	3	2.49	0.0128	0.94	0.346
Push	770	3	0.85	0.398	1.00	0.315
Resist	770	3	0.94	0.348	0.59	0.556
Retreat	770	3	0.61	0.541	0.50	0.618

Table 4.2: ANOVA statistics for the interaction between the effect of rank and tuning valence on the proportion of tuned neurons, while controlling for brain area.

	Rank				Brain area	
Behaviour	df - residuals	df - model	statistic	p	statistic	p
Male chemoinv.	47	6	0.74	0.482	< 0.01	1.0
Female chemoinv.	47	6	10.22	0.000206	< 0.01	1.0
Push	47	6	0.72	0.491	< 0.01	1.0
Resist	47	6	1.08	0.349	< 0.01	1.0
Retreat	47	6	< 0.01	0.991	< 0.01	1.0

mined in dominant and subordinate mice. A neuron was considered tuned to a cue based on a significant t-test between the baseline and response phases of the evoked PSTH. The sign of the t-statistic was used to determine the valence of the tuning, namely positive or negative with respect to the cue. The same neuron can therefore have multiple tunings depending on the stimulus. The percentage of cells with each tuning type for a given stimulus was then calculated for each mouse. Figure 4.3 shows the difference between the mean proportion of each tuning type in dominants and subordinates. A three-way ANOVA was used to test for an interaction between rank and tuning type when predicting the percentage of tuned neurons while controlling for the effect of brain area on tuning (See Table 4.2). A significant interaction between these terms was again found for tuning to female intruders, indicating that the ratio of positive to negative neurons moves in opposite directions depending on rank. Concretely, dominants have roughly 45% more positively tuned neurons in the VMH and 18% more in the MPOA compared to subordinates, suggesting a greater sensitivity to female social cues.

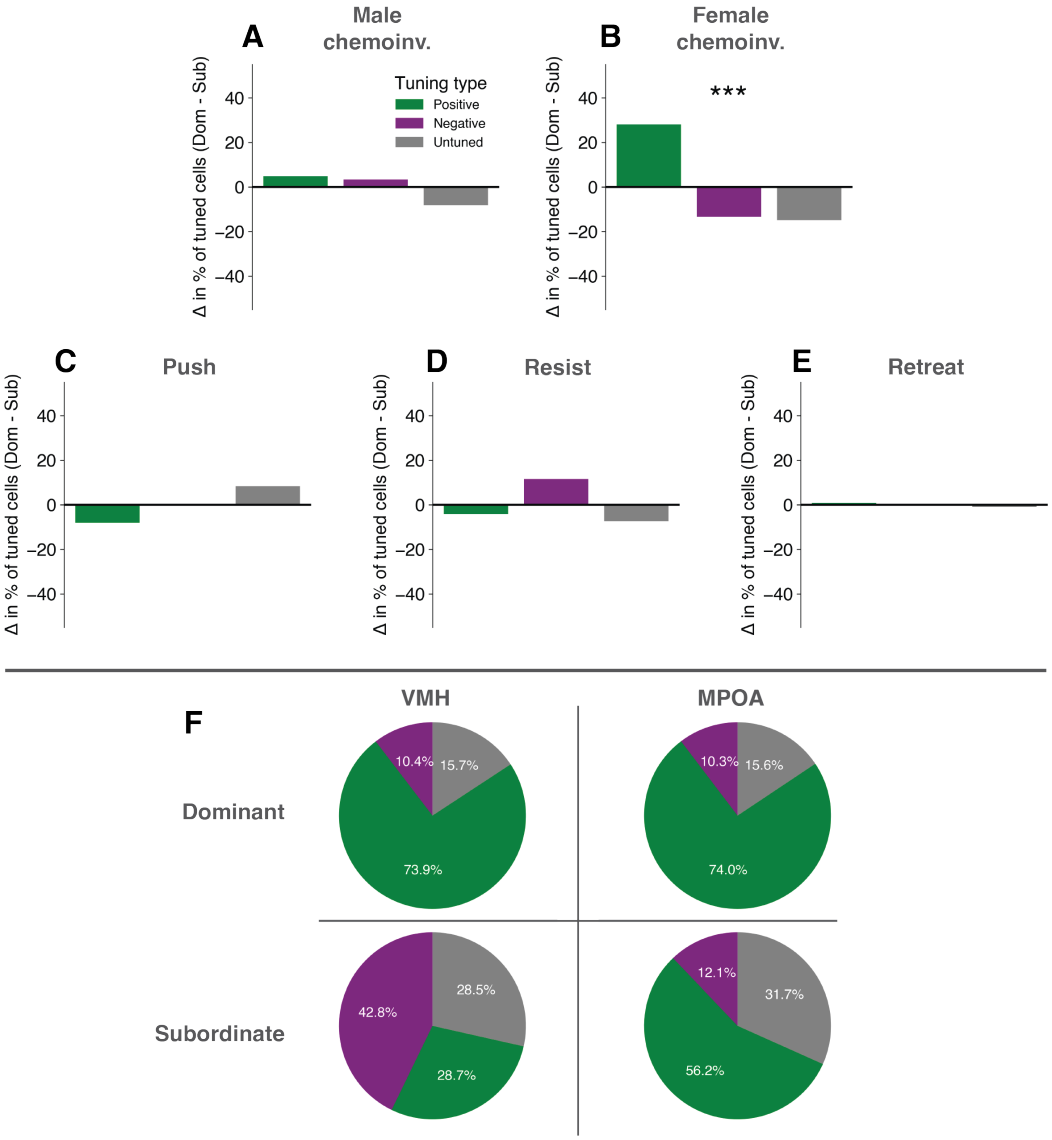

Figure 4.3: Dominants have more cells positively tuned and fewer cells negatively tuned to female conspecifics. **(A-E)** Differences in the mean proportion of neurons with positive, negative and neutral tuning between dominants and subordinates. Differences are shown across both the VMH and MPOA. Tuning is analysed for responses to chemoinvestigation of a male and female as well as pushing, resisting and retreating in the tube test. Statistics indicate a three-way ANOVA interaction effect between rank and tuning valence in predicting the proportion of tuned neurons in a recording ($N = 18$ mice). **(F)** The proportions of neurons of each tuning type in dominants and subordinates and in the VMH and MPOA during chemoinvestigation of a female intruder.

4.5 Behavioural correlates of modulation

In Chapter 3, I discussed that dominants have a higher behavioural interest in females and spend more time chemoinvestigating them. Given the evidence of hypothalamic gain and tuning modulation presented so far, I investigate whether these functional differences are also related to differences in behavioural phenotype, especially with regard to sexual behaviour. To that end, the mean evoked response amplitude ($F(1,16) = 3.48, p = 0.003$) and proportion of neurons positively tuned to the female intruder ($F(1,16) = 2.46, p = 0.0259$) was used to predict each male's duration of chemoinvestigatory interaction with that female (Figure 4.4). Both of these neural activity features significantly predicted the male social interest in the female, again without differences across brain areas, however, this relationship seems more robust in the VMH. Additionally, one of the VMH-implanted mice also exhibited sexual mounting of females and attack of male intruders during the recording. If hypothalamic amplitude and tuning modulation can result in a more robust approach to females, perhaps it can also improve the progression to sexual behaviour. Comparison of the response amplitudes in this mouse compared to controls shows that engaging in sexual behaviour ($t(279) = 3.37, p = 0.0008$), but not aggressive attack ($t(279) = 5.4, p = 0.591$), is associated with a higher response amplitude during the initial chemoinvestigation episode. These results are consistent with a lack of rank-dependent differences in aggressive behaviour or modulation of male intruder representations. Together these findings indicate that the rank-dependent differences in hypothalamic function can predict a sexual behavioural phenotype associated with dominance.

4.6 Representational Similarity Analysis

Both analyses of response amplitudes and tuning proportions suggest that female stimuli are more salient or rewarding compared to information about other males. This perhaps indicates a segregated representational space for female and male stimuli in the hypothalamus that would be necessary for distinct sex-specific behavioural responses, e.g., aggression towards male intruders and sexual behaviour towards fe-

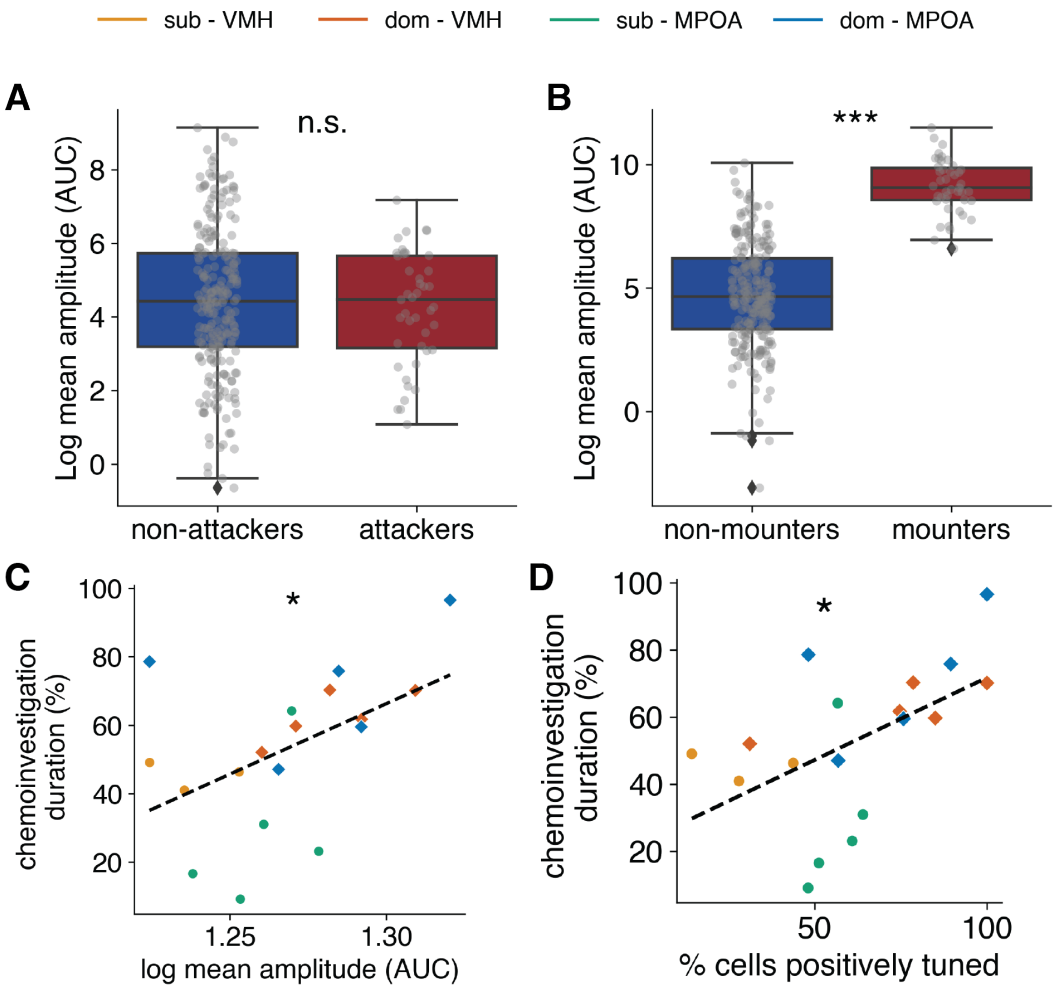

Figure 4.4: Higher response gain and tuning to female conspecifics in dominants predict chemoinvestigatory engagement and initiation of sexual behaviour. **(A)** Response amplitudes during the initial chemoinvestigation episode of a male intruder in mice that attacked the male intruder compared to non-attacking controls (attackers: $N = 43$ cells, 1 mouse, non-attackers: $N = 280$ cells, 7 mice). **(B)** Response amplitude during initial chemoinvestigation episode of a female intruder in mice that mounted the female compared to non-mounting controls. Data points indicate individual cells (mounters: $N = 43$ cells, 1 mouse, non-mounters: $N = 280$ cells, 7 mice). Both mounting and attack behaviours only occurred in the VMH cohort of recordings and hence only cells from this area are shown. Statistics indicate the results of mixed effects GLMs. **(C-D)** Linear regressions predicting the duration of female intruder chemoinvestigation based on the mean response amplitude **(C)** and the proportion of cells positively tuned to that behaviour **(D)**. Data points indicate mice ($N = 18$ mice). Error bars in panels **A** and **B** represent 95% CI.

male intruders. Indeed, other work has shown such segregation in terms of tuning in the VMH, focusing in particular on the role of sexual experience in increasing the proportion of VMH neurons exclusively tuned to one sex or the other but not both (Remedios et al., 2017). Nonetheless, some segregated tuning was still present in sexually naive males, supported by the results in this chapter and the ability of virgin males to distinguish the sexes and lead to opposite-sex sexual interest. The finding that low rank diminishes both response amplitudes and tuning to females therefore offers the hypothesis that male and female representations may be less segregated in subordinates, contributing to their lower sexual interest.

In this section the similarity of male and female intruder representations in the hypothalamus is analysed using two metrics: firstly, the proportion of neurons with mixed tuning for both sexes as opposed to selective tuning for one of the sexes (Figure 4.5) and secondly, the Euclidean distance between high-dimensional representations of the two sexes quantified using representational similarity analysis (RSA). Only mice where interaction with intruders of both sexes was recorded in the same session was used for these analyses, since finding cell correspondences across separate recording sessions can be unreliable. Mixed and sex-selective tuning was calculated as a proportion of the total number of tuned cells (excluding cells untuned to either male of female cues). Additionally, the cells in mixed tuning were separated into those that respond congruently to both male and female cues (e.g., excited by both sexes) or inversely (e.g., excited by males and inhibited by females). In both rank groups, the cells tuned to both sexes form the majority of the population compared to the cells tuned exclusively to only one of the sexes (Figure 4.5A). Proportions of mixed-tuned cells with congruent and inverse response patterns is very similar across ranks and therefore unlikely to drive a preference for female behavioural engagement. Contrary to the hypothesis, rank did not significantly affect the proportion of cells with mixed tuning (independent t-test: $t(11) = 2.09, p = 0.0605$). Nonetheless, there was a non-significant trend towards more mixed tuning in dominants and more selective tuning in subordinates. It is perhaps this trend which allowed a higher proportion of neurons with mixed

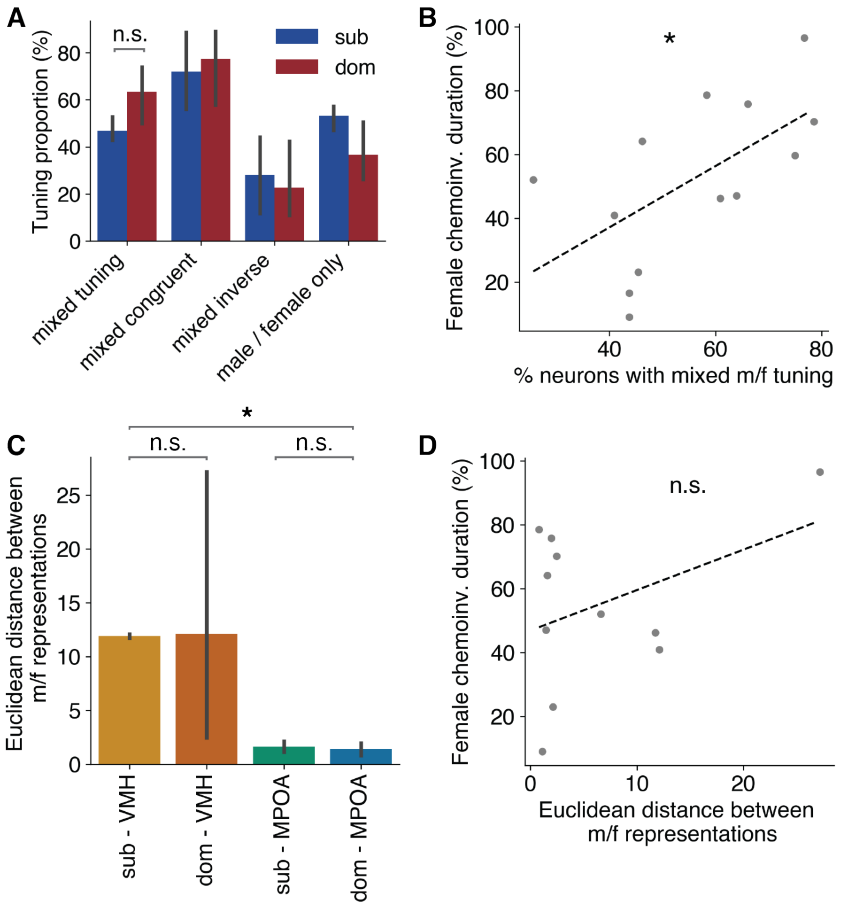

Figure 4.5: Representational separability of male and female conspecifics is not affected by dominance rank. **(A)** Comparison of the proportion of cells with mixed tuning for male and female conspecifics across ranks. Mixed congruent indicates the proportion of mixed cells with the same valence responses to both sexes, while mixed inverse indicates the proportion of cells with opposite valence responses to opposite sexes. Independent t-test, $N = 13$ mice, 6 dom, 7 sub. **(B)** The percentage of neurons with mixed-sex tuning predicts motivation to interact with females. Linear regression, $N = 13$ mice, 6 dom, 7 sub. **(C)** Euclidean distance between male and female representations across ranks and brain areas determined using representational similarity analysis. Two-way ANOVA, $N = 11$ mice, 6 dom, 5 sub. **(D)** The Euclidean distance between representations of male and female intruders does not predict the motivation to interact with females. Linear regression, $N = 11$ mice, 6 dom, 5 sub. Error bars in panels **A** and **C** represent 95% CI.

tuning to predict stronger behavioural engagement with female conspecifics (Figure 4.5B, linear regression: $p = 0.028$). In terms of Euclidean distance between representations obtained using RSA, a two-way ANOVA found more segregation in the VMH compared to the MPOA ($F(1,8) = 6.77, p = 0.032$), consistent with the differences in amplitude in Figure 4.2. However, within each area, rank does not affect the representational segregation of the sexes ($F(1,8) = 0.00006, p = 0.99$). In line with this finding, the Euclidean distance between representations of both sexes does not predict behavioural engagement with female conspecifics (linear regression: $p = 0.22$). In summary, based on two metrics there is no statistically robust evidence that dominance makes the representations of male and females more distinct in the hypothalamus. While a relationship between the proportion of cells with mixed tuning and behavioural engagement with females was found, this metric is insufficently associated with rank and could be a general feature of functional variability in the hypothalamus which does not arise from rank-dependent modulation.

4.7 Discussion

This chapter demonstrated an association between hgih dominance rank and enhanced hypothalamic tuning and excitability in response to female stimuli. Changes in both functional metrics predicted the male's chemoinvestigatory interest towards females as well as progression towards sexual behaviour. This suggests that the functional modulation of these areas my contribute to the rank-dependent behavioural differences investigated in Chapter 3. However, it also indicates an unexpected level of stimulus specificity, since it was initially hypothesised that widespread modulation of social stimuli would be observed. This could indicate that different social behaviours are modulated in anatomically segregated brain areas or that modulation of the sensory representation is specific to interactions with female conspecifics.

4.7.1 Limitations

There are two potential limitations of this analysis. Firstly, differences in responses to females may have been derived from the behavioural differences between ranks, where dominants could investigate the female more thoroughly and provide more sensory input to the brain. In vivo recordings of social behaviours certainly present unique challenges for robust separation of sensory-evoked responses from behaviour-associated activity. However, head-fixed recordings entail substantial ecological validity challenges when attempting to present social stimuli in a passive way, e.g., by presenting anaesthetised conspecifics or odorants such as urine. The freely-behaving paradigm was therefore preferred because it allows animals to explore others in a naturalistic way, while the sensory milieu of the conspecific is not limited through anaesthesia or by isolating a single sensory aspect chosen by the experimenter.

On the other hand, the strong responses associated with conspecific chemoinvestigation were not observed during free exploration of the home cage or inanimate objects such as food pellets. This suggests that chemoinvestigation-evoked responses largely reflect responsivity to social sensory stimulation rather than the act of chemoinvestigation itself. I therefore speculate that the rank-dependent differences in chemoinvestigation-evoked activity suggests a modulation of the sensory representation of social cues. In contrast, none of the tube test behaviour-evoked activities were modulated by rank, suggesting that there is no such thing as dominant or subordinate pushing or retreating. Once the behavioural decision is made, it appears to be represented and executed similarly in both groups. Additionally, the mean amplitude of the behaviour-evoked responses was substantially lower than the chemoinvestigation responses in both areas, suggesting stronger responsivity to sensory cues. I therefore propose that rank-dependent modulation of hypothalamic function primarily affects sensory rather than behavioural representations, although further experiments are needed to eliminate any behavioural contributions.

The second limitation is that rank-dependent differences may have been derived from the behaviour of the female intruders. Since estrus cycle states of the females were not monitored, some females in estrus may have been more sexually receptive than others and allowed more extensive chemoinvestigation by the female. While estrus cycle differences are certainly present in the dataset, they could not systematically vary depending on the dominance rank of the male resident. Estrus related behavioural and consequently activity related differences would therefore average out across the two dominance groups. A quantification of female intruder behaviour could address any remaining qualms about systematic variation in their behaviour.

4.7.2 The function of neuronal gain modulation

The example recording in Figure 4.1E shows that the amplitude of responses to bouts of chemoinvestigation decays over time along with the propensity of the resident to interact with the intruder. This suggests that the response amplitude may be conveying the salience or reward value of the conspecific, which declines as the resident becomes habituated to the intruder. In the context of rank, the higher amplitude responses in the dominants imply that they find female conspecifics more salient or rewarding, thus leading to a stronger motivation to interact with them behaviourally compared to subordinates. The modulation of response gain has been reported especially in the attention field with respect to sensory systems. A vigilant state associated with locomotion in mice results in depolarisation of the resting membrane potential in the V1 cortex, thus leading to increased spiking (Polack et al., 2013). This effect seems to be mediated by vasoactive intestinal peptide (VIP)-positive neurons in V1 as well as the auditory and barrel cortices in mice, whose activation in vigilant states induces the disinhibition of excitatory neurons (Fu et al., 2014). Work in V1 also showed that while there is a general increase in gain, there is also a decrease in the variability of the resting potential which decreases the rate of spontaneous firing (Polack et al., 2013). In this way, firing becomes more tightly tuned to a particular stimulus and the signal becomes less obscured by spontaneous firing. A similar mechanism may be at play in modulating the responses to social cues

in the hypothalamus. Indeed, work in the female VMH demonstrated an increased amplitude of male-evoked responses in sexually receptive compared to unreceptive females, along with an increase in positive tuning to male stimuli (Nomoto and Lima, 2015). Additionally, in the female MPOA, hormone-mediated response gain increases in neurotensin-expressing neurons led to increased interaction with male social cues (McHenry et al., 2017). Social status could therefore modulate male sexual motivation through an analogous mechanism.

The relationship between amplitude and interaction motivation was based on the total signal across all recorded cells in a mouse, suggesting that responses across the entire population may be integrated to determine the propensity to interact with the female. This mechanism would explain the differences in tuning as well - the higher proportion of positively tuned cells in dominants results in a higher amplitude of the summed responses across the population since the number of cells with subtracting inhibitory responses is lower. Both the MPOA and the VMH contain subpopulations, which trigger specific social behaviours in a projection-specific manner. By making more of these cells positively tuned to a conspecific, it biases the circuit towards producing a behavioural response and social engagement with the conspecific rather than no response at all. However, there is likely to be some selectivity in terms of subpopulations which experience increased excitability so that there is a bias towards dominant behavioural responses. While the molecular or functional identity of the cells was not available in my datasets, obtaining such information following miniscope recordings is possible, albeit technically challenging. The cells from in vivo calcium recordings can be registered to subsequently obtained single-cell RNA sequencing profiles (Xu et al., 2020). With this approach, it could be determined if response gain increases are constrained to cell subtypes which promote particular behavioural responses.

Chapter 5

Information encoding for hierarchical behaviour

5.1 Introduction

The previous chapter demonstrated that the VMH and MPOA are modulated by own dominance status. However, it remains to be seen whether these areas also represent the rank of the opponents as proposed in the information integration hypothesis. C-Fos studies by Nelson et al. (2019) showed that the VMH and MPOA show differential c-Fos expression in dominants compared to subordinates following several tube tests. This finding suggests the involvement of the hypothalamus in competitive behaviour in some capacity, however, it cannot reveal the exact variables that are being encoded. These differences could relate specifically to the relative frequency of tube test behaviours (i.e., pushing and retreating), it could also relate to the frequency of winning tests, the modulatory effects seen in the previous chapter, or representations of the opponent. This chapter therefore analyses the information encoding properties of these two areas in an effort to test the hypothesis that the hypothalamus integrates information about own and opponent dominance rank.

5.2 Encoding of variables relevant to competitive behaviour

5.2.1 Encoding of competitive context

A visual inspection of a recording containing a series of tube tests reveals temporally precise responses to the first contact with the opponent in the tube, but also a more stable signal presenting as binary state switching between episodes of tube testing and the intervening periods of free behaviour in the home cage (Figure 5.1). Furthermore, a visualisation of the population activity using principal component analysis (PCA) reveals distinct activity spaces inhabited during the tube test context and free home cage behaviour. This suggests encoding of a variable related to environmental context. Since these mice are very experienced with tube tests, they have likely formed an association between the tube environment and impending competition against a conspecific. A logistic regression model was trained to test whether this competitive context can be decoded from the population activity (Figure 5.1C). A two-way ANOVA testing for differences in decoder performance compared to a model trained on shuffled labels, while controlling for brain area was performed ($F(2,33) = 6.92, p = 0.003$). The real performance was significantly better than the shuffled data performance ($F(1,33) = 13.7, p = 0.0008$), while there were no differences in performance across brain areas ($F(1,33) = 0.1, p = 0.705$), showing that competitive context is encoded in both parts of the hypothalamus. Interestingly, the state probability extracted from the decoder indicates that the competitive state has a sharp onset when both mice enter the tube, and decays more slowly once the encounter is over (Figure 5.1D). This may be because the opponent is usually still in the vicinity and can sometimes attempt to reenter the tube and therefore still represent some level of threat.

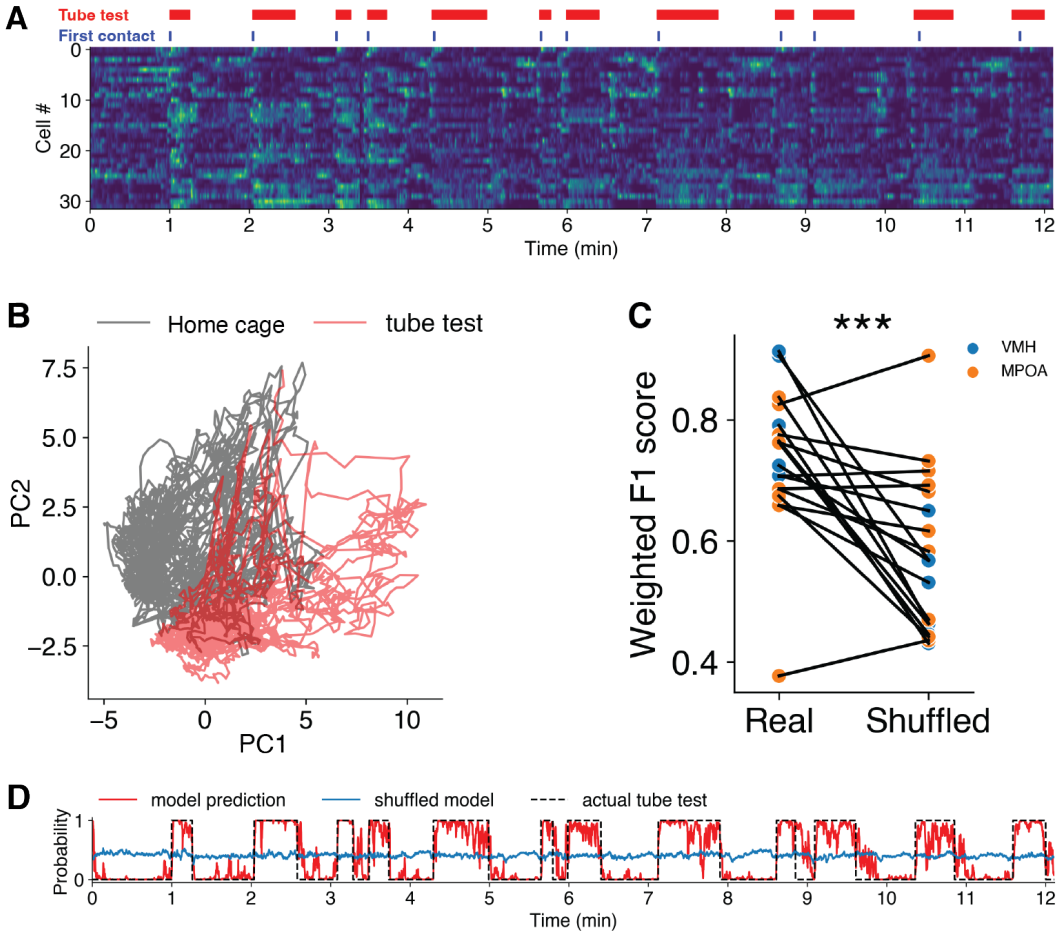

Figure 5.1: The tube test context has a unique representation in the hypothalamus. **(A):** Example VMH recording of a series of tube tests shows visually apparent state switching between testing episodes and intervening periods in the home cage. **(B)** Visualisation of the recording in **A** in PCA space shows separation between activity in the tube test context compared to the freely behaving home cage context. **(C)** Performance of a logistic decoder predicting whether the animal is in a tube test from hypothalamic activity. Two-way ANOVA: $N = 18$ mice, 10 MPOA, 8 VMH. **(D)** Decoder prediction of the tube test context from activity in **A**.

5.2.2 Encoding of tube test behaviours and winning

The competitive state appears independent of whether the tube test is actually won or lost. However, neural populations can encode multiple variables along orthogonal dimensions of population activity (Bernardi et al., 2020). Previous work has been able to decode tube test winning potential from the mPFC (Zhou et al., 2017; Padilla-Coreano et al., 2021), however, it has not been investigated whether this information is also passed down to subcortical areas involved in behaviour selection such as the hypothalamus. Indeed, labelling activity from winning and losing tube test trials in PCA space indicates minimal overlap suggesting that a "winning" state may also be encoded in addition to general competitive context (Figure 5.2A). To test this hypothesis, the same logistic model was fit to predict tube test outcomes. Only recordings that featured both winning and losing tube test trials could be used for this analysis, which was the case for 9 of the 18 animals recorded in total. A two-way ANOVA testing for performance differences between the decoder and a shuffled data model, while controlling for brain area ($F(2,15) = 19.4, p < 0.0001$), found tube test outcome decoding performance significantly better than the shuffled dataset ($F(1,15) = 37.0, p < 0.0001$) and no differences in performance between brain areas ($F(1,15) = 1.8, p = 0.203$, Figure 5.2C). Interestingly, an example model prediction in Figure 5.2E shows that predictions of the tube test outcome are accurate from the very beginning of the test, rather than becoming more reliable as the end of the tube test approaches. This could indicate that the mouse detects the rank of their opponent at first contact, determines their relative status, and foresees the eventual outcome of the encounter.

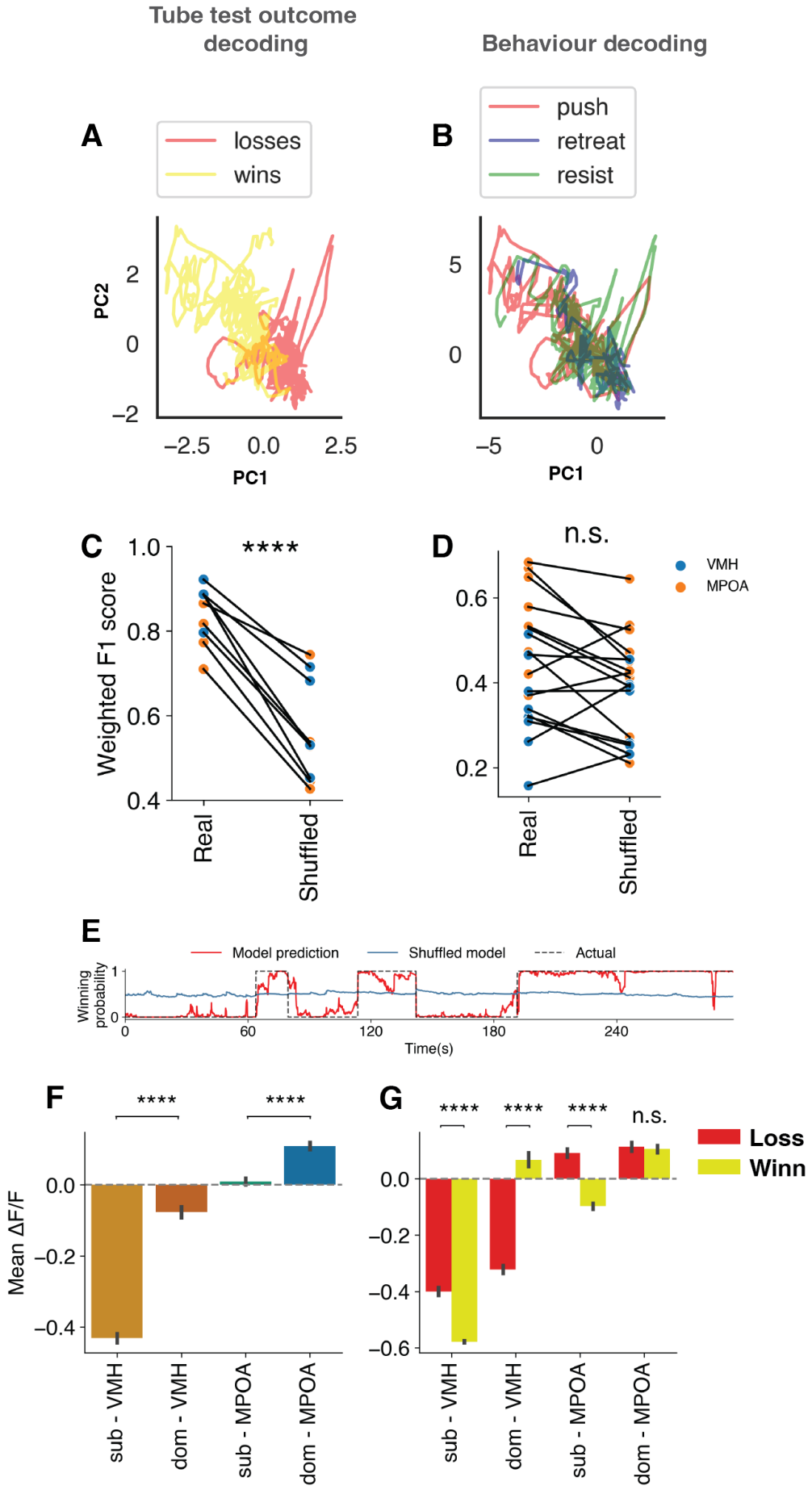
Tube test outcome decoding
Behaviour decoding
A
losses
wins
PC2
PC1
B
push
retreat
resist
PC1
C
****
Weighted F1 score
Real
Shuffled
D
n.s.
VMH
MPOA
Real
Shuffled
E
Model prediction
Shuffled model
Actual
Winning probability
Time(s)
F
****
****
Mean ΔF/F
sub - VMH
dom - VMH
sub - MPOA
dom - MPOA
G
****
****
****
n.s.
Loss
Winn
sub - VMH
dom - VMH
sub - MPOA
dom - MPOA

Figure 5.2: MPOA and VMH activity predicts tube test outcome, but not individual bouts of competitive behaviours. **(A-B)** Projections of population activity from the same animal into low dimensional space with respect to the two decoded variables. **(C)** Performance of the logistic decoder of tube test outcome (winning) from population activity. Two-way ANOVA: $N = 9$ mice, 5 MPOA, 4 VMH. **(D)** Performance of the logistic decoder of push, resist, and retreat behaviours from population activity. Two-way ANOVA: $N = 18$ mice, 10 MPOA, 8 VMH. **(E)** Decoder prediction of winning probability from population activity. **(F)** Mean fluorescence signal during the tube tests across ranks and brain areas. Statistics indicate mixed effects GLMs with Holm-Sidak correction. $N = 9$ mice, 5 MPOA, 4 VMH. **(G)** Mean fluorescence signal during tube tests separated based on winning. Statistics indicate mixed effects GLMs with Holm-Sidak correction. $N = 9$ mice, 5 MPOA, 4 VMH. Error bars represent 95% CI.

Both areas therefore encode two variables with slow dynamics - competitive context and winning state. While slow state encoding has been reported for the VMH, the MPOA is proposed to have comparatively rapid dynamics, exhibiting robust behaviour-evoked responses (Nair et al., 2023). Indeed, optogenetic manipulation of both areas demonstrated precise temporal control of specific social behaviours, suggesting that rapid behaviour-evoked activity could co-habit with more stable state variables. To investigate this second encoding role, the logistic decoder paradigm was used to predict individual behavioural episodes of pushing, retreating, and resisting behaviours. The representations of these three behaviours did not separate well in PCA space (Figure 5.2B) and the same ANOVA model ($F(2,33) = 8.2, p = 0.0013$) did not find decoder performance significantly above chance ($F(1,33) = 1.5, p = 0.157$, Figure 5.2D).

The MPOA and VMH therefore encode a slow competitive state rather than rapid behavioural changes in the tube test context. It also means that the winning state is not simply inferred from the frequency of either pushing or retreating behaviours in winning compared to losing trials. This result does not agree with previous studies into temporal dynamics of the two brain areas for which I propose several reasons: A technical source of this apparent discrepancy may be the relatively slow dynamics of the GCaMP construct (with a calcium transient duration of around 400 ms), compared to the very rapid nature of tube test behaviours. Pushing and retreat bouts can last less than a second and mice rapidly switch between these behaviours. In contrast, aggression and sexual behaviours in a freely behaving con-

text produce long and consistent bouts of behaviour with temporal progression, for example, from chemoinvestigation, to tail rattling, aggressive mounting, and finally to direct attack. These more consistent behaviours may be easier to resolve with the current calcium indicators. Furthermore, apparatus for tethered tube tests can result in frequent touching of the miniscope against the edges of the tube during behaviour, leading to motion artefacts. This deterioration of signal quality compared to freely behaving assays could obscure potentially weaker responses locked to behavioural bouts. Finally, these areas may simply employ a different encoding strategy for competitive behaviour compared to sexual or aggressive behaviour.

5.2.3 Hypothalamic activation during tube tests explains rank-dependent c-Fos differences in the VMH

Considering again the c-Fos differences reported by Nelson et al. 2019, these are most easily explained by an encoding of the winning state. Both dominants and subordinates enter the tube test, hence its encoding cannot produce distinct activations, while competitive behaviour frequency is different across ranks, but it is not encoded in these areas. Winning is the only variable whose frequency varies across ranks and is also encoded in the MPOA and VMH. Figure 5.2F shows the mean fluorescence signal across ranks and brain areas during the tube test. The VMH in subordinates is strongly inhibited compared to dominants in line with higher c-Fos expression in dominants. The differences are again smaller in the MPOA but in contrast with the c-Fos finding, where subordinates show higher MPOA c-Fos expression. This could be because c-Fos more accurately reflects the number of positively tuned cells, whereas the average fluorescence metric analysed here is affected by the amplitude of responses which is higher in dominants. A breakdown of activation signals based on the outcome of the tube test (Figure 5.2G) explains some of the general differences in VMH activation across ranks. While the subordinate VMH is inhibited irrespective of whether the mouse is winning or losing, there is a sign reversal in the dominant VMH, which is suppressed during losing and excited during winning. Furthermore, there are significant differences in the average fluorescence signal during winning and losing in the VMH of both ranks, which establishes a

straightforward criterion for the tube test outcome decoder. The situation is less clear in the MPOA, namely, subordinates exhibit MPOA activation during losing and inhibition during winning. Since subordinates are usually losing tests, this is consistent with high MPOA c-Fos activation in subordinates. There are no significant activation differences in the dominant MPOA. In this case, the decoder can rely on amplitude-independent features, such as identifying distinct subpopulations of neurons that are activated by winning compared to losing. Indeed, the distinct PCA activity subspaces inhabited by these two outcomes in Figure 5.2A shows that such features exist, since cell signals are standardised to a similar amplitude range before PCA transformation.

5.2.4 Social tuning properties of winner neurons

The linear decoder of tube test outcome allows the identification of neurons associated with winning and losing neurons based on the sign of their predictive weight in the model. A neuron's activation predicts winning when its model weight is positive and losing when it is negative. It was hypothesised that winner neurons may have other roles in social contexts that are not strictly competitive. For example, by also responding strongly to female stimuli they could constitute a single hypothalamic population that promotes not only competitive performance but a larger repertoire of dominant behaviours such as sexual interest in females. To interpret the role of these neurons in social interactions beyond competition in the tube test, the relationship between their model weight and their tuning to social cues was analysed in Figure 5.3. Tuning estimates were determined in the same manner as already seen in Chapter 4. Unfortunately, no significant relationship was observed with tuning to either female or male stimuli, or behaviours such as attack, sexual mounting or grooming (Table 5.1). The data also corroborates that encoding of the winning state does not rely on tuning to pushing, resisting, or retreating in the tube test. This suggests that the winning state is encoded as a unique representation in the hypothalamus that does not encompass other social states (e.g. sexual arousal) or specific behavioural programmes.

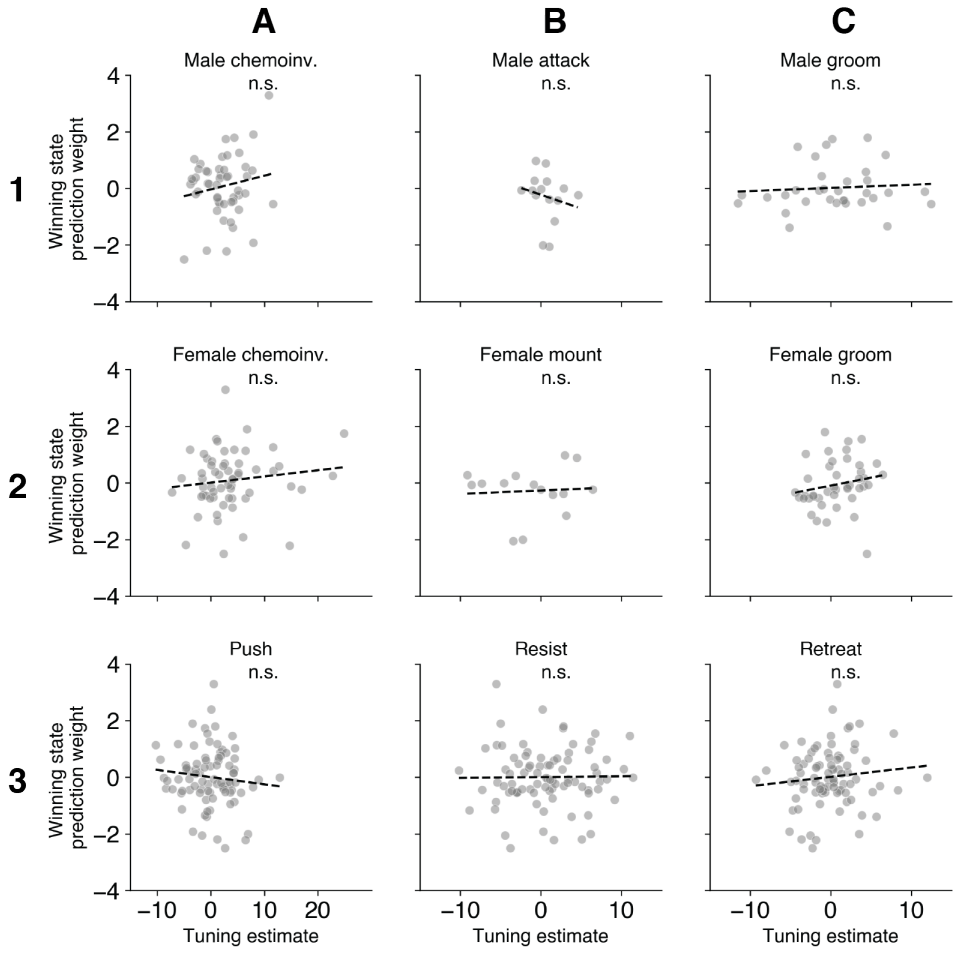

Figure 5.3: The tuning of winner neurons in noncompetitive social contexts. The weight of neurons in the tube test outcome decoder is correlated against estimates of their tuning to social cues and tube test behaviours. Significance symbols indicate the results of linear regressions with Holm-Sidak correction. $N = 334$ cells for tube test push, resist, retreat, male and female chemoinvestigation. $N = 43$ cells for male attack and female mount. $N = 97$ cells for male groom and $N = 154$ cells for female groom.

Table 5.1: Holm-Sidak corrected p-values for corresponding regression plots in Figure 5.3.

	A	B	C
1	0.555	0.765	0.901
2	0.688	0.924	0.555
3	0.688	0.924	0.687

5.3 Own and opponent rank encoding

So far rank has been treated as a variable that independently modulates social perception, however, adaptive hierarchical behaviour dynamically depends on the status of others as well. This is especially the case with middle-ranked animals, where the behavioural decision in the same circumstances can vary drastically depending on whether the opponent animal is just above or below one's own rank. Presumably, the brain must perform a subtraction between own and opponent rank and derive a representation of relative rank, which is perhaps the more behaviourally relevant variable. Studies so far have strongly focused on the encoding of own rank in the prefrontal cortex, however, this circuitry does not propose an obvious way in which own rank is integrated with representations of others. Extending the existing thalamocortical circuit into the hypothalamus offers an opportunity for an integration node, where the two information streams could meet. The following sections adopt a robust machine learning approach to determine which of these two variables are encoded in the VMH and the MPOA to test the model of the hypothalamus as an information integration node.

5.3.1 Encoding of own rank

5.3.1.1 Background

Based on the rank-dependent response amplitude and tuning differences observed in Chapter 4, it was hypothesised that this modulation of the representation of female social stimuli could be leveraged by a decoder to distinguish the own rank of an animal from hypothalamic activity. However, this approach faces the challenge that rank is stable within a recording session and activity samples for different ranks must therefore come from different animals. There is no direct correspondence between the recorded neurons from two different animals, meaning that there is no meaningful feature space for the decoder to use without first registering recordings from multiple animals into a common activity space. This is a non-trivial task, however, one approach used in the neural recording context is canonical correlation analysis (CCA) (Hotelling, 1936). This method leverages the assumption that dif-

ferent individuals use the same neural dynamics to produce a specific behaviour or sensory encoding (Safaie et al., 2023; Gallego et al., 2020). Recording a brain area produces a random sampling of the neurons, meaning that there is no direct correspondence between recording channels across animals, however, the underlying neural dynamic should still be recoverable in each random sample, provided that it is large enough. This leads to the conclusion that there exists a latent space in which neural activity from different animals is highly correlated. CCA optimises such a common latent space by maximising the Pearson correlations between the activities of two or more animals in that space (Figure 5.4). These correlation estimates also provide a direct measure of the representational similarity across animals.

5.3.1.2 Method validation

While the feature spaces do not have to be the same for CCA, the datasets must be temporally aligned. Since my recordings were freely behaving without a trial structure, the datasets were aligned based on the behavioural annotations of chemoinvestigation of male and female intruders. It has previously been reported that CCA correlations across animals performing the same behaviour are higher than across animals performing different behaviours consistent with the hypothesis of a signature neural dynamic for each behaviour (Safaie et al., 2023). This result was replicated in Figure 5.5, where activity is significantly more correlated across mice in the response portion of the behaviour evoked PSTH, when the animals are performing the same behaviour, compared to the baseline portion where behaviour is not synchronised across animals. A three-way ANOVA testing for differences in CCA correlation between the baseline and response phases of the behaviour-evoked signal while controlling for CCA mode and area ($F(3,1017) = 38.0, p < 0.0001$) found a significant main effect of behavioural synchrony on cross-animal correlations. ($F(1,1017) = 27.2, p < 0.0001$). Additional post hoc analyses found this to be the case in both the MPOA ($p < 0.0001$) and VMH ($p < 0.0001$, Tukey's correction). This serves as a confirmatory result for the validity of the method and that activity alignment across animals using behaviour-evoked PSTHs is meaningful. Only the response portions of the PSTHs were used from here onward for the evaluation of rank encoding.

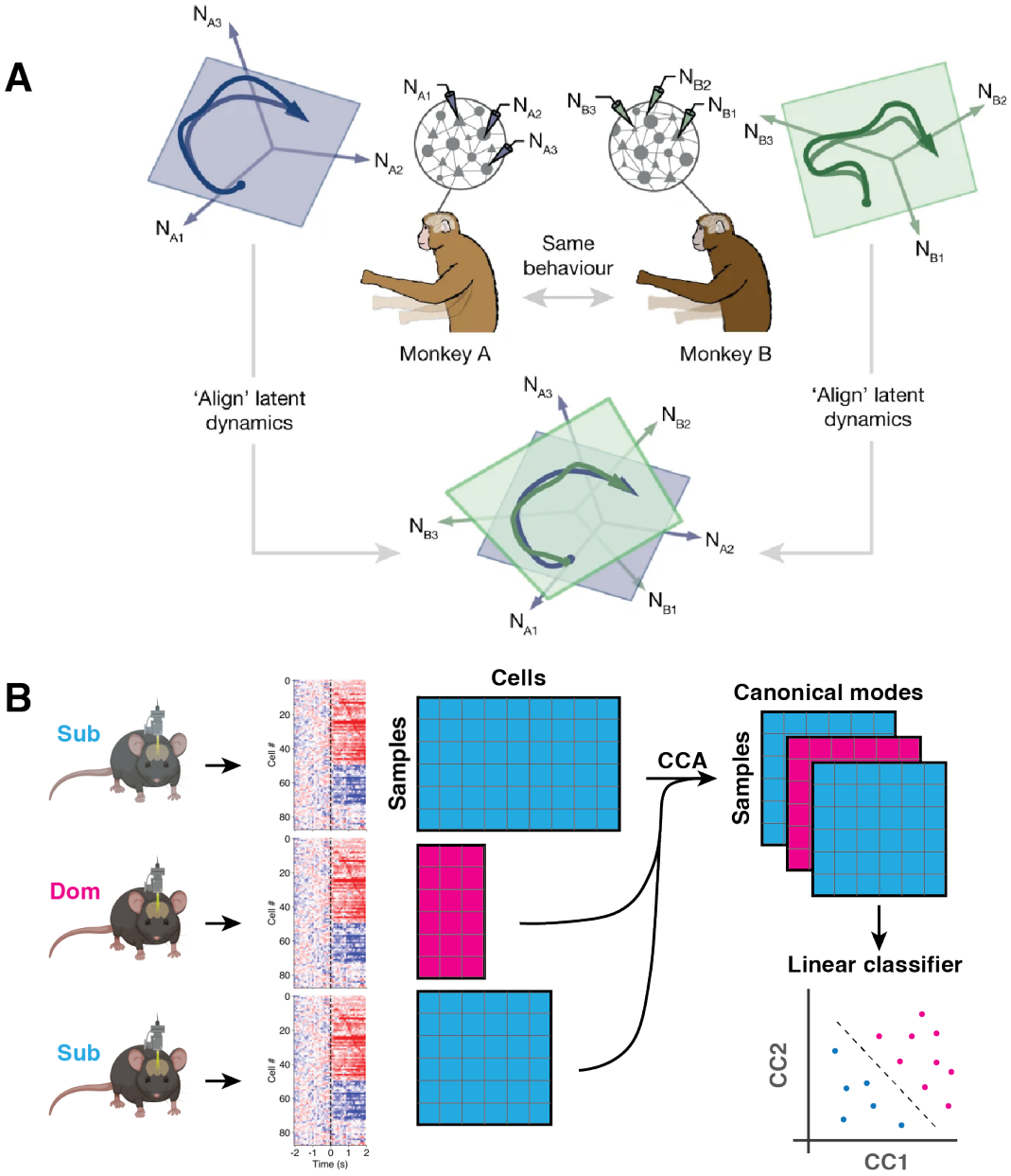

Figure 5.4: Canonical correlation analysis allows the identification of correlated latent variables across datasets with distinct feature spaces. (A) Two animals performing the same behaviour employ the same latent dynamics to perform the behaviour. While there is no direct correspondence between the neurons recorded in each animal, identification of correlated latents that exist in both animals allows alignment into a single common latent space. Adapted from Safaie et al. (2023) **(B)** Schematic of the own rank decoding strategy, illustrating the co-registration of cell sets from distinct mice into a single latent space using CCA, thus allowing the application of a linear classifier to decode the dominance rank of a mouse based on activity. Created using BioRender.com

5.3.1.3 Cross-animal correlations

The encoding of own rank was tested using two approaches using the CCA method: Firstly, mice of the same rank (rank congruent) are expected to have more correlated representations of conspecifics compared to mice of opposite ranks (rank incongruent). This was tested by co-registering the activity spaces of pairs of mice that were either rank congruent or incongruent and comparing the mean representational correlation estimated by CCA in these two groups. The canonical correlations between each pair of animals was 10-fold cross-validated. Figure 5.5 shows the representational correlations between rank congruent and incongruent pairs of animals. A three-way ANOVA testing the effect of rank congruence on representational correlations across mice while controlling for CCA mode and brain area ($F(3,507) = 52.8, p < 0.0001$) did not find a main effect of congruence ($F(1,507) = -0.54, p = 0.588$). Consequently, post hoc analyses for individual brain areas were not conducted.

5.3.1.4 Own rank decoding from a common latent space

The second approach was to co-register all mice into a single activity space and train a classifier to distinguish neural activity samples derived from dominant versus subordinate mice (Figure 5.4B). The activity trajectories associated with female chemoinvestigation in dominant and subordinate males is visualised in Figure 5.6, where the common CCA latent space has been further reduced in dimensionality using PCA for visualisation purposes. Consistent with the correlational analysis, the baseline activity inhabits a distinct part of the activity space, compared to the evoked responses in males of either rank. A support vector machine (SVM) classifier was able to distinguish the baseline and response phases of the PSTHs with high accuracy (permutation test: $p = 0.0039$ for both the VMH and MPOA, Holm-Sidak corrected). In contrast, there was a high overlap between the trajectories coming from animals of opposite ranks; consequently, the SVM classifier was unable to decode the rank of a male based on evoked responses to female conspecifics (permutation test: $p = 1.0$ for VMH, $p = 0.586$ for MPOA, Holm-Sidak corrected).

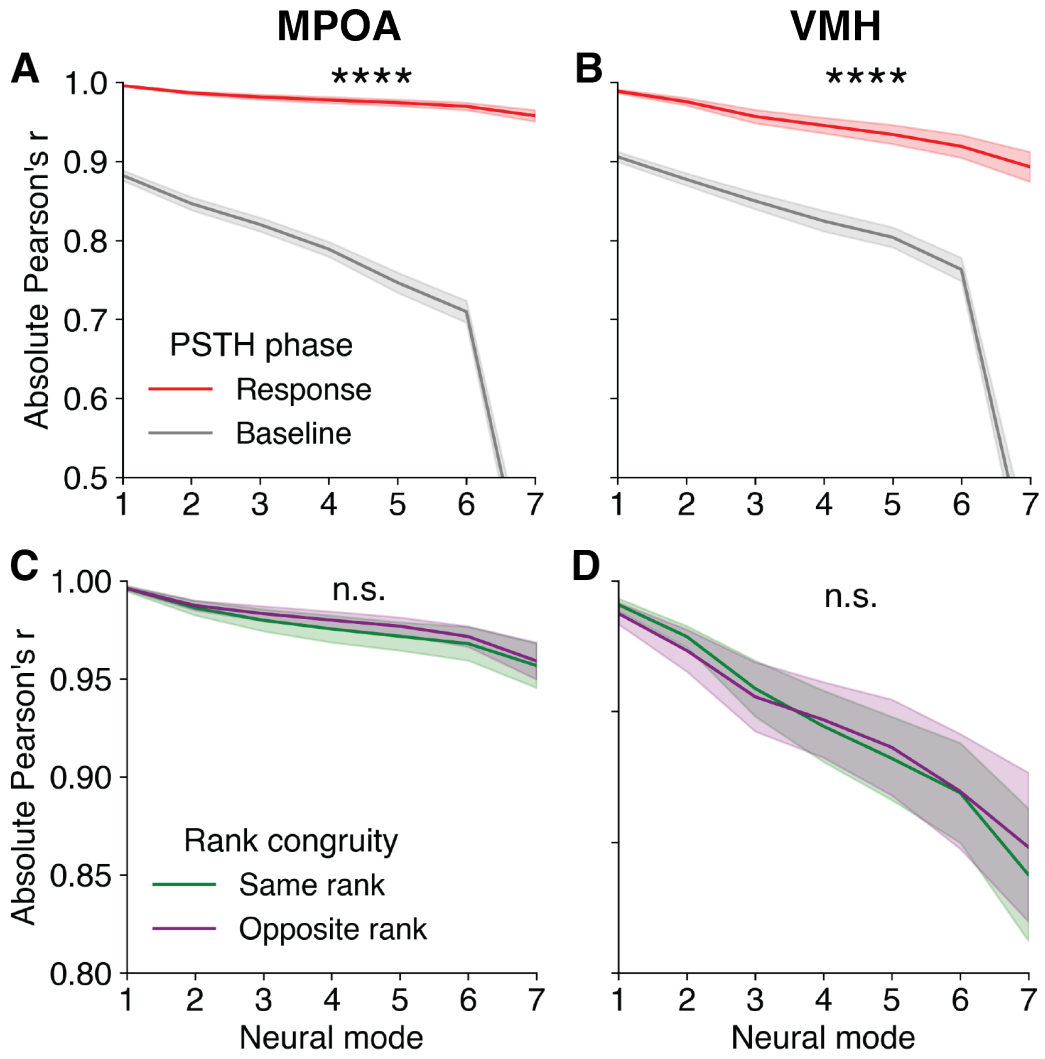

Figure 5.5: Hypothalamic representational similarity across males of the same or opposite dominance ranks using canonical correlation analysis. (A-B) CCA correlations across animals during behaviourally synchronised response phase of the evoked response, compared to the non-synchronised baseline phase in the MPOA ($N = 45$ animal pairs) and VMH ($N = 28$ animal pairs). Three-way ANOVA **(C-D)** CCA correlations across mice of the same rank or opposite ranks during chemoinvestigation of a female in the MPOA ($N = 30$ animal pairs) and VMH ($N = 26$ animal pairs). Three-way ANOVA. Error shading represents 95% CI.

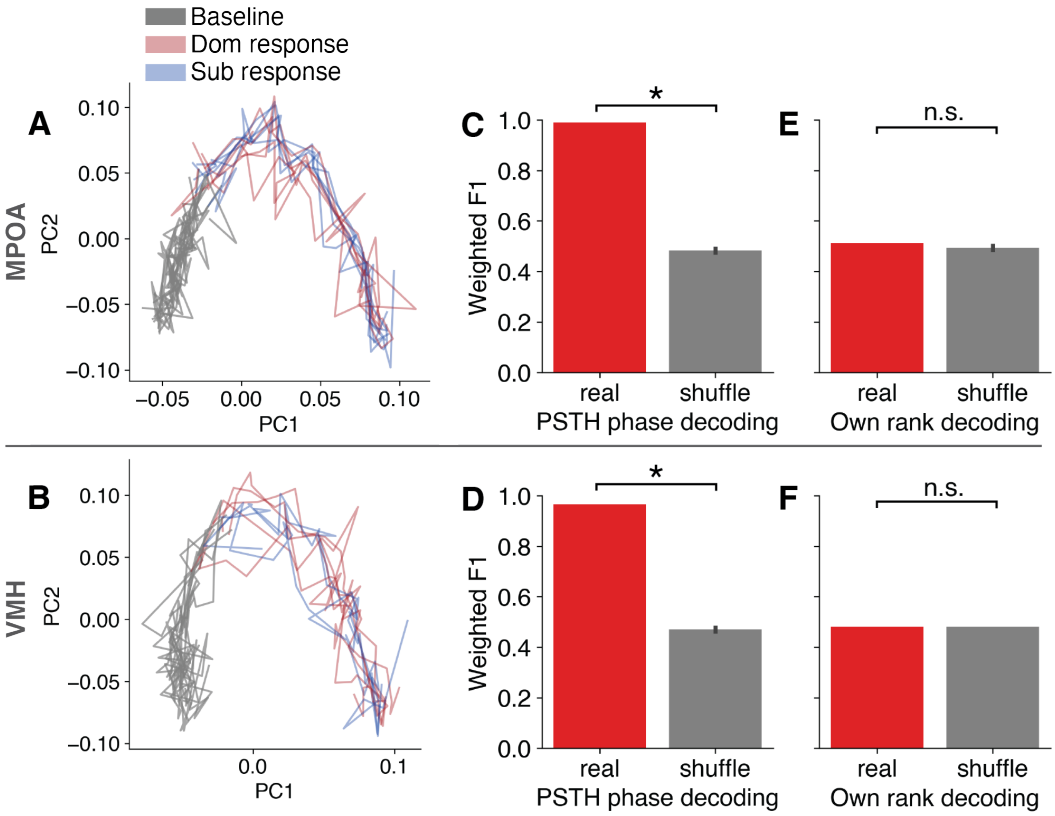

Figure 5.6: Decoding of own dominance rank from evoked responses to female conspecifics. **(A&B)** Visualisation of activity trajectories in response to female conspecifics in common CCA latent space visualised using PCA. Grey trajectories indicate the baseline phases of the PSTHs, whereas the red and blue trajectories show the dominant and subordinate response PSTHs phases respectively. $N = 10$ mice in MPOA group, $N = 8$ in VMH group. **(C&D)** Performance of an SVM classifier distinguishing the baseline and response phases of the PTSH. Permutation test, $N = 10$ mice in MPOA group, $N = 8$ in VMH group, 100 permutations. **(E&F)** Performance of an SVM classifier predicting own dominance rank from responses to female conspecifics. Permutation test, $N = 10$ mice in MPOA group, $N = 8$ in VMH group, 100 permutations, Holm-Sidak correction. Error bars represent 95% CI.

Interestingly, neither of the two CCA approaches showed evidence of own rank encoding in the hypothalamus in response to female social stimuli. The response amplitude-related differences reported in Chapter 4 are removed through feature standardisation before fitting the CCA model, hence any differences between ranks in CCA space would have to rely on distinct activity dynamics independent from signal amplitude. This is sufficient to preserve the temporal structure of the evoked responses since baseline and response PSTH phases are clearly separable but insufficient to decode own dominance rank. This leads to the conclusion that rank-dependent modulation in the hypothalamus primarily involves differences in the magnitude of responses to social stimuli, but not dynamical properties such as manifold topology or temporal evolution of the response.

5.3.2 Encoding of opponent rank

5.3.2.1 Background

In Chapter 3, I presented evidence that olfactory input is necessary to detect rank information about conspecifics. Past work has demonstrated sensitivity of the amygdalar and hypothalamic areas to pheromonal cues (Dhungel et al., 2011; Samuelsen and Meredith, 2009; Meredith, 1998) since they receive both volatile and non-volatile olfactory input (Dulac and Wagner, 2006), while work by Lee et al. (2021) provides additional support for the MeA and the VMH in particular as encoders of opponent rank. This study documented differential c-Fos expression in response to the presentation of urine derived from dominant or subordinate mice that were either familiar or unfamiliar to the subject mouse. Brain areas such as the premammillary nucleus, which only respond differently to familiar urine cues therefore likely encode social identity rather than dominance signals generally and can be excluded as candidates. The areas showing c-Fos differences in response to unfamiliar urine were the MeA, both subdivisions of the VMH and the ventrolateral periaqueductal grey (vlPAG), but not the MPOA. The vlPAG is involved in motor programme execution and might therefore reflect the differences in behavioural responses to urine of different ranks, such as avoiding dominant territorial markings. Conversely, the VMH and MeA have demonstrated sensory encoding functionality and therefore make for suitable candidates for encoders of opponent rank.

While this c-Fos study provides useful insights into potential candidates for opponent rank encoding, the tool itself lacks the temporal precision to demonstrate the encoding of any variable without follow-up functional recordings. Two papers with such recordings in the mPFC (Padilla-Coreano et al., 2021; Kingsbury et al., 2019) have indirectly investigated opponent rank encoding: The study by Padilla-Coreano et al. (2021) claims to separate relative dominants from relative subordinates using mPFC activity during reward-oriented competitive behaviour. This suggests an encoding of relative rank in the cortex, in other words, that both own and opponent rank variables are present there or are already integrated at an earlier node. The decoder was trained on activity trajectories from different mice registered into the same space using an adaptation of PCA, however, the way in which this was achieved is unclear since PCA alone is insufficient for the co-registration of distinct feature spaces. Even putting technical considerations aside, it is difficult to exclude the possibility that this analysis simply relies on an encoding of own rank (since that is very informative about relative rank in most encounters) or the encoding of effortful tube test behaviours (i.e. pushing), the encoding of which has previously been demonstrated in the mPFC (Zhou et al., 2017; Kingsbury et al., 2019). In the study by Kingsbury et al. (2019), the authors find that the mPFC activities are correlated across two mice competing in the tube test. They find that this partially results from cells tuned to the behaviour of the opponent mouse, demonstrating that the mPFC contains representations of opponent behaviour. A similar result was found for the VMH, where mirror-like cells were found that respond to both own and opponent aggression (Yang et al., 2023). However, none of these studies attempted to explicitly decode the rank of the opponent, which is addressed here.

5.3.2.2 Decoding strategy and generalisation requirements

A machine learning approach was adopted to train a classifier and predict the rank of an opponent conspecific based on the sensory representation in the hypothalamus of the recorded mouse. However, it is important to avoid the pitfall of allowing the model to use social identity to distinguish the opponents rather than their rank. If the hypothalamic representation of each conspecific is very high-dimensional and unique (consistent with the encoding of social identity), then it is possible to decode any arbitrary grouping of these conspecifics. In contrast, if the encoding is low-dimensional it is only possible to separate the conspecifics along a few activity axes, which are likely to correspond to more abstracted variables, such as conspecific sex, age, or indeed dominance rank (Bernardi et al., 2020). To address this, it is necessary to impose strict generalisability constraints on the decoder.

Figure 5.7A shows the paradigm used here: three male intruders of each rank were sequentially presented in a resident-intruder assay, where the recorded mouse was allowed to freely chemoinvestigate the intruders. The extracted population representations of each intruder visualised in Figure 5.7C show distinct patterns of neural activations for each intruder that resemble a combinatorial code. This raises the possibility that the classifier can detect a combinatorial encoding of each opponent, rather than amplitude-based encoding, where opponent rank correlates with the amplitude of the response. The ideal low-dimensional encoding space in this paradigm would allow the separation of intruders by rank, but different mice of the same rank would have overlapping representations. Training only on data from two of the intruders and testing on the taken-out third animal forces the decoder to learn a general representation of conspecific rank that is not specific to the unique identity signature of the two mice from the training data.

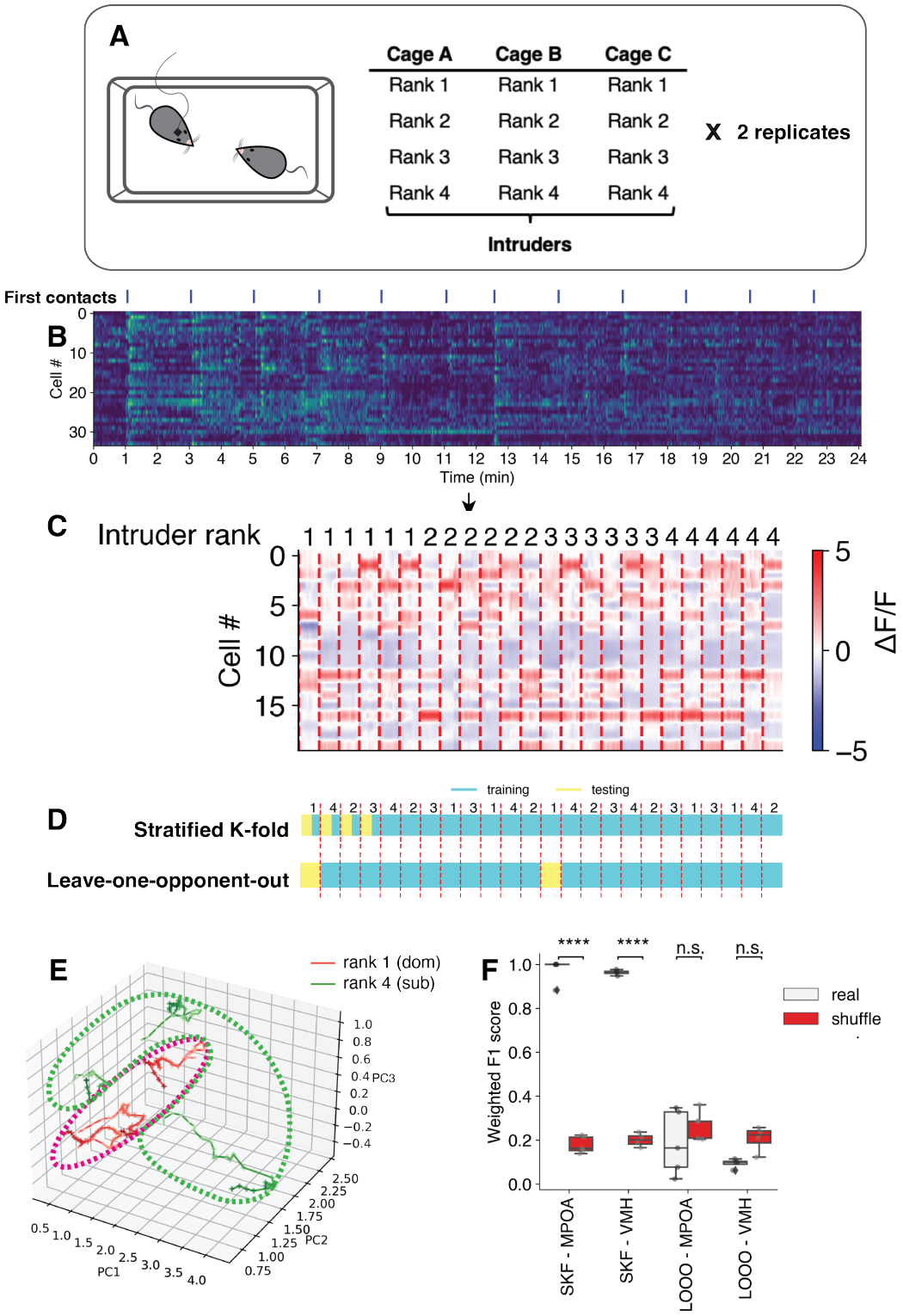
A
Cage A
Cage B
Cage C
Rank 1
Rank 2
Rank 3
Rank 4
X 2 replicates
Intruders
First contacts
B
Cell #
Time (min)
C
Intruder rank
Cell #
ΔF/F
D
training
testing
Stratified K-fold
Leave-one-opponent-out
E
rank 1 (dom)
rank 4 (sub)
PC1
PC2
PC3
F
Weighted F1 score
real
shuffle
****
****
n.s.
n.s.
SKF - MPOA
SKF - VMH
LOOO - MPOA
LOOO - VMH

Figure 5.7: Decoding of male intruder rank from hypothalamic activity. **(A)** Experimental paradigm diagram showing the full set of unfamiliar intruders introduced to the recorded mouse's cage in a resident intruder paradigm. The presentation order was randomised. **(B)** Truncated example recording showing evoked responses to initial chemoinvestigatory contact with each intruder. The signal from each cell is interpolated to values between 0 and 1 for visualisation purposes. **(C)** Extracted first contact responses for each intruder sorted by intruder rank (not in order of presentation). **(D)** Graphical comparison of two cross-validation strategies. Leave-one-opponent-out entirely removes all activity data pertaining to one of the intruders. This ensures that the model must learn a general representation of rank, rather than relying on social identity. The same intruder is presented twice, and data from both presentations is removed from training. **(E)** Example intruder representation trajectories in PCA space show very good separation between intruders, but also poor overlap between multiple intruders of the same rank, suggesting that each intruder is represented uniquely. **(F)** Logistic classifier performance using both cross-validation strategies. Permitting reliance on social identity to infer rank using the stratified K-fold strategy results in excellent performance, but the LOOO strategy does not perform better than the shuffled model. $N = 9$ mice, $N = 5$ MPOA, $N = 4$ VMH. Paired t-tests with Holm-Sidak correction. Error bars represent 95% CI.

This was achieved through a simple adjustment of the usual model cross-validation procedure: by leaving out all activity samples pertaining to one of the opponents in each of the cross-validation folds (leave-one-opponent-out or LOOO), the classifier performance reflects whether a previously unseen opponent (rather than individual activity sample) can be classified correctly in terms of rank. In contrast, stratified K-fold (SKF) based cross-validation allows distinct activity samples representing the same intruder to be simultaneously in the training and testing datasets (Figure 5.7D). Figure 5.7F shows the performance of the opponent rank classifier using both data splitting approaches. SKF results in extremely good classifier performance which indicates that neural representations of different opponents are very well separable, however, it is unclear whether this is due to social identity encoding or rank encoding (paired t-tests: MPOA - $t(9) = 31.2, p < 0.0001$, VMH - $t(7) = 54.6, p < 0.0001$, Holm-Sidak corrected). In contrast, performance using LOOO is not significantly better than decoding from shuffled data (paired t-tests: MPOA - $t(9) = 0.9, p = 0.434$, VMH - $t(7) = 3.0, p = 0.112$, Holm-Sidak corrected) indicating that the left-out opponents do not have a general rank representation in common with the training data intruders, in other words, every intruder is represented uniquely.

5.3.2.3 Assay refinements and dimensionality reduction

The difficulties in obtaining a generalisable encoding of opponent rank could result from the significant sources of variability with the potential to obscure signals related to opponent rank in this paradigm. Notably, there is behavioural variability in the way the recorded mouse investigates the opponent - their motivation to investigate falls somewhat throughout the assay, while anogenital chemoinvestigation can elicit stronger responses than sniffing other parts of the conspecific. Mice also rapidly switch between investigations of the home cage and of the intruder which is likely reflected in the activity. Additionally, manual annotation of sniffing used clear contact between the two mice as a criterion, however, olfactory cues could already be detected earlier from a distance. There is of course some degree of behavioural annotation error in time - representations that are similar, but shifted in time could lead to poorer decoding performance. Finally, there is clear decay in the response amplitudes to new intruders as the assay progresses (see Figure 5.7B for example). This is after bandpass spatial filtering of the recordings which should remove bleaching effects, suggesting that repeated presentation of intruders results in habituation and decreased salience. This results in variable intruder representation depending on when in the assay an intruder is presented.

To address some of these sources of variability, two adaptations of the original assay were trialled (Figure 5.8). The first simply replaces the resident-intruder paradigm with the tube test paradigm. It was expected that since the tube test forces an antagonistic encounter with a binary outcome, the chances of the opponents becoming less salient over time are lower. Additionally, it should ensure more reliable and unambiguous chemoinvestigatory contact, especially during pushing. The second approach dispenses with behavioural confounds entirely by anaesthetising the recorded animal and presenting urine belonging to opponents of different ranks. This allows for experimenter-controlled presentation of the stimulus. In addition to technical improvements, it is possible to analytically remove sources of noise or non-target variables from the data using dimensionality reduction (DR) methods. The hypothalamus encodes more than one variable - even if opponent rank encod-

ing is present, there is concurrent encoding of competitive context and winning state as discussed earlier in the chapter as well as other internal states such as aggression and sexual receptivity. Even if the intruder representations are higher-dimensional than ideal for the decoder, the data can be preprocessed to remove dimensions that contain irrelevant information. To this end, PCA was used as an unsupervised linear DR method, a basic autoencoder (AE) as an unsupervised non-linear method, and partial least squares (PLS) as a supervised linear method (Figure 5.8). In the PCA approach, the 3 principal components explaining the most data variability were retained for the decoder, while discarding the remaining components. The autoencoder constrained that data representation to 3 bottleneck neurons, therefore resulting in the same final dimensionality as PCA. PLS was used to find a single latent dimension which regressed well against opponent rank. With all three methods, the lower-dimensional latent space was fit only on the training segment of the cross-validation split, while the testing segment was projected to this latent space using the neuron weightings obtained from the training fit. A three-way ANOVA testing for effect of brain area, assay type and dimensionality reduction method on opponent rank decoder performance ($F(6,73) = 3.1, p = 0.00942$) only found a significant main effect for DR method ($F(3,73) = 5.6, p = 0.0016$), but not assay type ($F(2,73) = 0.8, p = 0.447$) or brain area ($F(1,73) = 0.2, p = 0.687$). Post hoc comparisons of DR methods did not find significantly different performance compared to no dimensionality reduction at all after Tukey's correction for multiple comparisons.

Another consideration was that the logistic model treats the opponent rank as a categorical variable, when it is in fact ordinal and does not recognise that rank 2 is closer to rank 1 compared to rank 4. Equally, model evaluation using the F1 score does not recognise that while a model classification of a rank 1 opponent as rank 2 is incorrect, it is closer to the true label than a prediction of rank 4. While the logistic decoder may fail to obtain better than chance classification performance when predictions are evaluated in a binary manner - i.e., as correct or incorrect - these predictions may still be closer to the true opponent rank than a random clas-

sification. To address this, an ordinal logistic decoder was implemented. Unlike the ordinary logistic decoder which fits a separate binary classifier for each rank label and chooses the one with the highest probability, the ordinal model fits a single set of feature weights and a set of thresholds which separate the ordinal categories. In addition, the performance of the ordinal model was evaluated using the ordinal mean absolute error, which calculates the mean distance between the true and predicted classification. The performance of this model is shown in Figure 5.8D. A three-way ANOVA testing for differences between the model performance and the shuffled control with pairing between results from the same mouse did not find a significant effect ($F(1,8) = 0.03, p = 0.866$). There were also no differences between brain areas ($F(1,8) = 0.3, p = 0.577$). Together, these results do not support the hypothesis that the hypothalamus contains a generalisable representation of opponent dominance rank.

5.3.2.4 Identity encoding

The conclusion that every intruder is represented uniquely is compatible with a social recognition function, where the area represents individual identities. An additional anecdotal observation during these experiments was that recorded mice became less interested in intruders that were all from the same cage. This behavioural effect was remedied by never presenting intruders from the same cage one after another, but it nevertheless suggests that mice can detect not only individual identities but also the group that a conspecific belongs to. In this section, I analysed whether the individual identity of the intruders or the cage they belong to can be decoded from the same data and the same leave-one-opponent-out generalisation requirement (Figure 5.9). Interestingly, neither cage identity (paired t-tests: MPOA - $t(5) = 1.3, p = 0.542$, VMH - $t(4) = 1.3, p = 0.542$, Holm-Sidak corrected) nor individual identity (paired t-tests: MPOA - $t(5) = 2.7, p = 0.112$, VMH - $t(1) = 1.3, p = 0.542$, Holm-Sidak corrected) can be decoded significantly better than the shuffled model. This suggests that hypothalamic representation of the same intruder varies drastically between presentations and perhaps more accurately reflects the instantaneous social interest in the conspecific rather than any features related to their identity.

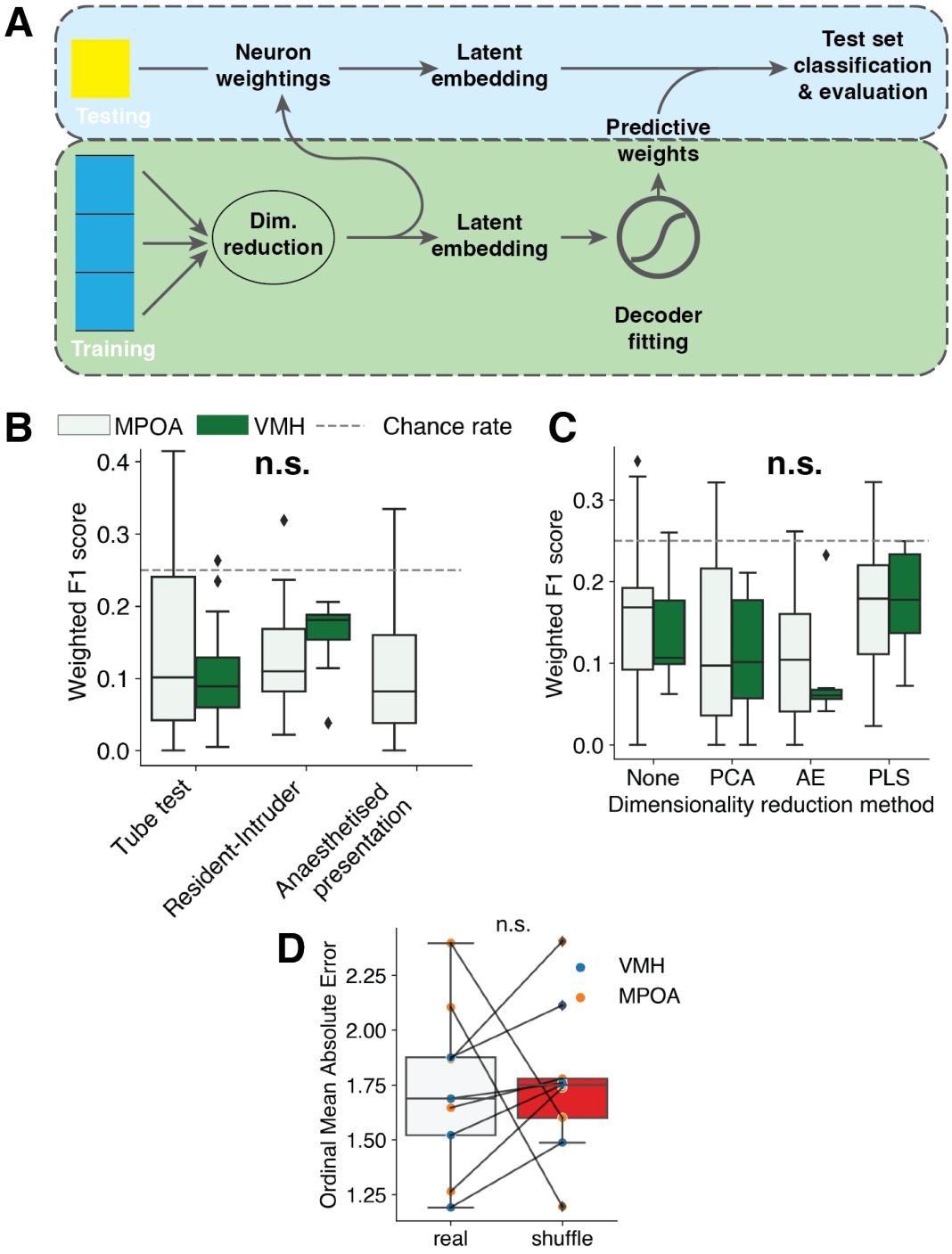

Figure 5.8: Effects of assay refinements and dimensionality reduction on opponent rank decoder performance. **(A)** Diagram of the decoder cross-validation procedure including learning of a lower-dimensional latent space from the training folds and projection of the testing fold into the latent space using the resulting neuron weights. **(B)** Performance differences between assay paradigms and brain areas. Three-way ANOVA, $N = 12$ mice for the resident-intruder assay, $N = 8$ mice for the tube test, and $N = 3$ mice for anaesthetised presentation. **(C)** Performance differences between dimensionality reduction methods compared to raw activity recordings. Three-way ANOVA, $N = 12$ mice. Significance labels in **B** and **C** indicate ANOVA main effects of assay type and dimensionality reduction method type in decoder performance respectively. **(D)** Performance of the ordinal logistic model in decoding intruder rank in the resident-intruder paradigm. Three-way ANOVA, $N = 9$ mice. Error bars represent 95% CI.

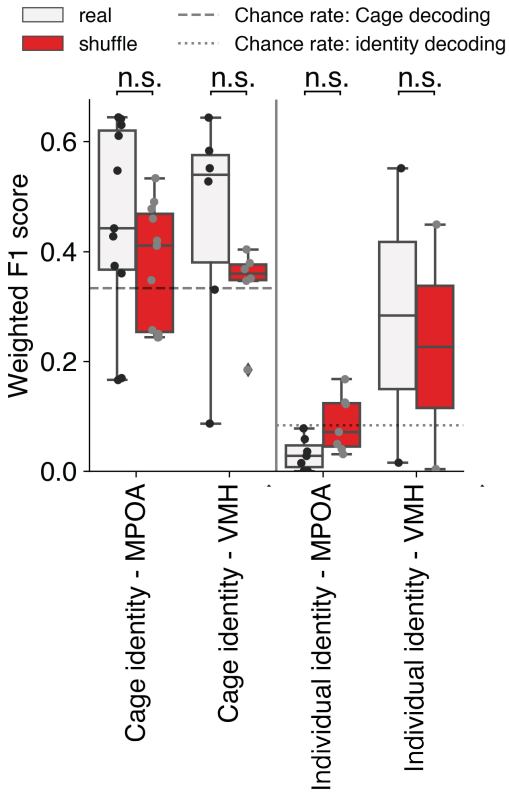

Figure 5.9: The hypothalamus does not encode social identity or cage identity of intruders. Performances of a logistic decoder classifying the cage identity or individual identity of male intruders. The chance rates differ between the two variables since the classifier can choose between 12 intruder identities, but only 3 cage identities, hence chance success is higher in the latter case. Paired t-tests with Holm-Sidak correction. $N = 6$ MPOA mice for both decoded variables, $N = 5$ VMH mice for cage identity decoding and $N = 2$ VMH mice for individual identity decoding. Error bars represent 95% CI.

5.4 Discussion

To produce adaptive hierarchical behaviour, an animal must detect the sensory signature of conspecifics in the environment. It must then extract the rank of these conspecifics, which is a more abstract variable invariant to the exact identity of the conspecific. This information can then be combined with knowledge of one's own status to construct a representation of relative rank. In parallel, the environmental circumstances are processed to determine whether the context is competitive (e.g. food is scarce and the mouse is hungry). In a competitive context, relative rank and perhaps other circumstances such as energy levels or previous injuries are used to

assess the likelihood of winning, thus producing a winning or losing state to promote either antagonistic or defensive behaviour. The aim of this chapter was to position the two hypothalamic nodes in this information hierarchy. Since neither encoding of own or opponent rank was found for either area, but encodings of competitive context and winning state were both robust, the hypothalamus is a more downstream node than initially hypothesised.

5.4.1 Competitive context encoding

Encoding of context has been observed especially in studies involving training in distinct and recognisable environments, for example, the colour of the assay box signalling to the mouse to perform a particular behaviour or conveying the task rules in the environment (Smith and Bulkin, 2014). Here there is also a degree of spontaneous training to the tube test environment which signals an antagonistic encounter with a conspecific. The behavioural response to a conspecific may vary drastically depending on context. For example, if food is abundant the presence of a conspecific near a food source may not be perceived as threatening and the two animals may ignore each other or even engage in affiliative interactions. In contrast, the same conspecific may be perceived as a threat when food is scarce and the context is therefore competitive. The competitive state may facilitate the engagement of more antagonistic behaviours such as aggression, non-aggressive demonstrations of strength, for example, tail rattling in mice, or defensive behaviours such as escape and freezing. Context in non-social paradigms has been shown to promote memory in learning. For example, recall of two lists of items is better if each list was learned and recalled in a separate environment (Smith and Bulkin, 2014). Encoding of the competitive context may serve an analogous function in learning one's own status. The context of the tube (and other environments associated with past competition) could allow easier recall of previous test experiences, whether they were won or lost and against which opponents.

There are also some alternative explanations for why the tube test context can be decoded. For example, the activity could reflect the unique sensory environment of the tube (e.g., the haptic feedback of being spatially constrained) or the dis-

tinct behavioural repertoire in the test. The latter scenario is less likely since I also showed that the hypothalamus does not represent the behavioural features of the tube test with sufficient fidelity for behavioural decoding. It could perhaps reflect unrelated behaviours, such as self-grooming in the home cage, however, this could not be tested since home cage behaviours were not recorded. The encoding of the unique sensory environment is a more probable explanation, however, that is effectively the same as the definition of environmental context. Nonetheless, it remains to be seen whether the contextual encoding seen here is completely unique to the tube test or whether it generalises to any competitive context. This can be tested by recording activity in multiple competition assays, determining whether competitive context can be decoded for all assays and if so, how much overlap there is between the cells that predict it in different tests. Ideally, a context encoder trained on the tube test would seamlessly generalise to activity in other assays.

5.4.2 Winning state encoding

The encoding of the winning state provides a straightforward explanation of the rank-dependent differences seen in c-Fos studies (Nelson et al., 2019; Lee et al., 2021). This is especially because both dominants and subordinates rapidly switch between pushing and retreating behaviours. The associated c-Fos signatures would be therefore present in both groups and less likely to result in a significant expression difference. In contrast, at the extremes of the hierarchy mice have a strong bias towards winning or losing tests, thus resulting in a more consistent activation difference. Furthermore, the differences in mean fluorescence signal in winning and losing trials in the VMH are consistent with the activation differences seen in the c-Fos data. Encoding of winning performance has previously been reported for the dmPFC (Zhou et al., 2017; Padilla-Coreano et al., 2021). Assuming that the thalamocortical dominance circuit is the primary encoder of own rank and the subcortical areas receive rank information as a modulatory input, the competition-relevant information in the hypothalamus could have its source in the mPFC. In this scenario, an animal's competitive performance could be controlled through prefrontal projections to the hypothalamus, as has been described for other subcortical areas (Franklin et al., 2017).

5.4.3 Limitations of own and opponent rank decoders

While several different approaches were taken to try to decode both own and opponent rank and the result is therefore convincing, there are some method limitations to discuss. One potential reason why CCA failed to find a latent space in which dominant and subordinate representations separate is that the method aims to find ways in which datasets are similar rather than to identify differences between them. Indeed, the high correlation between datasets along a latent serves as the very justification that it constitutes the same latent with the same dynamics in both datasets. Additionally, CCA has a dimensionality reduction aspect, since the canonical components can at most have the dimensionality of the original dataset with the smallest feature set (number of cells). Canonical components are ordered by correlation, meaning that the later components are more likely to contain the differences between the datasets. But since dimensionality was capped to 7 modes, these later components potentially containing rank-dependent variability have been removed.

An intuitive explanation for the high-dimensionality of the opponent encodings are behavioural afferent signals. It has been well documented that the majority of brain areas, including those that do not have a motor or behaviour execution function and including sensory brain areas, contain signals related to behaviour (Steinmetz et al., 2019). This has also been the assumption here, hence the attempts to reduce behavioural variability by using a more constrained assay - the tube test - over free chemoinvestigation and dispensing with behavioural confounds entirely through anaesthesia. The amount of representational variability remained very high in awake tube test recordings, while there were no convincing evoked responses to the urine presentations in the anaesthetised recordings. Perhaps the only approach that addresses both issues is an awake head-fixed recording with a controlled stimulus presentation, however, this is technically complex and would require some modification to the lens implant to allow fixation. Conversely, the assay and analytical adaptations reported here allowed the easy reuse of the same mice and data without custom apparatus.

Perhaps better decoder performances would be achieved by setting a less ambitious goal of decoding only the relative rank of the opponent. Indeed, there was an underlying assumption that relative rank representations must be derived by the animal from representations of the absolute ranks of both itself and the opponent. But making such estimates of absolute rank could be challenging for the mouse and it could use some heuristic to arrive at the relative rank directly. That said, the decoding of relative rank was not possible with this dataset, since the implanted animals were either of the highest or lowest rank, meaning that all opponents were either relatively lower or higher ranked than the recorded animal. Nevertheless, establishing whether a representation of absolute rank is even needed to understand relative rank is an interesting avenue for future research.

5.4.4 Functional alternative to the integration node hypothesis

If the hypothalamus does not encode opponent rank or even social identity, what about the conspecific does it actually encode? Certainly, the responses to the conspecific are very robust at least in awake recordings so they must carry some kind of information. There are two possible conclusions: either the encoding of opponents is in fact very high-dimensional, variable and contaminated with behavioural and internal state signals, or there is low-dimensional structure in these representations, but for a variable that was not measured here. Novelty or salience are good candidates for such as variable. While all presented opponents were unfamiliar to the recorded resident, there was a clear decline in signal amplitude towards the end of the assay, suggesting perhaps a decline in novelty in the task of repeatedly chemoinvestigating intruders. As discussed in Chapter 4, variability in response amplitude likely correlates with stimulus salience. But setting amplitude aside, why is the combination of neurons activated by each intruder in Figure 5.7C always different? This variability could be related to the other encoded variables, namely competitive context and winning state. In Figure 5.3 it was investigated whether these variables activate subpopulations of neurons which are also tuned to specific behavioural responses, namely, attack and sexual mounting. The MPOA and VMH drive such

social behaviours in a projection-specific manner, hence a winning state could already prime a particular behavioural response. However, no such association was found, although knowledge of the molecular identities of the cells would make this analysis more reliable.

Chapter 6

The circuit basis of rank-dependent modulation

6.1 Introduction

Chapter 4 demonstrated rank-dependent modulation of social perception, however, the origin of this modulatory input and it's circuit basis are unknown. The circuit model illustrated in Figure 6.1 proposes the known thalamocortical circuit as the encoder of a semi-stable dominance state, which in turn projects to and modulates the function of several subcortical areas involved in behavioural decision-making. Such monosynaptic modulatory input from the mPFC has been demonstrated through manipulation studies for several subcortical areas. For example, mPFC projections to the PAG (Franklin et al., 2017), NAc (Fetcho et al., 2023) and LH (Padilla-Coreano et al., 2021). The PAG is associated with behavioural (motor) programme execution, whereas the NAc encodes social reward (Dölen et al., 2013), a more upstream function in both the anatomical and computational sense. This suggests that mPFC projections carrying rank information modulate several computationally distinct nodes along the social pathway. It was therefore hypothesised that analogously to other subcortical structures, the most likely source of the modulatory effects in the MPOA and VMH may also be monosynaptic input from the mPFC. Less work

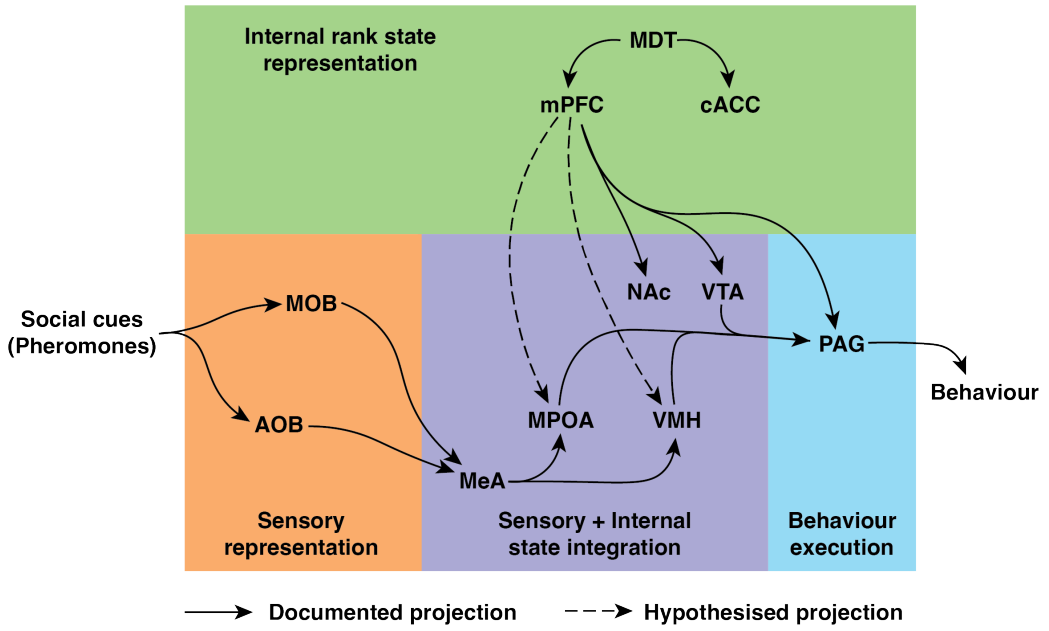

Figure 6.1: Circuit diagram of the subcortical nodes associated with social behaviour selection and the status-encoding thalamocortical circuit providing modulatory input.

has been done on cACC projections in the dominance context, however, this area may possess similar downstream projections that functionally oppose or moderate the mPFC inputs. This circuit model is tested in this chapter using a combination of anterograde viral tracing experiments to determine the existence of cortical projections to the MPOA and VMH, combined with optogenetic manipulation of these projections.

6.2 Viral tracing

The mPFC has several subdivisions along the dorsoventral axis: the rostral ACC most dorsally, followed by the prelimbic area (PL) and the infralimbic area (ILA) most ventrally. Recent work has mostly focused on the two dorsal areas (rACC and PL) as the dominance encoding areas (referred to below as dorsomedial prefrontal cortex or dmPFC), hence these subdivisions were targeted in the tracing experiments in Figure 6.2 in addition to the cACC. Shown are the most spatially constrained and accurate injections which do not contain visible projections in the hypothalamus. In addition, several other AAV serotypes and injection volumes were

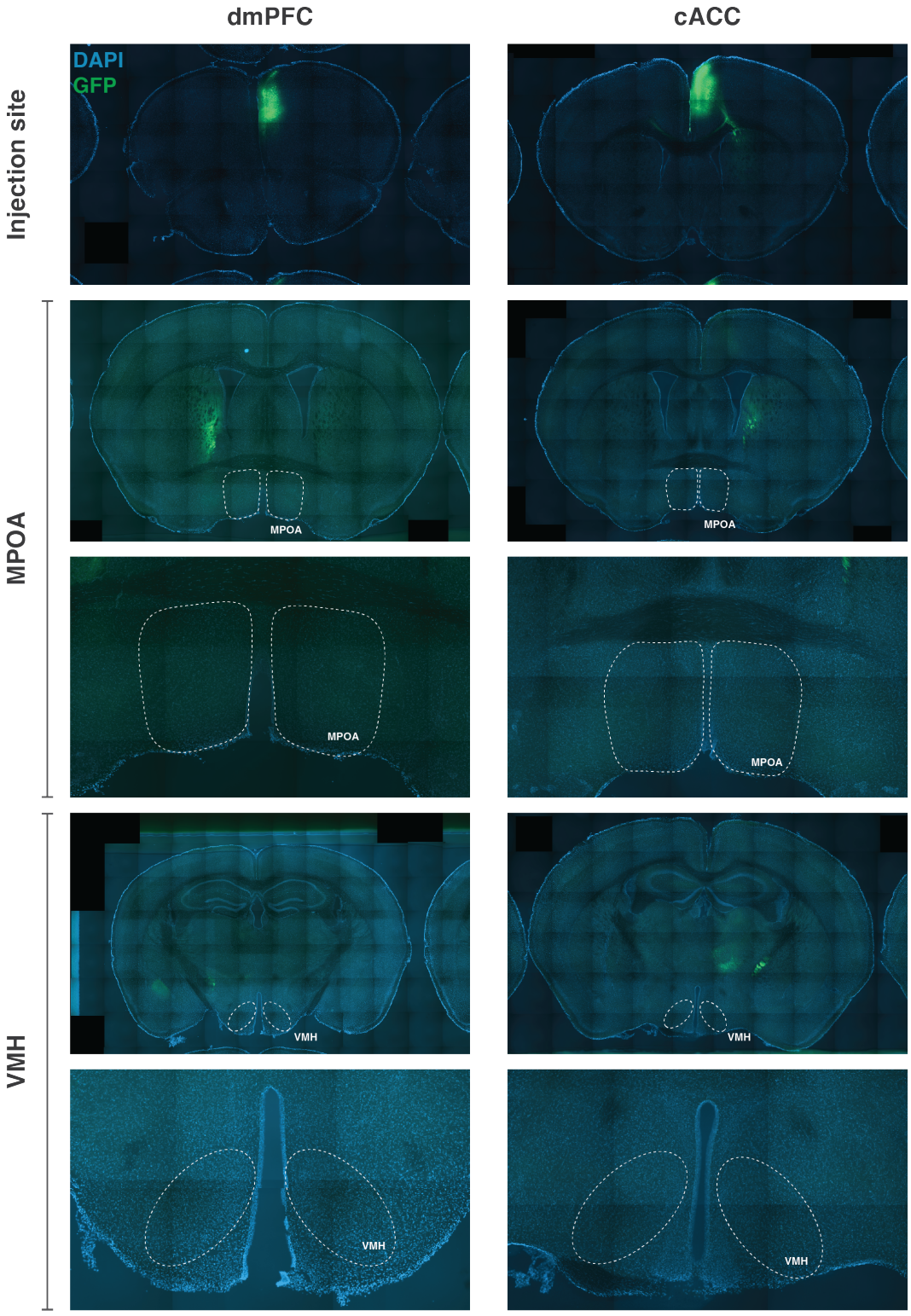

Figure 6.2: The dmPFC and cACC do not have notable projections to the hypothalamus. Epifluorescent miscroscopy of coronal brain slices injected with an AAV carrying a fluorescent tracer (GFP).

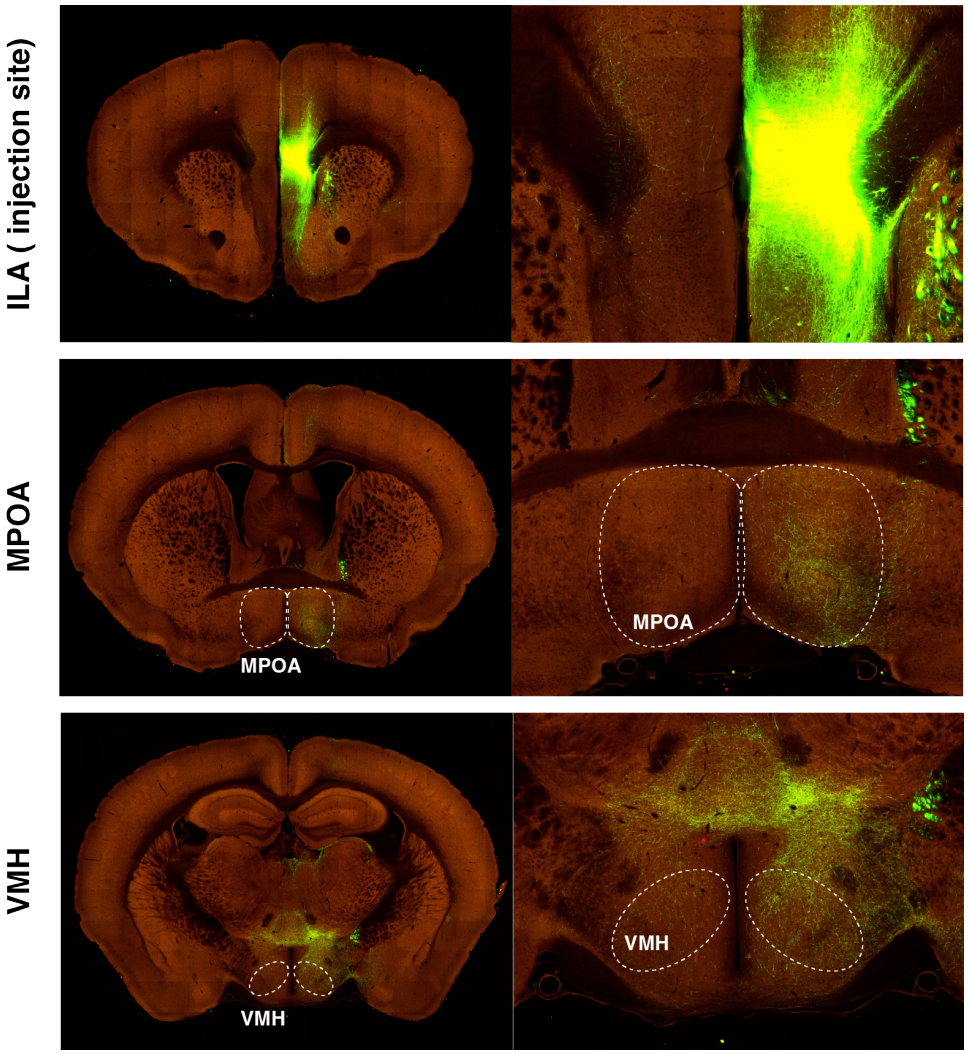

Figure 6.3: The infralimbic cortex sends significant projections to the MPOA and VMH. Epifluorescent miscroscopy of coronal brain slices injected with an AAV carrying a fluorescent tracer (GFP). Allen Mouse Brain Connectivity Atlas, experiment 157556400.

tested during the injection optimisation process resulting in more generous overall labelling throughout the brain, however, hypothalamic labelling remained consistently poor, especially in the VMH. Any weak labelling was considered insufficient to expect reliable responses from optostimulation.

In addition to the dmPFC, the infralimbic subdivision of the mPFC also receives abundant input from the mediodorsal thalamus (Graham et al., 2021) and shows increased c-Fos expression following an animal's ascent to more dominant status after removal of the previous dominant (Williamson et al., 2019). Impor-

tantly, ILA has much more substantial direct projections to both the MPOA and VMH, shown in tracing experiments from the Allen Connectivity Atlas (Experiment 157556400, Figure 6.3) (Allen Institute for Brain Science). Chemogenetic manipulation of ILA projections to the nucleus accumbens increases pushing behaviour in the tube test and social approach (Fetcho et al., 2023). Additionally, dominant Syrian hamsters showed elevated c-Fos expression in both the ILA and PL subdivision during acute social defeat compared to subordinates (Dulka et al., 2018). ILA was therefore considered a more promising mPFC subdivision to provide rank-dependent modulatory input to the hypothalamus.

6.3 Optogenetic manipulation

Manipulation of the hierarchy has been almost entirely demonstrated in the tube test context, which was also adopted here to leverage the verified stimulation protocols used in similar experimental designs. As shown in Figure 6.4A, mice of known hierarchical status were bilaterally injected with channelrhodopsin 2 expressing AAV in the ILA and implanted with a dual fibre-optic probe in either the MPOA or VMH. Panels 6.4B-F show representative injection and implant histology with more convincing MPOA fibres compared to the dmPFC injections, although VMH expression remained quite weak (panels C-D and E-F are from different animals). The tethered mouse underwent tube tests against all of its cagemates and the number of tube tests won in the light on and off conditions is shown in Figure 6.4G-H. Unfortunately, stimulation of ILA projections to either hypothalamic area did not consistently affect the number of tube tests won (paired t-test; MPOA: $t(7) = -0.73, p = 0.481$, VMH: $t(7) = -0.23, p = 0.826$). Additionally, there were concerns that 10 mW stimulation may be causing damage to the tissues underneath the fibre-optic implant. Hence, lower power levels were also piloted (Figure 6.4I), however, there were no differences in tube test winning depending on stimulation power (two-way ANOVA testing the effect of stimulation power while controlling for brain area being stimulated: $F(1,16) = 0.3, p = 0.615$). Again, there were no differences between brain areas ($F(1,16) = 0.008, p = 0.932$).

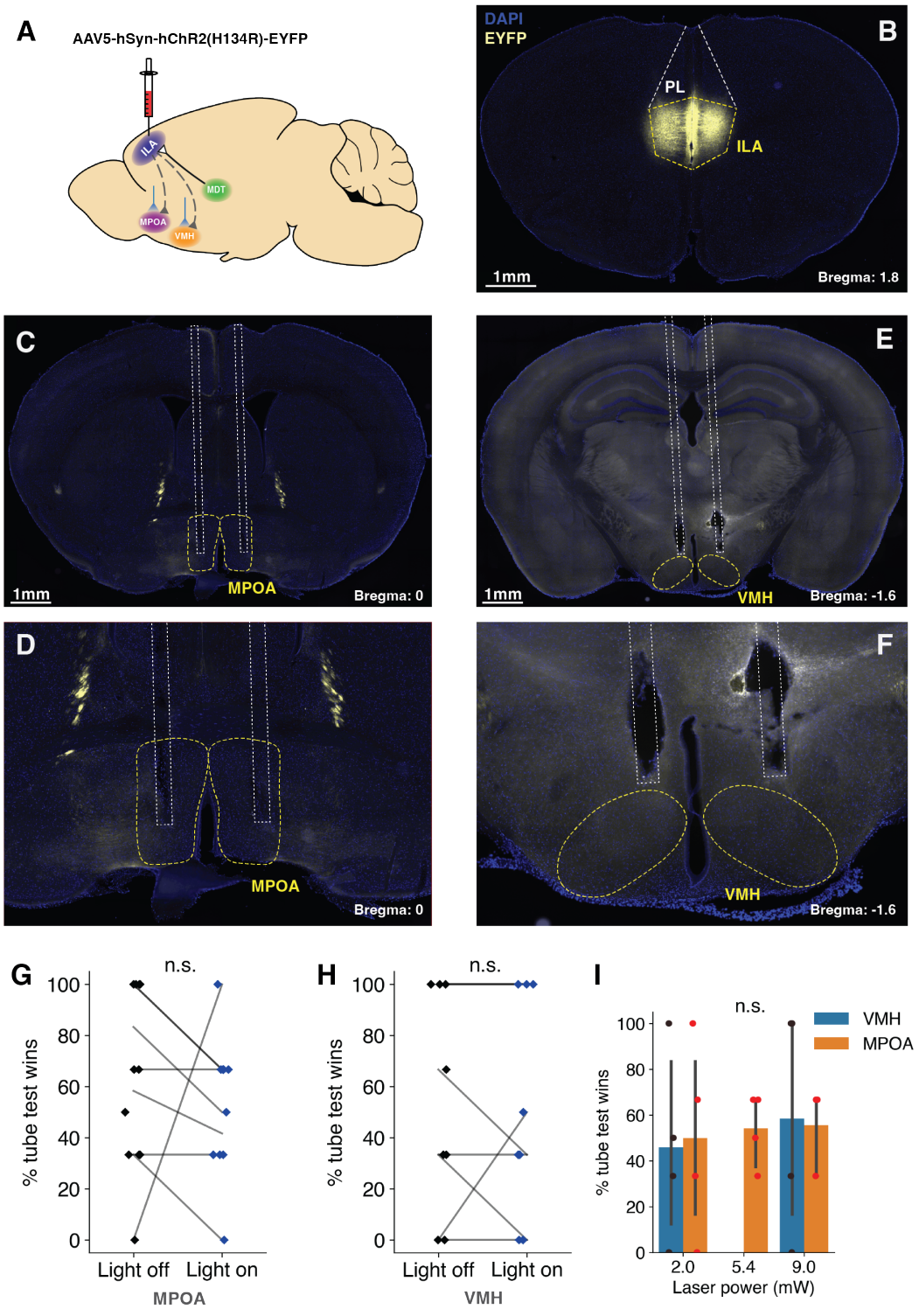

Figure 6.4: Optogenetic activation of infralimbic projections to the MPOA or VMH does not result in rank switching in the tube test. (**A**) Experimental design diagram. (**B-F**) Histology of the injection site (ILA) **(B)**, and implantation sites in the MPOA **(C-D)** and VMH **(E-F)** respectively. (**G-H**) Percentage of tube test wins against cagemate opponents in a round-robin design during optostimulation of ILA projections to the MPOA and VMH respectively. Paired t-tests, Holm-Sidak correction, $N = 8$ mice. (**I**) The effect of different stimulation powers on winning. Two-way ANOVA, $N = 8$ mice for 2 and 9 mW, $N = 4$ mice for 5.4 mW. Error bars represent 95% CI.

6.4 Discussion

The results in this chapter did not support the circuit hypothesis that monosynaptic prefrontal inputs to the hypothalamus cause the behavioural phenotype associated with dominance. One reason could be that since rank-dependent excitability differences were observed during free interaction with female conspecifics rather than tube test behaviours, this projection may also be affecting sexual rather than competitive behaviours. In this case, the tube test is unlikely to expose any stimulation-dependent differences in behaviour. Another caveat is that optical stimulation may not have reliably elicited opsin activation in ILA axon terminals, which was not explicitly verified in slice preparations.

These limitations aside, the very modest anatomical and functional inputs to the hypothalamus from the mPFC suggest two alternatives. Firstly, there may be intermediate nodes that convey the rank information to the hypothalamus via a multisynaptic connection. Secondly, modulation may be achieved via a diffusely secreted neuromodulator. Serotonin and dopamine are particularly promising candidates for this function. Dominance is associated with high serotonin levels (Raleigh, 1984; Moskowitz et al., 2001). Mice that are susceptible to social defeat experience inhibition of serotonergic dorsal raphe nucleus neurons by local inhibitory interneurons (Challis et al., 2013). This inhibition is achieved through mPFC inputs to the GABA-ergic interneurons in the raphe, thus suppressing serotonin secretion and in turn achieving widespread modulatory effects throughout the serotonin receptor-expressing regions of the brain. Work has also been done on resilience to social defeat and dopamine (DA). Mice that are resilient to social defeat have stronger dopaminergic inputs from the mesolimbic dopamine neurons to the nucleus accumbens, where DA terminals are more active when approaching the aggressive conspecific, compared to susceptible mice, which experience a dopamine peak at the onset of fleeing and the offset of attack from the aggressor (Willmore et al., 2022). There is additional evidence for dopaminergic involvement from the dominance field. A study from Xing et al. (2022) identified a functional segregation of mPFC cells into those expressing the D1 dopamine receptor which promote dominance and those expressing the D2 receptor which promote subordinacy.

Chapter 7

Conclusions

7.1 Brief summary

The basic computational loop of the brain involves the transformation of sensory inputs into progressively abstract representations of the environment. These representations are combined with internal states, beliefs, and past experiences to form a decision regarding the optimal behavioural response to the environment. Finally, these decisions trigger the execution of specific motor programmes that result in behaviour. Description of complete pathways which link sensory inputs through some cognitive representations of the environment to the behavioural output is therefore the principal goal in circuit neuroscience. At varying levels of mechanistic detail, such end-to-end circuit descriptions exist for several social behaviours (Chen and Hong, 2018), however, the current understanding of the social dominance system is limited to a description of own rank encoding as an internal state in the MDT-mPFC and MDT-cACC pathways, along with a status learning mechanism involving the plasticity of these projections. The aim of this thesis was to embed this thalamocortical pathway into a wider circuit that allows access to sensory information about conspecifics. The inclusion of two hypothalamic nodes involved in social cognition was expected to provide a mechanism for rank to modulate the sensory representations of social cues and influence behavioural decisions, as well as a mechanism for information about conspecific rank to interact with representations of own rank.

The following main hypotheses were investigated:

1. Dominance rank modulates sensory representations of conspecifics in the hypothalamus.

2. Modulation of social perception leads to distinct behavioural outcomes.

3. The hypothalamus serves as an integration node for representations of own and conspecific rank.

4. Rank-dependent modulatory input arrives to the hypothalamus via monosynaptic mPFC projections

An analysis of evoked responses to social cues found an increased amplitude of responses to female intruders in dominant males, as well as a higher proportion of positively tuned cells. The response amplitude was also higher in males who chose to mount the female. The direction of modulatory effects was the same in both areas, although the magnitude of the differences was generally higher in the VMH. Interestingly, no modulatory effects were found for representations of male conspecifics or tube test competitive behaviours. This suggests a primarily sensory modulatory influence limited to interactions with females. These findings support the first two hypotheses by showing that hypothalamic excitability to females systematically varies with dominance rank which is associated with increased social engagement with female conspecifics. That said, limitations regarding causality are discussed in the coming sections.

Regarding the third hypothesis, I first tested the assumption that rank recognition relies on olfaction in mice and demonstrated the necessity of this modality, as well as the sufficiency of either the volatile or non-volatile olfactory systems for this function. This provided two sensory pathways that could potentially interact with the thalamocortical dominance circuit. The hypothalamus is a region which receives processed input from both the volatile and non-volatile olfactory pathways. It shows differential c-Fos responses to urine cues from donors of different ranks, suggesting sensitivity to the status of conspecifics, while also exhibiting modulation by own

rank. The MPOA and VMH were therefore proposed as the integration nodes combining own and conspecific rank information. An analysis of the encoding of both variables showed that the MPOA and VMH do not robustly encode own nor conspecific rank, therefore rejecting the integration node hypothesis. While the initial model proposed that these two brain areas are firmly a part of the dominance circuit in the sense of encoding hierarchy-relevant variables, this evidence suggests that they might be more of a modulatory target of the dominance circuit, but not themselves involved in the encoding of rank. However, additional exploratory analysis of the information content in these areas revealed a robust encoding of competitive context as well as tube test winning. In the Chapter 5 discussion, I speculate that these variables are downstream of relative rank encoding, which is in turn downstream of own and other rank information. This is consistent with a model of the hypothalamus as a downstream modulation target of the dominance circuit.

Finally, I investigated the circuit basis of the modulatory input to the hypothalamus. I proposed that modulation is achieved via direct synaptic input from the mPFC. This model was based on other mPFC projections to the PAG and NAc, which drive social avoidance mimicking social defeat and tube test pushing respectively. I therefore hypothesised that the mPFC projects to multiple subcortical nodes and modulates multiple processes in the social cognition pathway. Tracing studies from the prelimbic subdivision of the mPFC did not show appreciable projections to the hypothalamus, hence the more promising infralimbic subdivision was selected for optogenetic manipulation. However, channelrhodopsin-mediated stimulation of ILA projections to either the MPOA or VMH did not affect winning potential in the tube test, therefore rejecting the monosynaptic mechanism of rank-dependent modulation. The main findings of the thesis are summarised as a graphical abstract in Figure 7.1.

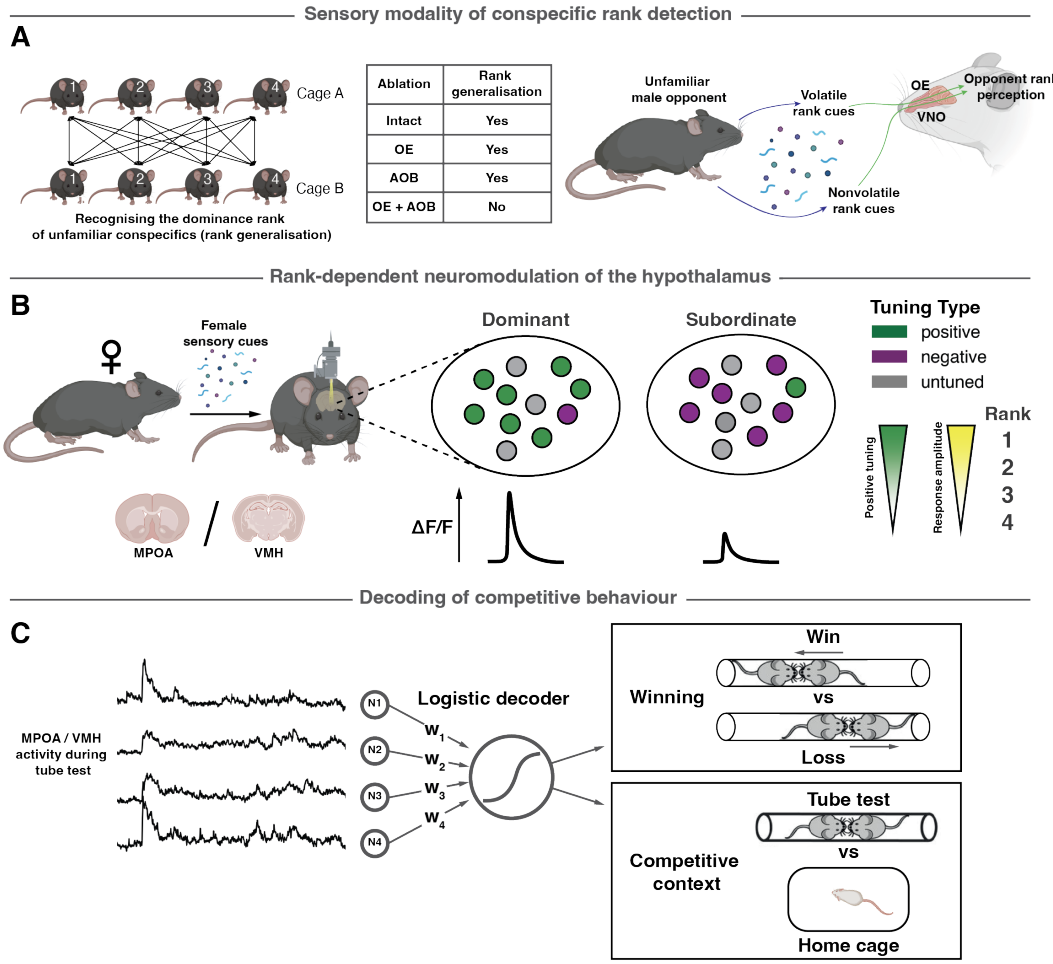

Figure 7.1: Graphical summary of main thesis findings. **(A)** Simultaneous but not individual ablation of both volatile (olfactory epithelium) and non-volatile (accessory olfactory bulb) olfaction impairs the ability of male mice to infer the rank of strangers. **(B)** High dominance rank is associated with a larger proportion of MPOA and VMH neurons that are positively tuned to female conspecifics. The amplitude of female-evoked neural responses is also higher. **(C)** MPOA and VMH activity during the tube test can be used to decode competitive environmental context and whether the mouse will win against its opponent. In contrast, bouts of competitive tube test behaviours, namely pushing, resisting and retreating, cannot be decoded from these two areas. Illustration created using BioRender.com.

7.2 Differences between the MPOA and VMH

Previous research on the roles of the VMH and MPOA in social behaviour creates the perspective of two areas with opposing functions. Where the VMH is broadly associated with either aggressive or defensive behaviour in generally antagonistic social interactions, MPOA is associated with more affiliative behaviour, especially parenting, sexual behaviour, and social approach. They also exhibit opposite sex preferences in terms of neuronal tuning, which is achieved through distinct modulatory effects from the bed nucleus of the stria terminalis, an area upstream of both the MPOA and VMH (Yang et al., 2022). While there are exceptions to this model (e.g., the canonical role of the VMH in mating (Yang et al., 2013)), this suggests that the two areas should likewise have an opposing function in the dominance context. However, throughout this thesis the modulatory effects on both areas as well as the information encoding properties were very similar between the two areas, differing mostly in the larger modulatory effects in the VMH. Indeed, in terms of evoked responses, they both exhibited a similar pattern of responding to a broad range of social sensory cues, where the amplitude of the response correlates with the novelty or salience of the stimulus. I believe this apparent absence of functional differences between the areas arises from the focus in this thesis on sensory representation, rather than tuning to stereotyped behaviours. I propose that the modulation of sensory responses can be uniform across areas which control very different or even mutually exclusive behaviours, since the behavioural outcome is instead determined by the downstream connectivity of each area. In other words, the population of cells whose sensory responses are enhanced by high social status overlaps with several subpopulations with different downstream projections which drive different behavioural responses. In this way, a homogeneous modulation of sensory response across areas is compatible with their distinct and even opposing roles in driving behaviour.

7.3 Redundant modulation of the hypothalamus and PAG

If the modulation of the hypothalamus is indeed causally linked to rank-dependent differences in behaviour, this raises the question of redundancy between the mPFC-PAG and hypothalamus-PAG mechanisms of affecting behavioural phenotype. The Franklin et al. (2017) study determined that mPFC projections selectively target the glutamatergic neurons in the dorsal and dorsolateral segments of the PAG, which have been specifically implicated in defensive behaviours (Deng et al., 2016). While the VMH exhibits a similar pattern of PAG innervation, the MPOA targets more lateral and ventral subdivisions (Allen Connectivity Atlas experiments 277615922 and 120280191 respectively). Hypothalamic projections to the brainstem are involved in a wider array of social behaviours and there is a degree of anatomical and subpopulation segregation of the mPFC and hypothalamic projections to the PAG. This suggests a model where rank modulates several brain areas which affects different aspects of social behaviour.

7.4 Behavioural causality

Conclusions about the behavioural function of the two hypothalamic nodes in this thesis have relied on correlative measures between modulatory effects on tuning and excitability and behavioural outcomes towards females. The gold standard of behavioural causality are of course manipulation experiments, however, this was complicated by the fact that optogenetic excitation of the VMH, for example, has known behavioural effects (Lin et al., 2011; Yang et al., 2013; Yates, 2015). It would therefore be difficult to claim that direct stimulation of the area mimics rank-dependent modulation. Instead, the excitation of projections from neurons known to carry rank-relevant information was considered the conceptually clearest way to make that argument, since none of the nodes in the known thalamocortical circuit project directly to the hypothalamus. However, having excluded all of the mPFC subdivisions - which were the most likely candidates - in Chapter 6, finding the ac-

tual source of the modulatory input may prove challenging. Nonetheless, in terms of simply demonstrating the behavioural causality of the modulation, a more promising route may be to identify a subpopulation of hypothalamic cells that are modulated, thus allowing selective optogenetic manipulation directly in the hypothalamus with a more persuasive argument that the intervention mimics rank-dependent modulation (see future directions).

7.5 Future directions

7.5.1 Subpopulation specific modulation

Previous chapters raised the possibility of subpopulation-specific modulation in the hypothalamus. Given the large increase in response amplitudes and positive tuning to females in dominant VMH, the subpopulations in this area that are associated with male sexual behaviour are of particular interest. Progesterone receptor (PR^+) expressing cells in the VMH, which have been shown to drive both male sexual behaviour and aggression (Yang et al., 2013), are good candidates for such a subpopulation. Dual colour miniscope recordings can be conducted, where non-conditional GCaMP expression can be combined with a static label of PR^+ cells, for example, via Cre-dependent expression of mCherry in a progesterone-Cre mouse line. It can then be compared whether the rank-dependent increases in response amplitude are enriched among the PR-expressing population of VMH cells. A more agnostic approach involves performing the same recordings as in this thesis, followed by post hoc colocalisation of the recorded cells with histological markers for a wider array of subpopulation biomarkers (Xu et al., 2020). The same approach can be used to investigate whether encoding of the winning state is likewise subpopulation-constrained. Identification of such a subpopulation would allow its direct manipulation in the hypothalamus to simulate the functional changes associated with rank. This could in turn confirm a causal relationship between the modulatory effects and their behavioural correlates identified in this thesis.

7.5.2 Source of the modulatory input

Given the negative result with respect to direct mPFC projections to the hypothalamus, the true source of modulatory input remains to be discovered. For the neurochemical hypothesis, where either serotonin or dopamine modulates the hypothalamus via diffuse secretion, the two chemicals can be administered locally to the hypothalamus through an implanted cannula. It can then be determined whether that mimics the effect of dominance on sexual behaviour or competitive behaviour in the tube test. In contrast, the identification of an upregulated synaptic input is more laborious. One approach is to express channelrhodopsin in areas with known input connectivity to the MPOA or VMH and analyse the strength of the light-evoked excitatory post-synaptic currents (eEPSC) during optostimulation. Since the two areas have a very large number of inputs between them, some reasonable criteria to narrow them down to a more manageable set of candidates include (1) areas that project to both the MPOA and VMH and (2) areas that have known involvement in hierarchy. The expected outcome is an increase in the eEPSC amplitude, analogous to increased input currents observed in the dominant MDT (Nelson et al., 2019).

7.5.3 Self vs. other encoding

The question of the encoding of self versus other likewise remains open. While this thesis focused specifically on rank, this is a wider question about the encoding of identity. Building on the discussion of the low-dimensional and abstract variables in the hypothalamus indicative of a relatively downstream area, one reason why the efforts to decode conspecific rank from this region failed may be that conspecific representation has already been heavily processed into more abstract variables by the time it reaches the hypothalamus. In other words, perhaps it is still possible to decode opponent rank from the AOB, but this is a detailed sensory description of the conspecific which is no longer detectable downstream. If rank is encoded simply in the amount of an MUP like darcin in the urine, then this would be a very simple sensory feature consistent with a very upstream encoding in the AOB.

An alternative to the model investigated in this thesis is offered by the MOB projection to the piriform cortex (PIR), which in turn projects to the MDT and the orbitofrontal cortex (OFC), both components of the existing dominance circuit (Tham et al., 2009). The OFC was identified as one of the two major sources of excitatory input into the MDT which then leads to heightened MDT excitability associated with dominance (Nelson et al., 2019). This pathway therefore offers a model where conspecific information interacts with the own rank circuit more directly, instead of anatomical segregation between the two streams joining at an integration node. Indeed, representations of own rank cannot be learned in a social vacuum but instead through a series of antagonistic encounters, or observation of the interactions among other group members (Leimar, 2021). Self-perceived rank is therefore a relative variable that exists in one's social context. It requires not only an awareness of how often one is winning in competitions against others but specifically who one is winning against. Since rank learning is facilitated by plasticity in the OFC-MDT-mPFC circuit, it makes sense for this circuit to receive information about not only winning but also the identity of the opponent. Future research can perform similar recordings to the one conducted in this thesis but instead in the PIR and even downstream OFC and MDT regions. It would be especially interesting to investigate whether there is any evolution in the information encoded along the pathway, for example, from opponent rank to relative rank encoding. Importantly, both the volatile and non-volatile pathways are sufficient and finding opponent rank encoding in the non-volatile pathway is similarly likely, despite its absence in the more downstream nodes of the pathway.

7.5.4 Circuit model

The dominance circuit now encompasses a multitude of brain areas and neurochemical systems with frequent recurrent connections. The field has described several individual pathways linking one or two areas in a way that promotes a particular rank phenotype, however, dominant behaviour alone may be an insufficient readout for disentangling the individual contributions of each area. Optogenetic manipulation of a behaviour can often implicate several distinct structures in a single behaviour,

but this makes it unclear whether an individual area is affecting the execution of the behaviour itself, perhaps a cognitive or emotional process, or the sensory perception of the environment. To propose a unified model of the dominance circuit, future work should adopt a more comprehensive approach to determining the information encoded in each circuit node. Efforts towards that goal have been made here by attempting to anatomically disentangle the representations of slow winning states, individual behavioural bouts, representations of own rank and opponent rank. However, in an ideal experiment, this approach entails simultaneous activity recordings from multiple brain areas, which also allows analysis of the information flow between areas. Computational modelling has shown that brain areas encode public variables that are passed onto downstream areas, but also private variables which remain in the area and are not communicated downstream (Semedo et al., 2019). Simultaneous recordings therefore allow not only information encoding analysis for each individual area but also the determination of which variables are communicated to the next node. Such data would be extremely useful for investigating the information hierarchy hypothesis discussed earlier in the thesis. While these experiments are feasible today, they are nonetheless technically ambitious in freely behaving contexts.

7.6 Conclusion

Both human and rodent work on social hierarchies suggests that low-status individuals have a more negative perception of other group members. An assumption of threat is applied indiscriminately, even to interactions with complete strangers based on past negative experiences with familiar conspecifics. This negative perception bias drives low social engagement, diminishes group belonging, and impairs the ability to increase one's rank by building rapport with others. Even if a low-ranking individual is placed into a new and unfamiliar group without a preexisting hierarchical structure, the existing perceptual biases will drive the group members into taking up hierarchical positions similar to those occupied in their previous community. The vicious cycle between low social status and social avoidance in turn

has serious negative consequences for physical and mental health outcomes. This work is the first to document rank-dependent differences in social perception at the level of specific nodes in the social pathway that correlate with behavioural social engagement. It therefore provides evidence of an important mechanism that may drive social isolation in low-status individuals with the associated consequences for health outcomes and maintenance of low status.

Bibliography

Allen Institute for Brain Science. Allen mouse connectivity atlas. URL `https://connectivity.brain-map.org/`.

Rachida Ammari, Francesco Monaca, Mingran Cao, Estelle Nassar, Patty Wai, Nicholas A. Del Grosso, Matthew Lee, Neven Borak, Deborah Schneider-Luftman, and Johannes Kohl. Hormone-mediated neural remodeling orchestrates parenting onset during pregnancy. *Science*, 382(6666):76–81, 10 2023. ISSN 0036-8075. doi: 10.1126/science.adi0576.

Alessio Avenanti, Angela Sirigu, and Salvatore M. Aglioti. Racial Bias Reduces Empathic Sensorimotor Resonance with Other-Race Pain. *Current Biology*, 20 (11):1018–1022, 6 2010. ISSN 0960-9822. doi: 10.1016/J.CUB.2010.03.071.

Nadège Bault, Mateus Joffily, Aldo Rustichini, and Giorgio Coricelli. Medial prefrontal cortex and striatum mediate the influence of social comparison on the decision process. *Proceedings of the National Academy of Sciences*, 108(38): 16044–16049, 9 2011. ISSN 0027-8424. doi: 10.1073/pnas.1100892108.

Silvia Bernardi, Marcus K. Benna, Mattia Rigotti, Jérôme Munuera, Stefano Fusi, and C. Daniel Salzman. The Geometry of Abstraction in the Hippocampus and Prefrontal Cortex. *Cell*, 183(4):954–967, 11 2020. ISSN 00928674. doi: 10.1016/j.cell.2020.09.031.

Lucy K. Bicks, Michelle Peng, Alana Taub, Schahram Akbarian, and Hirofumi Morishita. An Adolescent Sensitive Period for Social Dominance Hierarchy Plas-

ticity Is Regulated by Cortical Plasticity Modulators in Mice. *Frontiers in Neural Circuits*, 15, 5 2021. ISSN 1662-5110. doi: 10.3389/fncir.2021.676308.

Natalia Y. Bilenko and Jack L. Gallant. Pyrcca: Regularized Kernel Canonical Correlation Analysis in Python and Its Applications to Neuroimaging. *Frontiers in Neuroinformatics*, 10, 11 2016. ISSN 1662-5196. doi: 10.3389/fninf.2016.00049.

Erie D. Boorman, John P. O'Doherty, Ralph Adolphs, and Antonio Rangel. The Behavioral and Neural Mechanisms Underlying the Tracking of Expertise. *Neuron*, 80(6):1558–1571, 12 2013. ISSN 08966273. doi: 10.1016/j.neuron.2013.10.024.

W. J. Carr, Kenneth R. Kimmel, Steven L. Anthony, and David E. Schlocker. Female rats prefer to mate with dominant rather than subordinate males. *Bulletin of the Psychonomic Society*, 20(2):89–91, 8 1982. ISSN 0090-5054. doi: 10.3758/BF03330090.

Sonia A. Cavigelli and Hashim S. Chaudhry. Social status, glucocorticoids, immune function, and health: Can animal studies help us understand human socioeconomic-status-related health disparities? *Hormones and Behavior*, 62 (3):295–313, 8 2012. ISSN 0018506X. doi: 10.1016/j.yhbeh.2012.07.006.

Collin Challis, Janette Boulden, Avin Veerakumar, Julie Espallergues, Fair M. Vassoler, R. Christopher Pierce, Sheryl G. Beck, and Olivier Berton. Raphe GABAergic neurons mediate the acquisition of avoidance after social defeat. *Journal of Neuroscience*, 2013. ISSN 02706474. doi: 10.1523/JNEUROSCI.2383-13.2013.

M. R. A. Chance. Attention Structure as the Basis of Primate Rank Orders. *Man*, 2 (4):503, 12 1967. ISSN 00251496. doi: 10.2307/2799336.

Patrick Chen and Weizhe Hong. Neural Circuit Mechanisms of Social Behavior. *Neuron*, 98(1):16–30, 4 2018. ISSN 08966273. doi: 10.1016/j.neuron.2018.02.026.

Te-Yu Chen, Jiun-Hung Geng, Szu-Chia Chen, and Jia-In Lee. Living alone is associated with a higher prevalence of psychiatric morbidity in a population-based cross-sectional study. *Frontiers in Public Health*, 10, 11 2022a. ISSN 2296-2565. doi: 10.3389/fpubh.2022.1054615.

Yiwen Chen, Yuanjia Zheng, Jinglan Yan, Chuanan Zhu, Xuan Zeng, Shaoyi Zheng, Wenwen Li, Lin Yao, Yucen Xia, Wei-wei Su, and Yongjun Chen. Early Life Stress Induces Different Behaviors in Adolescence and Adulthood May Related With Abnormal Medial Prefrontal Cortex Excitation/Inhibition Balance. *Frontiers in Neuroscience*, 15, 1 2022b. ISSN 1662-453X. doi: 10.3389/fnins.2021.720286.

Ming-Yi Chou, Ryunosuke Amo, Masae Kinoshita, Bor-Wei Cherng, Hideaki Shimazaki, Masakazu Agetsuma, Toshiyuki Shiraki, Tazu Aoki, Mikako Takahoko, Masako Yamazaki, Shin-ichi Higashijima, and Hitoshi Okamoto. Social conflict resolution regulated by two dorsal habenular subregions in zebrafish. *Science*, 352(6281):87–90, 4 2016. ISSN 0036-8075. doi: 10.1126/science.aac9508.

Thomas A. Cleland. Construction of Odor Representations by Olfactory Bulb Microcircuits. pages 177–203. 2014. doi: 10.1016/B978-0-444-63350-7.00007-3.

Francesca R. D'Amato. Effects of male social status on reproductive success and on behavior in mice (Mus musculus). *Journal of Comparative Psychology*, 102 (2):146–151, 6 1988. ISSN 1939-2087. doi: 10.1037/0735-7036.102.2.146.

Robert O. Deaner, Amit V. Khera, and Michael L. Platt. Monkeys Pay Per View: Adaptive Valuation of Social Images by Rhesus Macaques. *Current Biology*, 15 (6):543–548, 3 2005. ISSN 09609822. doi: 10.1016/j.cub.2005.01.044.

Denys deCatanzaro and Boris B. Gorzalka. Postpubertal social isolation and male sexual behavior in rodents: Facilitation or inhibition is species dependent. *Animal Learning & Behavior*, 7(4):555–561, 12 1979. ISSN 0090-4996. doi: 10.3758/BF03209718.

H. Deng, X. Xiao, and Z. Wang. Periaqueductal Gray Neuronal Activities Underlie Different Aspects of Defensive Behaviors. *Journal of Neuroscience*, 36(29): 7580–7588, 7 2016. ISSN 0270-6474. doi: 10.1523/JNEUROSCI.4425-15.2016.

S. Dhungel, M. Masaoka, D. Rai, Y. Kondo, and Y. Sakuma. Both olfactory epithelial and vomeronasal inputs are essential for activation of the medial amygdala and preoptic neurons of male rats. *Neuroscience*, 199:225–234, 12 2011. ISSN 03064522. doi: 10.1016/j.neuroscience.2011.09.051.

Gül Dölen, Ayeh Darvishzadeh, Kee Wui Huang, and Robert C. Malenka. Social reward requires coordinated activity of nucleus accumbens oxytocin and serotonin. *Nature*, 501(7466):179–184, 9 2013. ISSN 0028-0836. doi: 10.1038/nature12518.

J Dominguez and E Hull. Dopamine, the medial preoptic area, and male sexual behavior. *Physiology & Behavior*, 86(3):356–368, 10 2005. ISSN 00319384. doi: 10.1016/j.physbeh.2005.08.006.

Carlos Drews. The Concept and Definition of Dominance in Animal Behaviour. *Behaviour*, 125(3-4):283–313, 1993. ISSN 0005-7959. doi: 10.1163/156853993X00290.

C. Dulac and S. Wagner. Genetic Analysis of Brain Circuits Underlying Pheromone Signaling. *Annual Review of Genetics*, 40(1):449–467, 12 2006. ISSN 0066-4197. doi: 10.1146/annurev.genet.39.073003.093937.

Catherine Dulac and A. Thomas Torello. Molecular detection of pheromone signals in mammals: From genes to behaviour. *Nature Reviews Neuroscience*, 4: 551–562, 2003. ISSN 14710048. doi: 10.1038/nrn1140.

Brooke N. Dulka, Kimberly S. Bress, J. Alex Grizzell, and Matthew A. Cooper. Social Dominance Modulates Stress-induced Neural Activity in Medial Prefrontal Cortex Projections to the Basolateral Amygdala. *Neuroscience*, 388:274–283, 9 2018. ISSN 03064522. doi: 10.1016/j.neuroscience.2018.07.042.

A.E. Elo. *The Rating of Chessplayers: Past and Present*. Ishi Press International, 2008. ISBN 9780923891275.

Andrew Erskine, Thorsten Bus, Jan T. Herb, and Andreas T. Schaefer. Autonomouse: High throughput operant conditioning reveals progressive impairment with graded olfactory bulb lesions. *PLOS ONE*, 14:e0211571, 3 2019. ISSN 1932-6203. doi: 10.1371/journal.pone.0211571.

Zhengxiao Fan, Hong Zhu, Tingting Zhou, Sheng Wang, Yan Wu, and Hailan Hu. Using the tube test to measure social hierarchy in mice. *Nature Protocols*, 2019. ISSN 17502799. doi: 10.1038/s41596-018-0116-4.

Ada T. Feldman and Delia Wolfe. Tissue Processing and Hematoxylin and Eosin Staining. pages 31–43. 2014. doi: 10.1007/978-1-4939-1050-2{_}3.

Robert N. Fetcho, Baila S. Hall, David J. Estrin, Alexander P. Walsh, Peter J. Schuette, Jesse Kaminsky, Ashna Singh, Jacob Roshgodal, Charlotte C. Bavley, Viraj Nadkarni, Susan Antigua, Thu N. Huynh, Logan Grosenick, Camille Carthy, Lauren Komer, Avishek Adhikari, Francis S. Lee, Anjali M. Rajadhyaksha, and Conor Liston. Regulation of social interaction in mice by a frontostriatal circuit modulated by established hierarchical relationships. *Nature Communications*, 14:2487, 4 2023. ISSN 2041-1723. doi: 10.1038/s41467-023-37460-6.

Steven W. Flavell, Nadine Gogolla, Matthew Lovett-Barron, and Moriel Zelikowsky. The emergence and influence of internal states. *Neuron*, 110(16): 2545–2570, 8 2022. ISSN 0896-6273. doi: 10.1016/J.NEURON.2022.04.030.

Tamara B Franklin, Bianca A Silva, Zinaida Perova, Livia Marrone, Maria E Masferrer, Yang Zhan, Angie Kaplan, Louise Greetham, Violaine Verrechia, Andreas Halman, Sara Pagella, Alexei L Vyssotski, Anna Illarionova, Valery Grinevich, Tiago Branco, and Cornelius T Gross. Prefrontal cortical control of a brainstem social behavior circuit. *Nature Neuroscience*, 20(2):260–270, 2 2017. ISSN 1097-6256. doi: 10.1038/nn.4470.

Olivier Friard and Marco Gamba. Boris: a free, versatile open-source event-logging software for video/audio coding and live observations. *Methods in Ecology and Evolution*, pages 1324–1330, 2016. ISSN 2041-210X. doi: 10.1111/2041-210X.12584.

Yu Fu, Jason M. Tucciarone, J. Sebastian Espinosa, Nengyin Sheng, Daniel P. Darcy, Roger A. Nicoll, Z. Josh Huang, and Michael P. Stryker. A cortical circuit for gain control by behavioral state. *Cell*, 156(6):1139–1152, 2014. ISSN 10974172. doi: 10.1016/j.cell.2014.01.050.

Matthew J. Fuxjager and Catherine A. Marler. How and why the winner effect forms: influences of contest environment and species differences. *Behavioral Ecology*, 21(1):37–45, 2010. ISSN 1465-7279. doi: 10.1093/beheco/arp148.

Matthew J. Fuxjager, Temitayo O. Oyegbile, and Catherine A. Marler. Independent and Additive Contributions of Postvictory Testosterone and Social Experience to the Development of the Winner Effect. *Endocrinology*, 152(9):3422–3429, 9 2011. ISSN 0013-7227. doi: 10.1210/en.2011-1099.

Juan A. Gallego, Matthew G. Perich, Raeed H. Chowdhury, Sara A. Solla, and Lee E. Miller. Long-term stability of cortical population dynamics underlying consistent behavior. *Nature Neuroscience*, 23(2):260–270, 2 2020. ISSN 1097-6256. doi: 10.1038/s41593-019-0555-4.

Sriparna Ghosal, Elias Gebara, Eva Ramos-Fernández, Alessandro Chioino, Jocelyn Grosse, Isabelle Guillot de Suduiraut, Olivia Zanoletti, Bernard Schneider, Antonio Zorzano, Simone Astori, and Carmen Sandi. Mitofusin-2 in nucleus accumbens D2-MSNs regulates social dominance and neuronal function. *Cell Reports*, 42(7):112776, 7 2023. ISSN 22111247. doi: 10.1016/j.celrep.2023.112776.

Kunal K Ghosh, Laurie D Burns, Eric D Cocker, Axel Nimmerjahn, Yaniv Ziv, Abbas El Gamal, and Mark J Schnitzer. Miniaturized integration of a fluorescence

microscope. *Nature Methods*, 8(10):871–878, 10 2011. ISSN 1548-7091. doi: 10.1038/nmeth.1694.

Kourtney Graham, Nelson Spruston, and Erik B. Bloss. Hippocampal and thalamic afferents form distinct synaptic microcircuits in the mouse infralimbic frontal cortex. *Cell Reports*, 37(3):109837, 10 2021. ISSN 22111247. doi: 10.1016/j.celrep.2021.109837.

Jan Gründemann, Yael Bitterman, Tingjia Lu, Sabine Krabbe, Benjamin F. Grewe, Mark J. Schnitzer, and Andreas Lüthi. Amygdala ensembles encode behavioral states. *Science*, 364(6437), 4 2019. ISSN 0036-8075. doi: 10.1126/science.aav8736.

Josée Guilmette, Isabelle Langlois, Pierre Hélie, and Alexander de Oliveira El Warrak. Comparative study of 2 surgical techniques for castration of guinea pigs (Cavia porcellus). *Canadian journal of veterinary research = Revue canadienne de recherche veterinaire*, 79(4):323–8, 10 2015. ISSN 1928-9022.

Huifen Guo, Qi Fang, Ying Huo, Yaohua Zhang, and Jianxu Zhang. Social dominance-related major urinary proteins and the regulatory mechanism in mice. *Integrative Zoology*, 10:543–554, 11 2015. ISSN 17494877. doi: 10.1111/1749-4877.12165.

Jennifer N. Gutsell and Michael Inzlicht. Empathy constrained: Prejudice predicts reduced mental simulation of actions during observation of outgroups. *Journal of Experimental Social Psychology*, 46(5):841–845, 9 2010. ISSN 0022-1031. doi: 10.1016/J.JESP.2010.03.011.

Sofia Håglin, Staffan Bohm, and Anna Berghard. Single or Repeated Ablation of Mouse Olfactory Epithelium by Methimazole. *Bio-protocol*, 11(8):e3983, 4 2021. ISSN 2331-8325. doi: 10.21769/BioProtoc.3983.

Patricia H. Hawley. The Ontogenesis of Social Dominance: A Strategy-Based Evolutionary Perspective. *Developmental Review*, 19(1):97–132, 3 1999. ISSN 0273-2297. doi: 10.1006/DREV.1998.0470.

Fiona Hollis, Michael A. van der Kooij, Olivia Zanoletti, Laura Lozano, Carles Cantó, and Carmen Sandi. Mitochondrial function in the brain links anxiety with social subordination. *Proceedings of the National Academy of Sciences*, 112(50): 15486–15491, 12 2015. ISSN 0027-8424. doi: 10.1073/pnas.1512653112.

H. Hotelling. Relations between two sets of variates. *Biometrika*, 28(3-4):321–377, 12 1936. ISSN 0006-3444. doi: 10.1093/biomet/28.3-4.321.

Shuo Huang, Zizhen Zhang, Eder Gambeta, Shi Chen Xu, Catherine Thomas, Nathan Godfrey, Lina Chen, Said M'Dahoma, Stephanie L. Borgland, and Gerald W. Zamponi. Dopamine Inputs from the Ventral Tegmental Area into the Medial Prefrontal Cortex Modulate Neuropathic Pain-Associated Behaviors in Mice. *Cell Reports*, 31(12):107812, 6 2020. ISSN 22111247. doi: 10.1016/j.celrep.2020.107812.

Fumiaki Imamura, Ayako Ito, and Brandon J. LaFever. Subpopulations of Projection Neurons in the Olfactory Bulb. *Frontiers in Neural Circuits*, 14, 8 2020. ISSN 1662-5110. doi: 10.3389/fncir.2020.561822.

Sayaka Inoue, Renzhi Yang, Adarsh Tantry, Chung-ha Davis, Taehong Yang, Joseph R. Knoedler, Yichao Wei, Eliza L. Adams, Shivani Thombare, Samantha R. Golf, Rachael L. Neve, Marc Tessier-Lavigne, Jun B. Ding, and Nirao M. Shah. Periodic Remodeling in a Neural Circuit Governs Timing of Female Sexual Behavior. *Cell*, 179(6):1393–1408, 11 2019. ISSN 00928674. doi: 10.1016/j.cell.2019.10.025.

Kentaro K. Ishii, Takuya Osakada, Hiromi Mori, Nobuhiko Miyasaka, Yoshihiro Yoshihara, Kazunari Miyamichi, and Kazushige Touhara. A Labeled-Line Neural Circuit for Pheromone-Mediated Sexual Behaviors in Mice. *Neuron*, 95(1):123–137, 7 2017. ISSN 08966273. doi: 10.1016/j.neuron.2017.05.038.

G. Trey Jenkins, Nicole Janich, Shiyou Wu, and Michael Shafer. Social isolation and mental health: Evidence from adults with serious mental illness. *Psychiatric*

Rehabilitation Journal, 46(2):148–155, 6 2023. ISSN 1559-3126. doi: 10.1037/prj0000554.

Sheri L. Johnson, Liane J. Leedom, and Luma Muhtadie. The Dominance Behavioral System and Psychopathology: Evidence from Self-Report, Observational, and Biological Studies. *Psychological Bulletin*, 138(4):692, 7 2012. ISSN 00332909. doi: 10.1037/A0027503.

Benedict C. Jones, Lisa M. DeBruine, Julie C. Main, Anthony C. Little, Lisa L. M. Welling, David R. Feinberg, and Bernard P. Tiddeman. Facial cues of dominance modulate the short-term gaze-cuing effect in human observers. *Proceedings of the Royal Society B: Biological Sciences*, 277(1681):617–624, 2 2010. ISSN 0962-8452. doi: 10.1098/rspb.2009.1575.

Ningdong Kang, Michael J. Baum, and James A. Cherry. A direct main olfactory bulb projection to the 'vomeronasal' amygdala in female mice selectively responds to volatile pheromones from males. *European Journal of Neuroscience*, 29(3):624–634, 2 2009. ISSN 0953-816X. doi: 10.1111/j.1460-9568.2009.06638.x.

Tomomi Karigo, Ann Kennedy, Bin Yang, Mengyu Liu, Derek Tai, Iman A. Wahle, and David J. Anderson. Distinct hypothalamic control of same- and opposite-sex mounting behaviour in mice. *Nature*, 589(7841):258–263, 1 2021. ISSN 0028-0836. doi: 10.1038/s41586-020-2995-0.

Ann Kennedy, Prabhat S. Kunwar, Ling-yun Li, Stefanos Stagkourakis, Daniel A. Wagenaar, and David J. Anderson. Stimulus-specific hypothalamic encoding of a persistent defensive state. *Nature*, 586(7831):730–734, 10 2020. ISSN 0028-0836. doi: 10.1038/s41586-020-2728-4.

Sepideh Keshavarzi, Robert K. P. Sullivan, Damian J. Ianno, and Pankaj Sah. Functional Properties and Projections of Neurons in the Medial Amygdala. *Journal of Neuroscience*, 34(26):8699–8715, 6 2014. ISSN 0270-6474. doi: 10.1523/JNEUROSCI.1176-14.2014.

Sepideh Keshavarzi, John M. Power, Eva H. H. Albers, Robert K. S. Sullivan, and Pankaj Sah. Dendritic Organization of Olfactory Inputs to Medial Amygdala Neurons. *The Journal of Neuroscience*, 35(38):13020–13028, 9 2015. ISSN 0270-6474. doi: 10.1523/JNEUROSCI.0627-15.2015.

Lyle Kingsbury, Shan Huang, Jun Wang, Ken Gu, Peyman Golshani, Ye Emily Wu, and Weizhe Hong. Correlated Neural Activity and Encoding of Behavior across Brains of Socially Interacting Animals. *Cell*, 178(2):429–446, 7 2019. ISSN 00928674. doi: 10.1016/j.cell.2019.05.022.

M. A. Kleshchev and L. V. Osadchuk. Social domination and reproductive success in male laboratory mice (Mus musculus). *Journal of Evolutionary Biochemistry and Physiology*, 2014. ISSN 00220930. doi: 10.1134/S0022093014030053.

Erik L. Knight and Pranjal H. Mehta. Hierarchy stability moderates the effect of status on stress and performance in humans. *Proceedings of the National Academy of Sciences*, 114(1):78–83, 1 2017. ISSN 0027-8424. doi: 10.1073/pnas.1609811114.

Johannes Kohl, Benedicte M. Babayan, Nimrod D. Rubinstein, Anita E. Autry, Brenda Marin-Rodriguez, Vikrant Kapoor, Kazunari Miyamishi, Larry S. Zweifel, Liqun Luo, Naoshige Uchida, and Catherine Dulac. Functional circuit architecture underlying parental behaviour. *Nature*, 556(7701):326–331, 4 2018. ISSN 0028-0836. doi: 10.1038/s41586-018-0027-0.

W Korzan, E Hoglund, M Watt, G Forster, O Overli, J Lukkes, and C Summers. Memory of opponents is more potent than visual sign stimuli after social hierarchy has been established. *Behavioural Brain Research*, 183(1):31–42, 10 2007. ISSN 01664328. doi: 10.1016/j.bbr.2007.05.021.

Earl T. Larson, Donald M. O'Malley, and Richard H. Melloni. Aggression and vasotocin are associated with dominant–subordinate relationships in zebrafish. *Behavioural Brain Research*, 167(1):94–102, 2 2006. ISSN 01664328. doi: 10.1016/j.bbr.2005.08.020.

Won Lee, Amber Khan, and James P. Curley. Major urinary protein levels are associated with social status and context in mouse social hierarchies. *Proceedings of the Royal Society B: Biological Sciences*, 284:20171570, 9 2017. ISSN 0962-8452. doi: 10.1098/rspb.2017.1570.

Won Lee, Hollie N. Dowd, Cyrus Nikain, Madeleine F. Dwortz, Eilene D. Yang, and James P. Curley. Effect of relative social rank within a social hierarchy on neural activation in response to familiar or unfamiliar social signals. *Scientific Reports*, 11:2864, 2 2021. ISSN 2045-2322. doi: 10.1038/s41598-021-82255-8.

Olof Leimar. The Evolution of Social Dominance through Reinforcement Learning. *The American Naturalist*, 197(5):560–575, 5 2021. ISSN 0003-0147. doi: 10.1086/713758.

Ying Li, Alexander Mathis, Benjamin F. Grewe, Jessica A. Osterhout, Biafra Ahanonu, Mark J. Schnitzer, Venkatesh N. Murthy, and Catherine Dulac. Neuronal Representation of Social Information in the Medial Amygdala of Awake Behaving Mice. *Cell*, 171(5):1176–1190, 11 2017. ISSN 00928674. doi: 10.1016/j.cell.2017.10.015.

Romain Ligneul, Ignacio Obeso, Christian C. Ruff, and Jean-Claude Dreher. Dynamical Representation of Dominance Relationships in the Human Rostromedial Prefrontal Cortex. *Current Biology*, 26(23):3107–3115, 12 2016. ISSN 09609822. doi: 10.1016/j.cub.2016.09.015.

Romain Ligneul, Romuald Girard, and Jean-Claude Dreher. Social brains and divides: the interplay between social dominance orientation and the neural sensitivity to hierarchical ranks. *Scientific Reports*, 7(1):45920, 4 2017. ISSN 2045-2322. doi: 10.1038/srep45920.

Dayu Lin, Maureen P. Boyle, Piotr Dollar, Hyosang Lee, E. S. Lein, Pietro Perona, and David J. Anderson. Functional identification of an aggression locus in the mouse hypothalamus. *Nature*, 470:221–226, 2 2011. ISSN 0028-0836. doi: 10.1038/nature09736.

Sheila J. Linz and Bonnie A. Sturm. The Phenomenon of Social Isolation in the Severely Mentally Ill. *Perspectives in Psychiatric Care*, pages n/a–n/a, 2 2013. ISSN 00315990. doi: 10.1111/ppc.12010.

Mengyu Liu, Dong-Wook Kim, Hongkui Zeng, and David J. Anderson. Make war not love: The neural substrate underlying a state-dependent switch in female social behavior. *Neuron*, 110(5):841–856, 3 2022. ISSN 08966273. doi: 10.1016/j.neuron.2021.12.002.

Liching Lo, Shenqin Yao, Dong Wook Kim, Ali Cetin, Julie Harris, Hongkui Zeng, David J. Anderson, and Brandon Weissbourd. Connectional architecture of a mouse hypothalamic circuit node controlling social behavior. *Proceedings of the National Academy of Sciences of the United States of America*, 2019. ISSN 10916490. doi: 10.1073/pnas.1817503116.

Kenneth C. Luzynski, Doris Nicolakis, Maria Adelaide Marconi, Sarah M. Zala, Jae Kwak, and Dustin J. Penn. Pheromones that correlate with reproductive success in competitive conditions. *Scientific Reports*, 11(1):21970, 11 2021. ISSN 2045-2322. doi: 10.1038/s41598-021-01507-9.

Yuqian Ma, Jin Bao, Yuanwei Zhang, Zhanjun Li, Xiangyu Zhou, Changlin Wan, Ling Huang, Yang Zhao, Gang Han, and Tian Xue. Mammalian Near-Infrared Image Vision through Injectable and Self-Powered Retinal Nanoantennae. *Cell*, 177(2):243–255, 4 2019. ISSN 00928674. doi: 10.1016/j.cell.2019.01.038.

Takeo Machida, Yumiko Yonezawa, and Tetsuo Noumura. Age-associated changes in plasma testosterone levels in male mice and their relation to social dominance or subordinance. *Hormones and Behavior*, 1981. ISSN 10956867. doi: 10.1016/0018-506X(81)90013-1.

Jenna A. McHenry, James M. Otis, Mark A. Rossi, J. Elliott Robinson, Oksana Kosyk, Noah W. Miller, Zoe A. McElligott, Evgeny A. Budygin, David R. Rubinow, and Garret D. Stuber. Hormonal gain control of a medial preoptic

area social reward circuit. *Nature Neuroscience*, 2017. ISSN 15461726. doi: 10.1038/nn.4487.

Michael Meredith. Vomeronasal, Olfactory, Hormonal Convergence in the Brain: Cooperation or Coincidence? *Annals of the New York Academy of Sciences*, 855(1):349–361, 11 1998. ISSN 0077-8923. doi: 10.1111/j.1749-6632.1998.tb10593.x.

Jeffrey R. Moffitt, Dhananjay Bambah-Mukku, Stephen W. Eichhorn, Eric Vaughn, Karthik Shekhar, Julio D. Perez, Nimrod D. Rubinstein, Junjie Hao, Aviv Regev, Catherine Dulac, and Xiaowei Zhuang. Molecular, spatial, and functional single-cell profiling of the hypothalamic preoptic region. *Science*, 2018. ISSN 10959203. doi: 10.1126/science.aau5324.

D. S. Moskowitz, Gilbert Pinard, David C. Zuroff, Lawrence Annable, and Simon N. Young. The Effect of Tryptophan on Social Interaction in Everyday Life: A Placebo-Controlled Study. *Neuropsychopharmacology 2001 25:2*, 25 (2):277–289, 2001. ISSN 1740-634X. doi: 10.1016/s0893-133x(01)00219-6. URL `https://www.nature.com/articles/1395662`.

Michael R. Murphy, Paul D. MacLean, and Sue C. Hamilton. Species-Typical Behavior of Hamsters Deprived from Birth of the Neocortex. *Science*, 213(4506): 459–461, 7 1981. ISSN 0036-8075. doi: 10.1126/science.7244642.

Aditya Nair, Tomomi Karigo, Bin Yang, Surya Ganguli, Mark J. Schnitzer, Scott W. Linderman, David J. Anderson, and Ann Kennedy. An approximate line attractor in the hypothalamus encodes an aggressive state. *Cell*, 186:178–193.e15, 1 2023. ISSN 00928674. doi: 10.1016/j.cell.2022.11.027.

Alexandre Naud, Eloise Chailleux, Yan Kestens, Céline Bret, Dominic Desjardins, Odile Petit, Barthélémy Ngoubangoye, and Cédric Sueur. Relations between Spatial Distribution, Social Affiliations and Dominance Hierarchy in a Semi-Free Mandrill Population. *Frontiers in Psychology*, 7, 5 2016. ISSN 1664-1078. doi: 10.3389/fpsyg.2016.00612.

A. C. Nelson, C. B. Cunningham, J. S. Ruff, and W. K. Potts. Protein pheromone expression levels predict and respond to the formation of social dominance networks. *Journal of Evolutionary Biology*, 28:1213–1224, 6 2015. ISSN 1010061X. doi: 10.1111/jeb.12643.

Adam C. Nelson, Vikrant Kapoor, Eric Vaughn, Jeshurun A. Gnanasegaram, Nimrod D. Rubinstein, Venkatesh N Murthy, and Catherine Dulac. Molecular and Circuit Architecture of Social Hierarchy. *bioRxiv*, 2019. doi: 10.1101/838664.

Randy J. Nelson and Brian C. Trainor. Neural mechanisms of aggression. *Nature Reviews Neuroscience*, 8(7):536–546, 7 2007. ISSN 1471-003X. doi: 10.1038/nrn2174.

Christof Neumann, Julie Duboscq, Constance Dubuc, Andri Ginting, Ade Maulana Irwan, Muhammad Agil, Anja Widdig, and Antje Engelhardt. Assessing dominance hierarchies: validation and advantages of progressive evaluation with Elo-rating. *Animal Behaviour*, 82(4):911–921, 10 2011. ISSN 00033472. doi: 10.1016/j.anbehav.2011.07.016.

Hamed Nili, Cai Wingfield, Alexander Walther, Li Su, William Marslen-Wilson, and Nikolaus Kriegeskorte. A Toolbox for Representational Similarity Analysis. *PLoS Computational Biology*, 10(4):e1003553, 4 2014. ISSN 1553-7358. doi: 10.1371/journal.pcbi.1003553.

Kensaku Nomoto and Susana Q. Lima. Enhanced Male-Evoked Responses in the Ventromedial Hypothalamus of Sexually Receptive Female Mice. *Current Biology*, 25(5):589–594, 3 2015. ISSN 09609822. doi: 10.1016/j.cub.2014.12.048.

Ken-ichi Ohta, Shingo Suzuki, Katsuhiko Warita, Kazunori Sumitani, Chiaki Tenkumo, Toru Ozawa, Hidetoshi Ujihara, Takashi Kusaka, and Takanori Miki. The effects of early life stress on the excitatory/inhibitory balance of the medial prefrontal cortex. *Behavioural Brain Research*, 379:112306, 2 2020. ISSN 01664328. doi: 10.1016/j.bbr.2019.112306.

Nancy Padilla-Coreano, Kanha Batra, Makenzie Patarino, Zexin Chen, Rachel Rock, Ruihan Zhang, Sebastien Hausmann, Javier Weddington, Reesha Patel, Yu Zhang, Hao-Shu Fang, Laurel Keyes, Avraham Libster, Gillian Matthews, James Curley, Ila Fiete, Cewu Lu, and Kay Tye. A cortical-hypothalamic circuit decodes social rank and promotes dominance behavior. *Nature Portfolio*, 2021. ISSN 2693-5015. doi: 10.21203/rs.3.rs-94115/v1.

Dustin J. Penn, Sarah M. Zala, and Kenneth C. Luzynski. Regulation of Sexually Dimorphic Expression of Major Urinary Proteins. *Frontiers in Physiology*, 13, 3 2022. ISSN 1664-042X. doi: 10.3389/fphys.2022.822073.

Pierre Olivier Polack, Jonathan Friedman, and Peyman Golshani. Cellular mechanisms of brain state-dependent gain modulation in visual cortex. *Nature Neuroscience*, 16(9):1331–1339, 2013. ISSN 10976256. doi: 10.1038/nn.3464.

Felicia Pratto, Jim Sidanius, Lisa M. Stallworth, and Bertram F. Malle. Social dominance orientation: A personality variable predicting social and political attitudes. *Journal of Personality and Social Psychology*, 67(4):741–763, 10 1994. ISSN 1939-1315. doi: 10.1037/0022-3514.67.4.741.

Chaoling Qu, Tamara King, Alec Okun, Josephine Lai, Howard L. Fields, and Frank Porreca. Lesion of the rostral anterior cingulate cortex eliminates the aversiveness of spontaneous neuropathic pain following partial or complete axotomy. *Pain*, 152(7):1641–1648, 7 2011. ISSN 0304-3959. doi: 10.1016/j.pain.2011.03.002.

Michael J. Raleigh. Social and Environmental Influences on Blood Serotonin Concentrations in Monkeys. *Archives of General Psychiatry*, 41(4):405, 4 1984. ISSN 0003-990X. doi: 10.1001/archpsyc.1984.01790150095013.

Nathaniel J. Ratcliff, Kurt Hugenberg, Edwin R. Shriver, and Michael J. Bernstein. The Allure of Status: High-Status Targets Are Privileged in Face Processing and Memory. *Personality and Social Psychology Bulletin*, 37(8):1003–1015, 8 2011. ISSN 0146-1672. doi: 10.1177/0146167211407210.

Ryan Remedios, Ann Kennedy, Moriel Zelikowsky, Benjamin F. Grewe, Mark J. Schnitzer, and David J. Anderson. Social behaviour shapes hypothalamic neural ensemble representations of conspecific sex. *Nature*, 2017. ISSN 14764687. doi: 10.1038/nature23885.

Sarah A Roberts, Deborah M Simpson, Stuart D Armstrong, Amanda J Davidson, Duncan H Robertson, Lynn McLean, Robert J Beynon, and Jane L Hurst. Darcin: a male pheromone that stimulates female memory and sexual attraction to an individual male's odour. *BMC Biology*, 8(1):75, 12 2010. ISSN 1741-7007. doi: 10.1186/1741-7007-8-75.

Annika Rosengren, Kristina Orth-Gomér, and Lars Wilhelmsen. Socioeconomic differences in health indices, social networks and mortality among Swedish men. A study of men born in 1933. *Scandinavian Journal of Social Medicine*, 26(4): 272–280, 10 1998. ISSN 0300-8037. doi: 10.1177/14034948980260040801.

Mostafa Safaie, Joanna C. Chang, Junchol Park, Lee E. Miller, Joshua T. Dudman, Matthew G. Perich, and Juan A. Gallego. Preserved neural dynamics across animals performing similar behaviour. *Nature*, 623(7988):765–771, 11 2023. ISSN 0028-0836. doi: 10.1038/s41586-023-06714-0.

Chad L Samuelsen and Michael Meredith. The vomeronasal organ is required for the male mouse medial amygdala response to chemical-communication signals, as assessed by immediate early gene expression. *Neuroscience*, 164(4):1468–1476, 12 2009. ISSN 03064522. doi: 10.1016/j.neuroscience.2009.09.030.

Robert M. Sapolsky. Social Status and Health in Humans and Other Animals. *Annual Review of Anthropology*, 33(1):393–418, 10 2004. ISSN 0084-6570. doi: 10.1146/annurev.anthro.33.070203.144000.

Diego Scheggia, Filippo La Greca, Federica Maltese, Giulia Chiacchierini, Maria Italia, Cinzia Molent, Fabrizio Bernardi, Giulia Coccia, Nicolò Carrano, Elisa Zianni, Fabrizio Gardoni, Monica Di Luca, and Francesco Papaleo. Reciprocal cortico-amygdala connections regulate prosocial and selfish choices in mice.

Nature Neuroscience, 25(11):1505–1518, 11 2022. ISSN 1097-6256. doi: 10.1038/s41593-022-01179-2.

Roberta Schellino, Sara Trova, Irene Cimino, Alice Farinetti, Bart C. Jongbloets, R. Jeroen Pasterkamp, Giancarlo Panzica, Paolo Giacobini, Silvia De Marchis, and Paolo Peretto. Opposite-sex attraction in male mice requires testosterone-dependent regulation of adult olfactory bulb neurogenesis. *Scientific Reports*, 6 (1):36063, 10 2016. ISSN 2045-2322. doi: 10.1038/srep36063.

João D. Semedo, Amin Zandvakili, Christian K. Machens, Byron M. Yu, and Adam Kohn. Cortical Areas Interact through a Communication Subspace. *Neuron*, 102 (1):249–259, 4 2019. ISSN 08966273. doi: 10.1016/j.neuron.2019.01.026.

Stephen V. Shepherd, Robert O. Deaner, and Michael L. Platt. Social status gates social attention in monkeys. *Current Biology*, 16(4):R119–R120, 2 2006. ISSN 09609822. doi: 10.1016/j.cub.2006.02.013.

Leon Sloman. The Evolutionary Model of Psychiatric Disorder. *Archives of General Psychiatry*, 41(2):211, 2 1984. ISSN 0003-990X. doi: 10.1001/archpsyc.1984.01790130107016.

David M. Smith and David A. Bulkin. The form and function of hippocampal context representations. *Neuroscience & Biobehavioral Reviews*, 40:52–61, 3 2014. ISSN 01497634. doi: 10.1016/j.neubiorev.2014.01.005.

Stefanos Stagkourakis, Giada Spigolon, Grace Liu, and David J. Anderson. Experience-dependent plasticity in an innate social behavior is mediated by hypothalamic LTP. *bioRxiv*, 2020. doi: 10.1101/2020.07.21.214619.

Stefanos Stagkourakis, Giada Spigolon, Markus Marks, Michael Feyder, Joseph Kim, Pietro Perona, Marius Pachitariu, and David J Anderson. Anatomically distributed neural representations of instincts in the hypothalamus. *bioRxiv*, 2023. doi: 10.1101/2023.11.21.568163.

John S. Stamm. The function of the median cerebral cortex in maternal behavior of rats. *Journal of Comparative and Physiological Psychology*, 48(4):347–356, 1955. ISSN 0021-9940. doi: 10.1037/h0042977.

Nicholas A. Steinmetz, Peter Zatka-Haas, Matteo Carandini, and Kenneth D. Harris. Distributed coding of choice, action and engagement across the mouse brain. *Nature*, 576(7786):266–273, 12 2019. ISSN 0028-0836. doi: 10.1038/s41586-019-1787-x.

Lisa Stowers and Stephen D Liberles. State-dependent responses to sex pheromones in mouse. *Current Opinion in Neurobiology*, 38:74–79, 6 2016. ISSN 09594388. doi: 10.1016/j.conb.2016.04.001.

Lisa Stowers, Timothy E. Holy, Markus Meister, Catherine Dulac, and Georgy Koentges. Loss of sex discrimination and male-male aggression in mice deficient for trp2. *Science*, 295:1493–1500, 2 2002. ISSN 0036-8075. doi: 10.1126/science.1069259.

Stephen Takács, Regine Gries, and Gerhard Gries. Sex Hormones Function as Sex Attractant Pheromones in House Mice and Brown Rats. *ChemBioChem*, 18(14): 1391–1395, 7 2017. ISSN 1439-4227. doi: 10.1002/cbic.201700224.

Wendy W.P. Tham, Richard J. Stevenson, and Laurie A. Miller. The functional role of the medio dorsal thalamic nucleus in olfaction. *Brain Research Reviews*, 62 (1):109–126, 12 2009. ISSN 01650173. doi: 10.1016/j.brainresrev.2009.09.007.

D H Thor and W J Carr. Sex and aggression: competitive mating strategy in the male rat. *Behavioral and Neural Biology*, 26(3):261–265, 7 1979. ISSN 01631047. doi: 10.1016/S0163-1047(79)91256-1.

Elizabeth A. Tibbetts, Juanita Pardo-Sanchez, and Chloe Weise. The establishment and maintenance of dominance hierarchies. *Philosophical Transactions of the Royal Society B*, 377(1845), 2 2022. ISSN 14712970. doi: 10.1098/RSTB.2020.0450.

M A van der Kooij, F Hollis, L Lozano, I Zalachoras, S Abad, O Zanoletti, J Grosse, I Guillot de Suduiraut, C Canto, and C Sandi. Diazepam actions in the VTA enhance social dominance and mitochondrial function in the nucleus accumbens by activation of dopamine D1 receptors. *Molecular Psychiatry*, 23(3):569–578, 3 2018. ISSN 1359-4184. doi: 10.1038/mp.2017.135.

Justin A. Varholick, Jeremy D. Bailoo, Ashley Jenkins, Bernhard Voelkl, and Hanno Würbel. A Systematic Review and Meta-Analysis of the Relationship Between Social Dominance Status and Common Behavioral Phenotypes in Male Laboratory Mice. *Frontiers in Behavioral Neuroscience*, 14, 1 2021. ISSN 1662-5153. doi: 10.3389/fnbeh.2020.624036.

Alexandra Veyrac, Guan Wang, Michael J. Baum, and Julie Bakker. The main and accessory olfactory systems of female mice are activated differentially by dominant versus subordinate male urinary odors. *Brain Research*, 1402:20–29, 7 2011. ISSN 00068993. doi: 10.1016/j.brainres.2011.05.035.

Fei Wang, Jun Zhu, Hong Zhu, Qi Zhang, Zhanmin Lin, and Hailan Hu. Bidirectional Control of Social Hierarchy by Synaptic Efficacy in Medial Prefrontal Cortex. *Science*, 334(6056):693–697, 11 2011. ISSN 0036-8075. doi: 10.1126/science.1209951.

Li Wang, Vaishali Talwar, Takuya Osakada, Amy Kuang, Zhichao Guo, Takashi Yamaguchi, and Dayu Lin. Hypothalamic Control of Conspecific Self-Defense. *Cell Reports*, 26(7):1747–1758, 2 2019. ISSN 22111247. doi: 10.1016/j.celrep.2019.01.078.

Dongyu Wei, Vaishali Talwar, and Dayu Lin. Neural circuits of social behaviors: innate yet flexible. *Neuron*, 109(10):1600, 5 2021. ISSN 10974199. doi: 10.1016/J.NEURON.2021.02.012.

Yingliang Wei, Jun Tang, Jianzhu Zhao, Jiajian Liang, Zhiyuan Li, and Song Bai. Association of loneliness and social isolation with mental disorders among medical residents during the COVID-19 pandemic: A multi-center cross-sectional

study. *Psychiatry Research*, 327:115233, 9 2023. ISSN 01651781. doi: 10.1016/j.psychres.2023.115233.

Wesley K. Whitten. Modification of the oestrous cycle of the mouse by external stimuli associated with the male. *The Journal of endocrinology*, 13(4):399–404, 1956. ISSN 00220795. doi: 10.1677/joe.0.0130399.

Wesley K Whitten. Pheromones and Mammalian Reproduction. In A Mclaren, editor, *Advances in Reproductive Physiology*, pages 155–177. Academic Press, New York, 1966.

Richard G Wilkinson. Socioeconomic determinants of health: Health inequalities: relative or absolute material standards? *BMJ*, 314(7080):591–591, 2 1997. ISSN 0959-8138. doi: 10.1136/bmj.314.7080.591.

Cait M. Williamson, Won Lee, Russell D. Romeo, and James P. Curley. Social context-dependent relationships between mouse dominance rank and plasma hormone levels. *Physiology and Behavior*, 2017. ISSN 1873507X. doi: 10.1016/j.physbeh.2016.12.038.

Cait M. Williamson, Won Lee, Alexandra R. DeCasien, Alesi Lanham, Russell D. Romeo, and James P. Curley. Social hierarchy position in female mice is associated with plasma corticosterone levels and hypothalamic gene expression. *Scientific Reports*, 2019. ISSN 20452322. doi: 10.1038/s41598-019-43747-w.

Lindsay Willmore, Courtney Cameron, John Yang, Ilana B. Witten, and Annegret L. Falkner. Behavioural and dopaminergic signatures of resilience. *Nature*, 611 (7934):124–132, 11 2022. ISSN 0028-0836. doi: 10.1038/s41586-022-05328-2.

Zheng Wu, Anita E. Autry, Joseph F. Bergan, Mitsuko Watabe-Uchida, and Catherine G. Dulac. Galanin neurons in the medial preoptic area govern parental behaviour. *Nature*, 509(7500):325–330, 5 2014. ISSN 0028-0836. doi: 10.1038/nature13307.

Bo Xing, Nancy R. Mack, Yu-Xiang Zhang, Erin P. McEachern, and Wen-Jun Gao. Distinct Roles for Prefrontal Dopamine D1 and D2 Neurons in Social Hierarchy. *The Journal of Neuroscience*, 42(2):313–324, 1 2022. ISSN 0270-6474. doi: 10.1523/JNEUROSCI.0741-21.2021.

Shengjin Xu, Hui Yang, Vilas Menon, Andrew L. Lemire, Lihua Wang, Fredrick E. Henry, Srinivas C. Turaga, and Scott M. Sternson. Behavioral state coding by molecularly defined paraventricular hypothalamic cell type ensembles. *Science*, 370(6514), 10 2020. ISSN 0036-8075. doi: 10.1126/science.abb2494.

Bin Yang, Tomomi Karigo, and David J. Anderson. Transformations of neural representations in a social behaviour network. *Nature*, 608(7924):741–749, 8 2022. ISSN 0028-0836. doi: 10.1038/s41586-022-05057-6.

Cindy F. Yang, Michael C. Chiang, Daniel C. Gray, Mahalakshmi Prabhakaran, Maricruz Alvarado, Scott A. Juntti, Elizabeth K. Unger, James A. Wells, and Nirao M. Shah. Sexually Dimorphic Neurons in the Ventromedial Hypothalamus Govern Mating in Both Sexes and Aggression in Males. *Cell*, 153(4):896–909, 5 2013. ISSN 00928674. doi: 10.1016/j.cell.2013.04.017.

Taehong Yang, Daniel W. Bayless, Yichao Wei, Dan Landayan, Ivo M. Marcelo, Yangpeng Wang, Laura A. DeNardo, Liqun Luo, Shaul Druckmann, and Nirao M. Shah. Hypothalamic neurons that mirror aggression. *Cell*, 186(6):1195–1211, 3 2023. ISSN 00928674. doi: 10.1016/j.cell.2023.01.022.

Darran Yates. Going on the defensive. *Nature Reviews Neuroscience*, 16(5):247–247, 5 2015. ISSN 1471-003X. doi: 10.1038/nrn3952.

Tingting Zhou, Hong Zhu, Zhengxiao Fan, Fei Wang, Yang Chen, Hexing Liang, Zhongfei Yang, Lu Zhang, Longnian Lin, Yang Zhan, Zheng Wang, and Hailan Hu. History of winning remodels thalamo-PFC circuit to reinforce social dominance. *Science*, 2017. ISSN 10959203. doi: 10.1126/science.aak9726.

Caroline F. Zink, Yunxia Tong, Qiang Chen, Danielle S. Bassett, Jason L. Stein, and Andreas Meyer-Lindenberg. Know Your Place: Neural Processing of Social

Hierarchy in Humans. *Neuron*, 58(2):273–283, 4 2008. ISSN 08966273. doi: 10.1016/j.neuron.2008.01.025.